UNIVERSITÉ LAVAL

Fabrication and Characterization of New and Highly Hydrophobic Hollow Fiber Membranes for CO_2 Capture in Membrane Contactors

Thèse

Sanaz Mosadegh Sedghi

Doctorat en génie chimique
Philosophiae Doctor (Ph.D.)

Québec, Canada

Résumé

Dans ce projet de doctorat, des membranes microporeuses (fibres creuses) et hautement hydrophobes à base de polyéthylène basse densité (LDPE) pour utilisation dans la capture du CO_2 dans des contacteurs gaz-liquide à membrane (GLMC), ont été fabriquées en utilisant une nouvelle méthode simple, sans solvant ou diluants, autant écologique qu'économique, et qui ne nécessite aucun post-traitement mécanique ou thermique. Pour produire des fibres creuses et contrôler leur porosité, on combine deux techniques, l'extrusion et le lavage de sel. Un mélange de LDPE et de particules de NaCl de différentes concentrations en sel conduit à la production des fibres (par extrusion) qui sont ensuite immergées dans l'eau pour éliminer le sel emprisonné dans le polymère et obtenir autant une structure microporeuse qu'une surface rugueuse hautement hydrophobe. La nouvelle méthode constitue une alternative très prometteuse aux méthodes actuellement utilisées pour la fabrication des membranes hydrophobes, principalement basées sur un processus d'inversion de phase qui implique des solvants toxiques et coûteux.

Les membranes fabriquées ont été caractérisées en termes de morphologie, densité, porosité et distribution de taille des pores, hydrophobicité, pression de percée et propriétés mécaniques. Comme le phénomène de mouillage des membranes en contact avec les solutions absorbantes est la cause principale de la réduction de l'efficacité des GLMC à long terme, une étude approfondie sur la compatibilité membrane/liquide absorbant a été réalisée. La stabilité morphologique, chimique et thermique des membranes en contact avec différentes solutions aqueuses d'alcanolamines à base de monoéthanolamine (MEA) et 2-amino-2-hydroxyméthyl-1,3-propanediol (AHPD), ainsi que des mélanges MEA/PZ (pipérazine) et AHPD/PZ, a été investiguée en détail.

Abstract

In this work, highly hydrophobic low density polyethylene (LDPE) hollow fiber membranes aiming to be used for CO_2 capture in gas-liquid membrane contactors (GLMC) were fabricated using a simple, novel method, without solvent or diluents, economic and environmentally friendly, which does not require any mechanical or thermal post-treatments. In order to produce hollow fibers and control their porosity, the process combines melt extrusion and template-leaching techniques. A mixture of LDPE and NaCl particles first produce blends with different salt contents. A microporous structure and a rough highly hydrophobic surface can then be produced by leaching the salt particles from the hollow fiber matrix via immersion in water. The new method represents a very promising alternative to conventional membrane fabrication approaches which are mainly based on phase inversion process that involves toxic and expensive solvents.

The fabricated membranes were characterized in terms of morphology, density, porosity and pore size distribution, hydrophobicity, breakthrough pressure and mechanical properties. Since the phenomenon of membrane wetting by liquid absorbents is the major cause of the reduction of long-term efficiency of GLMC, a comprehensive study on the compatibility between membrane and absorbent liquid was performed. Morphological, chemical and thermal stability of LDPE membranes in contact with different aqueous alkanolamine solutions including monoethanolamine (MEA) and 2-amino-2-hydroxymethyl-1,3-propanediol (AHPD), as well as blends of MEA/PZ (piperazine) and AHPD/PZ, was investigated in detail.

Table of content

List of Tables

List of Figures

Nomenclature

AEDP	2-amino-2-ethyl-1,3-propanediol
AHPD	2-amino-2-hydroxymethyl-1,3- propanediol
AMP	2-amino-2-methyl-1-propanol
B (-)	Shape factor
$CaCl_2$	Calcium chloride
CO_2	Carbon dioxide
d_i (m)	Inner diameter of hollow fiber
d_{lm} (m)	Logarithmic mean diameter
d_O (m)	Outer diameter of hollow fiber membrane
D_{ij} (m^2/s)	Molecular diffusion coefficient
D_{kj} (m^2/s)	Knudsen diffusion coefficient
D_L (m^2/s)	Diffusion coefficient of the solute in liquid phase
DEA	Diethanolamine
DETA	Diethylenetriamine
DMEAD	Dimethylethanolamine
DMFD	Dimethylformamide
ESA	Electric swing adsorption
f_1	Fraction of solid on a rough surface
f_2	Fraction of air on a rough surface
GLMC	Gas-Liquid membrane contactor
HALS	Hindered amine light stabilizers
IGCC	integrated gasification combined cycle
ipp	Isotactic polypropylene
K_{OG} (m/s)	Overall mass transfer coefficient based on the gas phase
k_S (m/s)	Mass transfer coefficient of porous support in composite membranes
k_C (m/s)	Mass transfer coefficient of dense coating in composite membranes

k_G (m/s)	Gas side mass transfer coefficient
k_m (m/s)	Membrane mass transfer coefficient
k_L (m/s)	Liquid phase mass transfer coefficient
k_{mg} (m)	Mass transfer coefficient through gas-filled pores
k_{ml} (m/s)	Mass transfer coefficient in the liquid filled pores
LDPE	Low density polyethylene
M	Distribution coefficient between gas and liquid
MDEA	Methyl diethanolamine
MEA	Monoethanolamine
MEK	Methyl ethyl ketone
MS-S	Melt-spinning and stretching
MWCNT	Multi-walled carbon nanotube
NaCl	sodium chloride
NIPS	Non-solvent induced phase separation
OH	Hydroxyl group
PA	Polyamide
PE	Polyethylene
$PE^{\bullet}$	Polyethylene alkyl radical
$PEOO^{\bullet}$	Polyethylene peroxy radical
$PEOOH$	Polyethylene hydroperoxide
PEG	Polyethylene glycol
PES	Polyethersulfone
PET	Poly(ethylene terephthalate)
PFA	Poly(tetrafluoroethylene-co-perfluorinated alkyl vinyl ether)
PFPE	Perfluoropolyether
PGMA	Poly(glycidylmethacrylate)
PI	Polyimide
PMMA	Poly(methyl methacrylate)
PP	Polypropylene

PS	Polystyrene
PSA	Pressure swing adsorption
PSF	Polysulfone
PTFE	Polytetrafluoroethylene
PU	Polyurethane
PVA	Poly vinyl alcohol
PVDF	Polyvinylidene fluoride
PZ	Piperazine
R (s/m)	Mass transfer resistance
R_a	Mean surface roughness
R_{max}	Maximum surface roughness
R_s	RMS value
r_P (m)	Maximum membrane pore radius
SD	Standard deviation
SEBS	Styrene-ethylene-butadiene-styrene
TETA	Triethylenetetramine
TIPS	Temperature induced phase separation
TSA	Temperature swing adsorption
V	Variety of volatile species generated from $PEOOH$ degradation
W	Weight of hollow fiber membrane
x^* (-)	Wetting ratio
Z_i	The vertical scanner tip position at a given position of the image
Z_{ave}	The average Z value
Z_{cp}	The Z value of the center plane

Greek letters

α	Number of volatile species generated from $PEOOH$ degradation
ΔP_c	Breakthrough pressure (kPa)
δ (m)	Membrane thickness

ε (-)	Porosity
γ_L (mN/m)	Solution surface tension
γ_S (mN/m)	Solid-vapor surface tension
γ_{SL} (mN/m)	Solid-liquid surface tension
γ_S^d (mN/m)	Dispersion component of solid-vapor surface tension
γ_L^d (mN/m)	Dispersion component of the liquid-vapor surface tension
γ_{CL} (mN/m)	Critical surface tension
θ (°)	Contact angle between liquid and membrane
θ_{eff} (°)	Effective contact angle
ρ_0 (kg/m^3)	Density of blank hollow fiber
ρ_1 (kg/m^3)	Density of porous hollow fiber membrane
τ (-)	Tortusity

Acknowledgment

This dissertation could not have been completed without the aid and support of countless people. First, I would like to express my deepest appreciation to my supervisor Maria Iliuta for her continuous support of my Ph.D. research. Without her guidance and persistent help, completing this dissertation would not have been possible. Furthermore, I would like to express my gratitude to my co-supervisors Denis Rodrigue and Josée Brisson for the useful comments, remarks and engagement through this Ph. D. project.

I would like to thank the Natural Sciences and Engineering Research Council of Canada (NSERC), the FRQNT Centre Québécois sur les Matériaux Fonctionnels (CQMF) and FQRNT Centre in Green Chemistry and Catalysis (CGCC) for financial support and the Centre de Recherche sur les Matériaux Avancés (CERMA) for technical support.

I would like to thank my beloved family, my mother, my father and my sister Bahareh who supported me spiritually throughout the entire process. Their kindness has always encouraged me to persistently go further in my research.

I would like to express my love and appreciation to my husband, Hamid, for his patience, encouragement and motivation. His sincere overall support derived me to complete this Ph. D. research project. I could not have imagined having a better friend than him in all my life.

Foreword

This thesis consists of 6 chapters. The first part of Chapter 1 (Introduction) deals with the importance of CO_2 capture and available methods for its mitigation (especially post-combustion techniques), gas separation using membrane contactors and membrane fabrication and characterisation. The second part of Chapter 1 represents a comprehensive review on the wetting phenomenon, a major concern in membrane contactors, which is in direct relationship with the aim of this thesis (fabrication of highly hydrophobic polymeric membranes). It also deals with membrane stability, another important parameter to be taken into account in industrial applications. The effect of several parameters including the properties of absorbents (operational conditions, flow rate, type and concentration) and membranes (hydrophobicity, pore size and porosity) on wetting phenomenon, as well as different methods to prevent membrane wetting, along with their advantages and drawbacks are discussed in detail. This section is the subject of a review paper. The Introduction chapter ends with Conclusions and Objectives of this work. Chapters 2-4 describe the hollow fiber membrane fabrication (as the main objective of this thesis) and the investigation on the stability of the fabricated membranes in contact with alkanolamine solutions. The general conclusions and suggestions for future works are given in Chapter 5.

This thesis was prepared based on the following published or submitted papers in/to scientific journals, in which the author has the main contribution:

1. Sanaz Mosadegh-Sedghi, Denis Rodrigue, Josée Brisson, Maria C. Iliuta, Wetting phenomenon in membrane contactors-Causes and preventions, *J. Membr. Sci*., Accepted for publication (Chapter 1, section 1.1.7).

2. Sanaz Mosadegh-Sedghi, Denis Rodrigue, Josée Brisson, Maria C. Iliuta, Highly hydrophobic microporous low-density polyethylene hollow fiber membranes by melt extrusion coupled with salt-leaching technique, *Polym. Adv. Technol.* 24 (2013) 584-592 (Chapter 2).

3. Sanaz Mosadegh-Sedghi, Josée Brisson, Denis Rodrigue, Maria C. Iliuta, Chemical alteration of LDPE hollow fibers exposed to monoethanolamine solutions used as absorbent for CO_2 capture process, *Sep. Purif. Technol*. 80 (2011) 338-344 (Chapter 3).

4. Sanaz Mosadegh-Sedghi, Josée Brisson, Denis Rodrigue, Maria C. Iliuta, Morphological, chemical and thermal stability of microporous LDPE hollow fiber membranes in contact with single and mixed amine based CO_2 absorbents, *Sep. Purif. Technol*. 96 (2012) 117-123 (Chapter 4).

The results of the present thesis were (will be) also presented in the following academic conferences:

1. Sanaz Mosadegh-Sedghi, Elodie Blanchard, Denis Rodrigue, Josée Brisson, Maria C. Iliuta, Chemical impact of MEA based absorbents on polyethylene membranes intended to be used in membrane contactors, *32nd Canadian High Polymer Forum* 2010, Ste-Adèle, Quebec, Canada.

2. Sanaz Mosadegh-Sedghi, Denis Rodrigue, Josée Brisson, Maria C. Iliuta, Characterization of LDPE Hollow Fibers for Membranes Applications, *Int. Conf. on Environ. Pollution and Remediation* 2011, Ottawa, Ontario, Canada.

3. Sanaz Mosadegh-Sedghi, Denis Rodrigue, Josée Brisson, Maria C. Iliuta, Characterization of Neat and Used Microporous LDPE Hollow Fiber Membranes for CO_2 Capture in Membrane Contactors, *PPS Americas Conference* 2011, Niagara Falls, Ontario, Canada.

4. Sanaz Mosadegh-Sedghi, Denis Rodrigue, Josée Brisson, Maria C. Iliuta, Fabrication of Highly hydrophobic microporous LDPE hollow fiber membranes by melt-extrusion and salt-leaching technique, 63*th Canadian Chem. Eng. Conf.* 2013, Fredericton, Ontario, Canada. (oral presentation).

Chapter 1

Introduction

1.1. Literature review

1.1.1. CO_2 capture and storage (CCS)

Carbon dioxide (CO_2) is known to be the main greenhouse gas. Today, the important CO_2 emissions are known to have an impact on global climate change. From continuous monitoring, global concentrations of CO_2 in the atmosphere have increased from pre-industrialisation levels (around 1860) of approximately 280 parts per million by volume (ppmv) to approximately 316 ppmv in 1958 and rapidly increased to approximately 369 ppmv today (UNEP, 2005). The global CO_2 concentration is predicted to rise to levels above 750 ppmv by 2100 if no action is taken to redress the current situation.

Power generation from fossil fuel-fired power plants (e.g. coal and natural gas) is the single largest source of CO_2 emissions (Freund, 2003). However, fossil fuel fired power plants play a vital role in meeting energy demands. For instance, coal-fired power plants could be operated flexibly in meeting with varying demand. With growing concerns over the increasing atmospheric concentration of anthropogenic greenhouse gases, effective CO_2 emission abatement strategies such as Carbon Capture and Storage (CCS) are required to combat this trend (Yang et al., 2008). CCS consists in the separation of CO_2 from industrial and energy-related sources, transport to a storage location and long-term isolation from the atmosphere (Wang et al., 2011). From this definition, CCS consists of three basic stages: (a) separation of CO_2; (b) transportation and (c) storage. As an alternative to storage, the captured CO_2 can also find applications in different industrial processes, like catalytic conversion in high-value products (CO_2 valorisation by chemical conversion) (Ma et al., 2009).

1.1.2. CO_2 Capture Strategies

The objective of CO_2 capture is to produce a concentrated stream, ready for use. Depending on the concentration of CO_2 in the gas stream, the pressure of the gas stream

and the fuel type (gas or solid), the potential pathways to sequestration are divided into different categories as described next.

1.1.2.1. Pre-combustion

The pre-combustion process is essentially based on the decarbonization of carbonaceous fuels. In this case, the primary fuel in a reactor is processed with controlled oxygen or air to produce a mixture consisting of carbon monoxide and hydrogen (synthesis gas). Subsequently, additional hydrogen, together with CO_2, is produced through the water gas shift reaction in a second reactor (shift reactor). The resulting mixture of H_2 and CO_2 can then be separated into two purified gas streams (Pires et al., 2011). CO_2 can be used in different industrial processes or stored, while hydrogen is a carbon-free energy carrier that can be combusted to generate power and/or heat, as well as used in industrial processes (like catalytic hydrogenation). Fuel conversion steps are more elaborated and costly compared to the post-combustion systems. The high concentrations of CO_2 produced by the shift reactor (typically 15 to 60% by volume on a dry basis) and the high pressures often encountered in these applications are more favorable for CO_2 separation. Pre-combustion is however an interesting process that can be used in power plants that employ integrated gasification combined cycle (IGCC) technology.

1.1.2.2. Post Combustion

Post-combustion capture involves removal of CO_2 from flue gas, which comes for example from the thermal power plant combustion chamber as shown in Fig.1.1. Existing power plants use air for combustion and generate a flue gas at atmospheric pressure and typically have a CO_2 concentration of less than 15% (Figueroa et al., 2008). Thus, the thermodynamic driving force for CO_2 capture from flue gas is low creating a technical challenge for the development of cost effective advanced capture processes (Figueroa et al., 2008). The low concentration of CO_2 in power-plant flue gas (13-15% for coal-fired power plants, 7-8% for gas-fired power plants) implies handling of large volumes of gas, which results in large equipment sizes and high capital costs. Technologies based on chemical absorption appear to be best adapted to this separation. Other technologies like

adsorption, membranes, and cryogenic capture are less suitable for post-combustion capture than pre-combustion capture, mainly for the following reasons (Mondal et al., 2012):

- A much lower partial pressure of CO_2 in post-combustion exhaust gases than in syngas originating from a gasifier or a reformer.
- The presence of larger quantities of dusts, impurities such as SOx and NOx, and non-condensable gases, particularly oxygen.

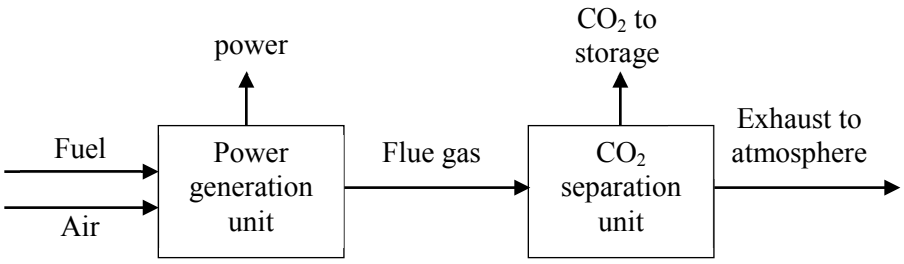

Figure 1.1. Principle of post-combustion CO_2 capture.

1.1.2.3. Oxyfuel combustion

In these systems, fuel is combusted with pure oxygen instead of air to produce a flue gas that mainly contains water vapor and CO_2. This results in production of a flue gas with high CO_2 concentrations (larger than 80% by volume) (IPCC, 2005). The water vapour is then removed by cooling and compressing the gas stream. Oxyfuel combustion requires the upstream separation of oxygen from air, with a purity of 95–99% oxygen assumed in most current designs (IPCC, 2005). Further treatment of the flue gas may be needed to remove air pollutants and non-condensed gases (such as nitrogen) from the flue gas before CO_2 is sent to storage. As a method of CO_2 capture in boilers, oxyfuel combustion systems are still in the demonstration phase. Oxyfuel systems are also being studied in gas turbine systems, but conceptual designs for such applications are still in the research phase.

1.1.3. Post-combustion CO_2 Capture Techniques

In order to capture CO_2 different techniques have been developed which are described in Fig. 1.2.

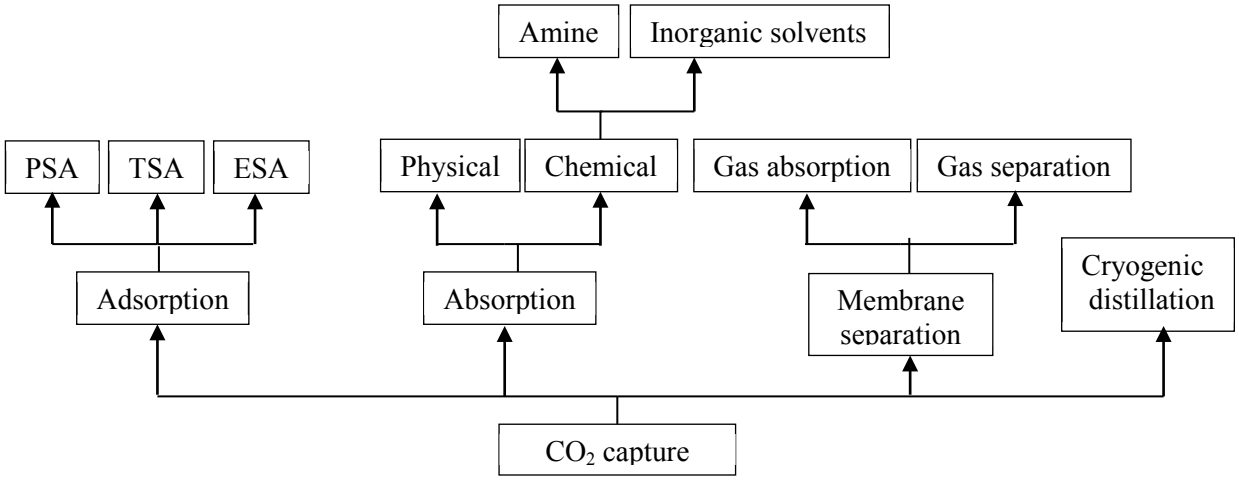

Figure 1.2. CO_2 capture techniques.

1.1.3.1. Adsorption

Adsorption is a physical process that involves the attachment of a gas or liquid to a solid surface. The properties of the adsorbed particles (molecular size, molecular weight and polarity) and the adsorbent surface (polarity, pore size and spacing) determine the adsorption quality (Pires et al., 2011). Since adsorption is an exothermic process, the regeneration of the adsorbents through desorption can be performed by rising the temperature (temperature swing adsorption, TSA), reducing the pressure (pressure swing adsorption, PSA) or through passing a high voltage electricity (electric swing adsorption, ESA). Adsorbents, which could be applied to CO_2 capture, include for example activated carbon, alumina, metallic oxides and zeolites (IEA GHG, 1993; Zhao et al., 2007; Hedin et al., 2013).

Adsorption presents lower energy requirements when compared to absorption (Drage et al., 2009). However, current adsorption systems may not be suitable for application in large-scale power plant flue gas treatment. At such scale, the low adsorption capacity of most available adsorbents may pose significant challenges. In addition, the flue gas streams to be treated must have high CO_2 concentrations because of the generally low selectivity of most available adsorbents. For instance, zeolites have a stronger affinity for water vapour (IEA, 2004; IEA, 2007; Zhao et al., 2007).

1.1.3.2. Physical absorption

This process involves the absorption of CO_2 into a physical solvent, based on Henry's law. Physical absorption takes place at low temperatures or high pressures. Regeneration can be achieved using heat, pressure reduction or both. As such, the main energy requirements originate from the flue gas pressurization. Physical absorption is therefore not economical for flue gas streams with CO_2 concentration lower than 15 vol% (Chakravati et al., 2001, IEA, 2004). Typical solvents are Selexol (dimethyl ethers of polyethylene glycol) and Rectisol (methanol) (IEA GHG, 1993).

1.1.3.3. Chemical absorption

Chemical absorption involves the reaction of CO_2 with a chemical solvent to form a weakly bonded intermediate compound which may be regenerated with the application of heat, producing the original solvent and a CO_2 stream (IPCC, 2005). Since this process involves chemical reactions between a chemical absorbent and CO_2, it can be accelerated at temperatures higher than room temperature. Among all CO_2 capture techniques, chemical absorption in liquids (absorbent solutions) is the most well-established technology due to its highest CO_2 removal efficiency (up to 90%) (Gabelman, 1999). The selectivity of this form of separation, offered by the chemical absorbent, is relatively high. In addition, a relatively pure CO_2 stream (around 98%) could be produced. These factors make chemical absorption well suited for CO_2 capture for industrial flue gases. Commonly used chemical absorbents are aqueous solutions of alkanolamines, especially monoethanolamine (MEA). But alkanolamines like MEA can easily be degraded in the presence of oxygen (Davidson, 2007). Oxygen levels of less than 1 ppm in flue gas are recommended for use with MEA when corrosion inhibitors are not employed (IEA GHG, 1993).

1.1.3.4.Cryogenic distillation

The cryogenic process concerns the separation of CO_2 from the flue gas stream by condensation. At atmospheric pressure, CO_2 condenses at −56.6 °C (IEA GHG, 1993). Considering its high refrigeration cost, this process is suitable for treating flue gas streams with high CO_2 concentrations (Pires et al., 2011). Cryogenic distillation has the advantage that it enables direct production of liquid CO_2, which is more economical for transport by

ships or pipelines. The most promising application for cryogenic distillation is the separation of CO_2 from gases with high CO_2 partial pressures, such as in pre-combustion or oxyfuel combustion (Wang et al., 2011).

1.1.3.5. Membrane separation

In membrane-based separation, selectivity is provided by the membranes themselves. This process normally uses thin polymeric films. Permeation rates would differ based on the relative sizes of the molecules or diffusion coefficients in the membrane material. The driving force for the permeation is the difference in partial pressure of the components at either sides of the membrane (Wang et al., 2011; Pires et al., 2011). The gas permeation processes have advantages of applicability in industrial processes (air separation, hydrogen recovery and carbon dioxide capture from natural gas); and high packing density, which requires small installations (Bounaceur et al., 2006). However, the selectivity of this separation process is low and thus only a fraction of the CO_2 is captured. In addition, the purity of the captured CO_2 is low for the same reason (IEA, 2004; IEA GHG, 1993). Multistage separation is employed to capture a higher proportion of CO_2, incurring extra capital and operating costs (Chakravati et al., 2001; IEA, 2004; IEA GHG, 1993).

1.1.4. Gas-Liquid Membrane Contactors (GLMC)

Although absorption columns have been of industrial interest for decades, an important disadvantage of these systems arises from the direct contact of two fluid phases, which can lead to operational difficulties such as foaming, emulsions, unloading and flooding (Falk-Pedersen and Dannström, 1997; deMontigny et al., 2005). Non-dispersive contact via a microporous membrane is an alternative technology that overcomes these disadvantages. In addition, the main challenge of maximizing the mass transfer rate is to produce as much interfacial area as possible (Li and Chen, 2005; Mansourizadeh and Ismail, 2009). For packed columns, this requires a good selection of packing material and uniform distribution of fluids, and for bubble columns the design challenge is how to minimize the bubble or droplet size of the dispersed phase, which is very difficult. Gas liquid membrane contactors (GLMC), using microporous membranes, offer substantially

more interfacial area per unit volume than columns (Dindore et al., 2004, Pubby and Sastre, 2013). This advantage is much more notable when using hollow fiber membranes with remarkably higher packing factor (interfacial area to the total volume of contactor). Falk-Pedersen and Dannström (1997) reported 72% reduction in size and 66% reduction in weight for membrane contactors compared with conventional columns (Table 1.1).

Table 1.1. Comparison of conventional absorber and membrane gas/liquid contactor **(**Falk-Pedersen and Dannström, 1997).

	Column	**Membrane contactor**
Size (width, length, height) (m)	4.5 × 4.5 × 21.8	4.5 × 4.5 × 5
Weight (tons)	70	24

Nishikawa et al. (1995) also showed that the overall volumetric mass transfer coefficient of hollow-fiber gas-liquid contactors is more than 5 times larger than that of a conventional packed bed, which suggests that using membrane contactors has the advantage of making the absorber more compact. Compared with flat membranes, hollow fiber membranes have attracted more attention, since they provide more interfacial area per unit volume, typically 30 times more than the area achievable in conventional gas absorbers (Gabelman and Hwang, 1999; Kosaraju et al., 2005). In addition to the mentioned advantages, membrane contactors provide the following benefits: *operational flexibility*, which arises from independent flow of gas and liquid which can then be manipulated independently, *economy,* which is attributed to the impact nature of these devices which makes them less energy consuming and *ease of linear scaled-up* (Li and Chen, 2005).

In a membrane contactor, the gas mixture and the liquid absorbent are fed to the contactor in counter-current or co-current flows. Fig. 1.3 shows the scheme of a typical membrane contactor with counter-current gas and liquid flows.

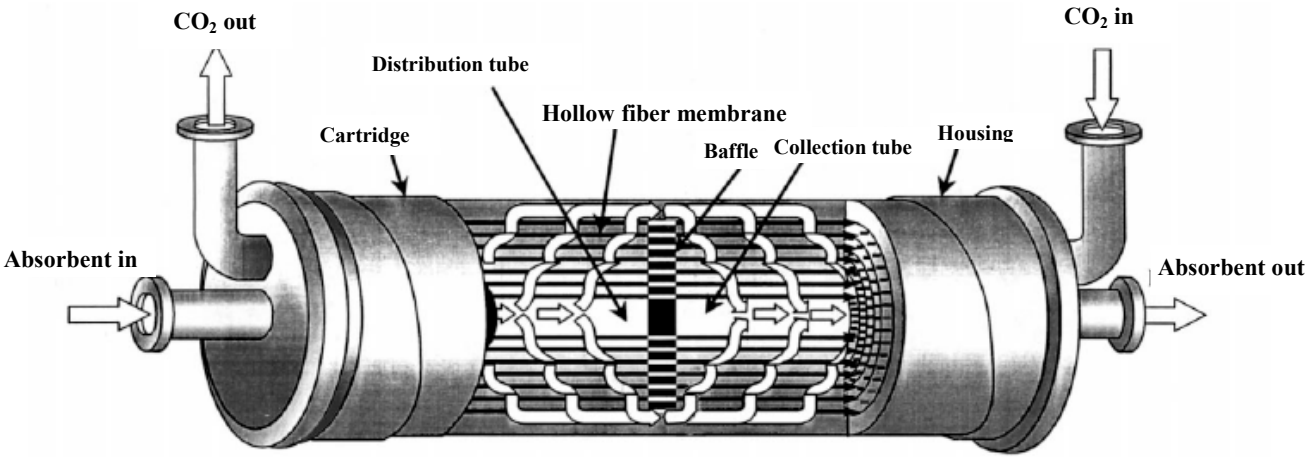

Figure 1.3. Typical scheme of a hollow fiber membrane contactor (Gabelman and Hwang, 1999)**.**

As shown in Fig. 1.4, gas molecules penetrate through the wall of the membranes and meet the liquid absorbent on the other side. Membranes used in these systems act as an interface between the gas and the liquid in order to prevent the dispersion of one phase in the other. In addition, in membrane contactors the permeated gas is absorbed rapidly by the liquid absorbent, thereby maintaining the concentration difference as the driving force on both sides of the membrane.

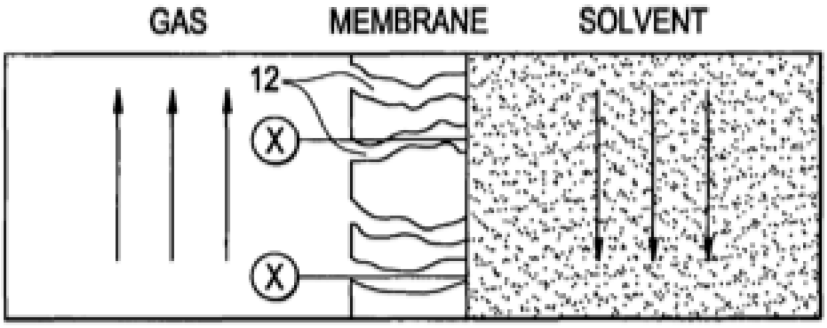

Figure 1.4. Gas penetration through a membrane in a membrane contactor (Falk-Pedersen and Dannström, 1997).

1.1.5. Criteria for the selection of membrane and absorbent in membrane contactors

CO_2 absorption in membrane contactors have been studied in the literature using different membrane materials, including polypropylene (PP) (Rangwala, 1996; Falk-Pedersen and Dannström, 1997; Kumar et al., 2002; Lin et al., 2008), polytetrafluoroethylene (PTFE) (Matsumoto et al., 1995; Kim and Yang, 2000; deMontigny et al., 2006; Lu et al., 2010), polyvinylidene fluoride (PVDF) (Dindore et al., 2004; Zhang et al., 2008; Rongwong et al., 2009) and polysulfone (PS) (Mansourizadeh and Ismail, 2010; Rahbari-Sisakht et al., 2012), as well as different absorbents, including monoethanolamine (MEA) (Falk-Pedersen and Dannström, 1997; Kim and Yang, 2000; Zhang et al., 2008; Lv et al., 2010; Chen et al., 2011), diethanolamine (DEA) (Rangwala, 1996; Kumar et al., 2002, Wang et al., 2004a), hindered amine solutions (Lin et al., 2008; Bougie and Iliuta, 2010) and activated salts (Kumar et al., 2002; Yan et al., 2007; Lu et al., 2009).

Membranes selected to be used in membrane contactors should have specific properties including high porosity, small pore size (ideally around 0.1 μm), low surface energy (to minimize its wettability in contact with absorbents) and high chemical stability (Dindore et al., 2004).

The selection of liquid absorbents should also be based on criteria including high reactivity with CO_2 (Yang and Cussler, 1986), high surface tension to reduce its wetting tendency in contact with membranes (Kruelen et al., 1993), chemical compatibility with the membrane to prevent possible chemical reactions between the absorbent and membrane (Barbe et al., 2000; Wang et al., 2004a), low vapor pressure (if the solvent is volatile, its vapor can fill the membrane pores and even penetrate through the membrane into the gas phase, which will increase the total mass-transfer resistance) (Kim and Yang, 2000), and high thermal stability to avoid decomposition during regeneration (Li et al., 2005).

1.1.6. Hollow fiber membrane fabrication

Based on their structure, membranes are characterized as in Fig. 1.5. Gas permeation through dense membranes occurs by solution diffusion. These kinds of membranes are commercially desirable when they are cast as very thin films. Unlike

homogeneous microporous membranes, heterogeneous membranes have non-uniform pore structures. Heterogeneous membranes, having a thin, dense top layer are called asymmetric membranes. Heterogeneous membranes, having a dense top layer created in a separate step (e.g. coating) are known as thin-film composite membranes. Generally, there are two main techniques for membrane fabrication including *melt-spinning* and *solution spinning* which will be discussed next.

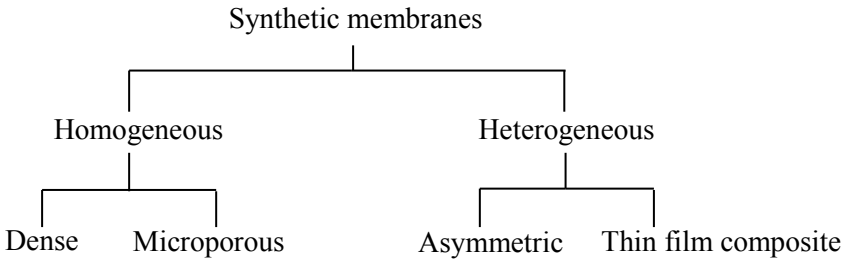

Figure 1.5. Membrane classification based on their different structures (Puri, 1990).

1.1.6.1. Melt spinning

This process uses either a single or twin-screw extruder to melt and transport the polymer melt through a die (spinneret). The die used for melt-spinning of fibers typically has the cross-section shown in Fig. 1.6. The polymer solution is pushed through the outside annulus and the core gas is used to maintain and control the diameter of the extruded fiber (Puri, 1990).

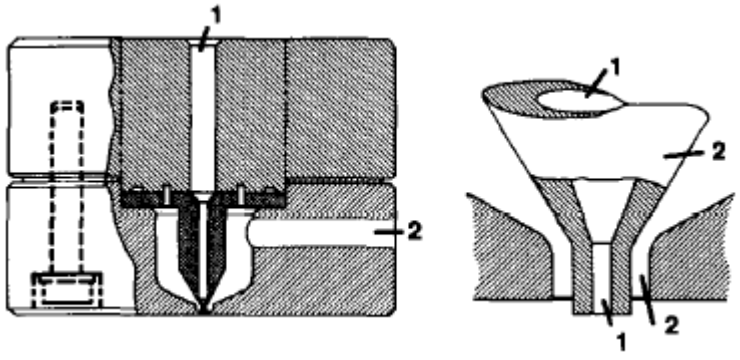

Figure 1.6. Cross-section of a typical hollow fiber membrane spinneret: 1) air, 2) polymer melt (Puri 1990).

Melt-spinning is a solvent-free method of membrane fabrication and leads to the formation of homogeneous membranes with a dense structure. In order to form a microporous structure, spinning should be coupled with another technique. The techniques used for homogeneous microporous membrane fabrication are described here:

1.1.6.2. Melt-spinning and stretching (MS-S)

This process comprises the melt-spinning of a polymer, followed by a stretching step, in which the micropores are formed due to the mechanical force (Kim et al., 1994). The general hollow fiber membrane fabrication procedure via MS-S method is described in Fig. 1.7.

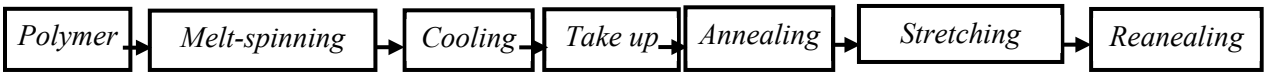

Figure 1.7. Microporous hollow fiber membrane preparation procedure via melt-spinning and stretching.

The polymer goes through the spinning process to form dense membrane precursors, which are then annealed at a temperature close to the polymer melting point to develop their crystallinity. A simple scheme of a hollow fiber spinning apparatus typically used is illustrated in Fig. 1.8. The dense precursors are stretched either in one (cold stretching) or two (cold and hot stretching) steps to form a microporous structure. The microporous membranes are then re-annealed to maintain their original dimensions and avoid shrinkage (Kim et al., 1994).

Since melt-spinning and stretching does not employ any solvent or diluent, it is a very clean and economical process. In addition, this process does not involve any phase separation and therefore, is easy to handle. In addition, membranes prepared by this method have quite high mechanical strength, due to the high degree of molecular orientation (Kim et al., 1995). There are several reports in the literature concerning the fabrication of microporous membranes, including PP (Kim et al., 1994, Kim et al., 1995, Mei et al., 2002), PVDF (Du et al., 2007), PE (Kim et al., 2008, Xi et al., 2008, Shen et al., 2002),

PVDF/PU (Hu et al., 2011), and PVDF/PU/PEG (Hu et al., 2010) using the MS-S technique.

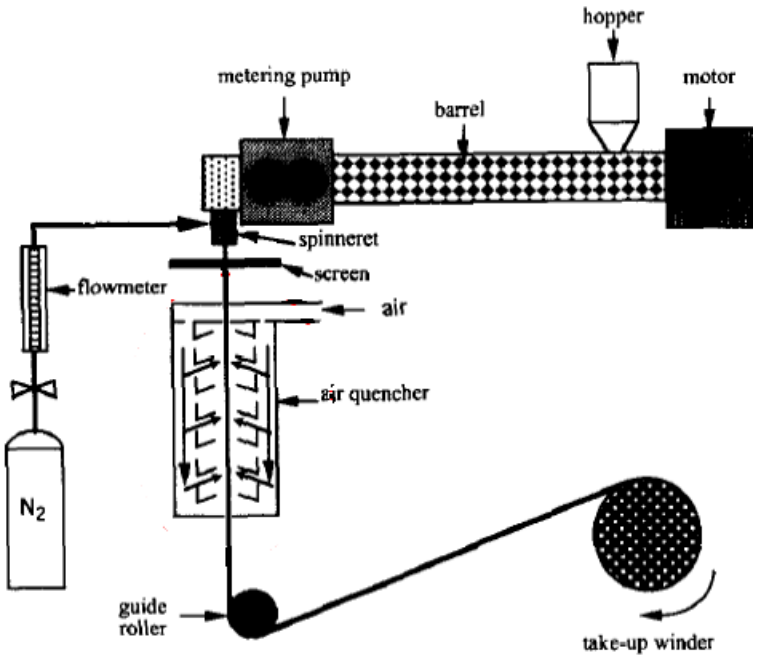

Figure 1.8. Hollow fiber spinning apparatus (Kim et al., 1994).

1.1.6.2.1. Micropore formation mechanism

MS-S method is applied to semi-crystalline polymers including an amorphous phase as well as a crystalline one. Such polymers, under high stresses applied on the polymer melt during extrusion, form a row lamellar structure which is developed during the annealing process (Keller and Marchin, 1967; Shen et al., 2002). The highly oriented, row nucleated lamellar structures usually have the unique properties of "hard elastic" polymers: high orientation, high modulus, and high elastic recovery. The term "hard elastic" is commonly used since its modulus of elasticity is much higher than those of classical elastic or rubbery polymers with similar recovery properties at strains of less than 50% extension. This type of hard elastic behavior has been reported in polyethylene, polypropylene, polyoxymethylene, and nylon-6,6 when effectively annealed (Yu and Wilkes, 1996). Afterwards, during stretching, the crystalline phase forms lamellae stacks, while the amorphous phase forms micropores and microfibrils, acting as connections between

lamellae stacks (Kim et al., 2008). The morphology of PE hollow fiber membranes fabricated via MS-S process, including micropores, lamellae stacks and microfibrils, is depicted in Fig. 1.9.

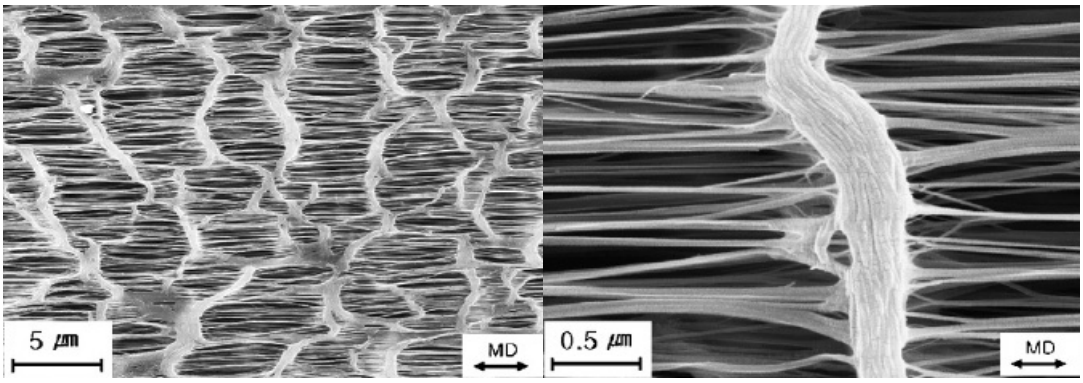

Figure 1.9. a) Inner surface images of membrane prepared from annealed hollow fiber precursors by hot stretching, b) (a) at higher resolution (Kim et al., 2008).

1.1.6.2.2. Effect of MS-S parameters

As defined in the literature, in the MS-S process, the membrane structure is affected by spinning (extrusion) parameters including the *melt-draw ratio,* defined as the ratio of take up speed and extrusion rate (extrusion rate is the volumetric flow rate of the spun fiber coming out of the spinneret to the annular cross-sectional area of the spinneret), *spinneret temperature*, which is the temperature of the die zone where the hollow fiber melt comes out of the extruder and *annealing temperature,* as well as stretching parameters including *temperature*, *rate*, and *ratio* (Kim et al., 1994, Kim et al., 1995, Kim et al., 2008, Du et al., 2007, Xi et al., 2008)

The parameters studied in the literature as well as their impacts on membrane structure are presented in Table 1.2.

Table 1.2. Effect of melt-spinning and stretching on hollow fiber membranes structures.

	Spin.T[a]	Melt-draw ratio	Take up S[b]	Anneal. T[c]	Stretch. R[d]	Stretch. ratio	Stretch.T[e]	Ref.
Crystallinity		Direct	Direct	Direct		-		Kim et al., 1994
		-	-			Direct		Kim et al., 1995
		-	-			-		Du et al., 2007
		-	-			-		Kim, 2008
Bubble point pressure	Direct	Reverse		Reverse		-		Kim et al., 1994
	-	-		-		Reverse		Kim et al., 1995
	-	-		-		-		Du et al., 2007
Pore size		Direct		-	-	-		Kim et al., 1994
		-		-	-	-		Kim et al., 1995
		-		Direct	Direct	-		Du et al., 2007
		-		-	-	-		Kim, 2008
		-		-	Reverse	Direct		Xi et al., 2008
Porosity		-		-	-	-	-	Kim et al., 1994
		-		-	-	Direct	-	Kim et al., 1995
		Direct		Direct	Direct	-	-	Du et al., 2007
		-		-	-	-	-	Kim, 2008
		-		-	Direct	Direct	Direct	Xi et al., 2008

Table 1.2. Effect of melt-spinning and stretching on hollow fiber membranes structures (continued).

	Spin.T[a]	Melt-draw ratio	Take up S[b]	Anneal. T[c]	Stretch. R[d]	Stretch. ratio	Stretch. T[e]	Ref.
Elastic recovery		Direct		direct				Du et al., 2007
		cte		-				Kim, 2008
Fiber inner diameter		cte						Kim et al., 1995
		Reverse						Du et al., 2007
Fiber thickness		Reverse						Kim et al., 1995
		-						Du et al., 2007
Contact angle						Direct		Xi et al., 2008

[a] Spinneret temperature, [b] Take up speed, [c] Annealing temperature, [d] Stretching rate, [e] Stretching temperature

1.1.6.2.2.1. Effect of extrusion parameters

The influence of melt extrusion parameters including melt-draw ratio, annealing temperature, and spinneret temperature on membrane properties has been investigated in the literature (Kim et al., 1994; Chu et al., 2012). It was concluded that the melt-draw ratio and spinneret temperature can influence the degree of orientation of the hollow fiber membrane, while annealing temperature does not affect this property. Instead, crystallinity is affected by the annealing temperature, as well as the take up speed. Fig. 1.10 shows that birefringence increases with increasing melt-draw ratio due to higher stresses applied on the hollow fiber passing through the spinneret. In addition, the viscosity and consequently the stress of the polymer melt increases at lower temperature. Therefore, birefringence increases with decreasing spinneret temperature (Fig 1.10), whereas birefringence (i.e. molecular orientation of the hollow fiber membranes) was not influenced by annealing temperature (Fig. 1.10g). Crystallinity of hollow fiber membranes was identified with sample density. The density of the sample (i.e. crystallinity) increases with increasing melt-draw ratio (Fig. 1.10b) and annealing temperature (Fig. 1.10b), while it is not affected by the spinning temperature (Fig. 1.10e).

It was also concluded that the bubble point pressure (breakthrough pressure) was dependant on melt-draw ratio, spinning temperature and annealing temperature as shown in Fig. 1.10c and 1.10f and 1.10i. As the melt-draw ratio increased, the bubble point pressure decreased (due to the increase in d_{max} (maximum pore diameter) in eq. 2.1), which is attributed to the changes in morphology and crystalline order. Similarly, when the sample was spun at lower temperature, it had a more ordered structure and consequently lower bubble point pressure. The annealing step also helped the hollow fibers to have a more ordered structure; i.e. smaller bubble point pressure via recrystallization and rearrangement of the polymer chain.

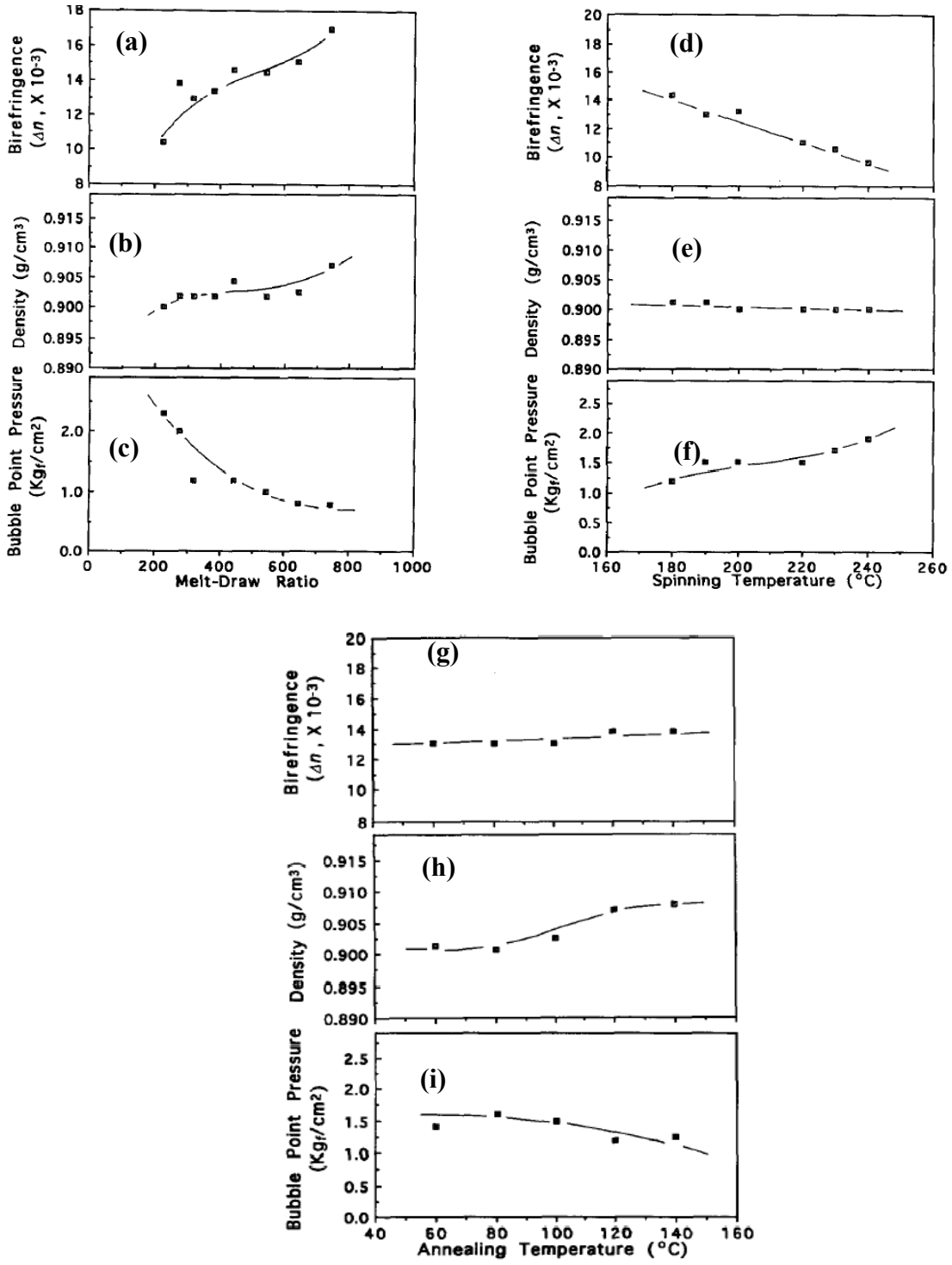

Figure 1.10. a), b) and c) effect of drawing ratio, d), e) and f) effect of spinneret temperature and g), h) and i) effect of annealing temperature on structure and properties of PP hollow fiber membranes (Kim et al., 1994).

1.1.6.2.2.2. Effect of stretching parameters

1.1.6.2.2.2.1. Effect of stretching temperature

Xi et al. (2008) proposed a *two-step stretching* process to produce polyethylene hollow fiber membranes via a melt-spinning and stretching method. These steps are composed of the cold stretching step at 40°C, followed by a hot stretching step at temperatures higher than 55°C. They focused on the effect of stretching temperature, rate and ratio on hollow fiber membrane structure. It was indicated that during the cold stretching process, crystalline lamellae will be separated by the formation of a large number of voids. As stretching continues at higher temperatures (hot stretching), the voids are interconnected and micropores are formed. It was concluded that porosity of PE hollow fiber membranes, as well as N_2 permeation, were induced by rising stretching temperature (Fig. 1.11).

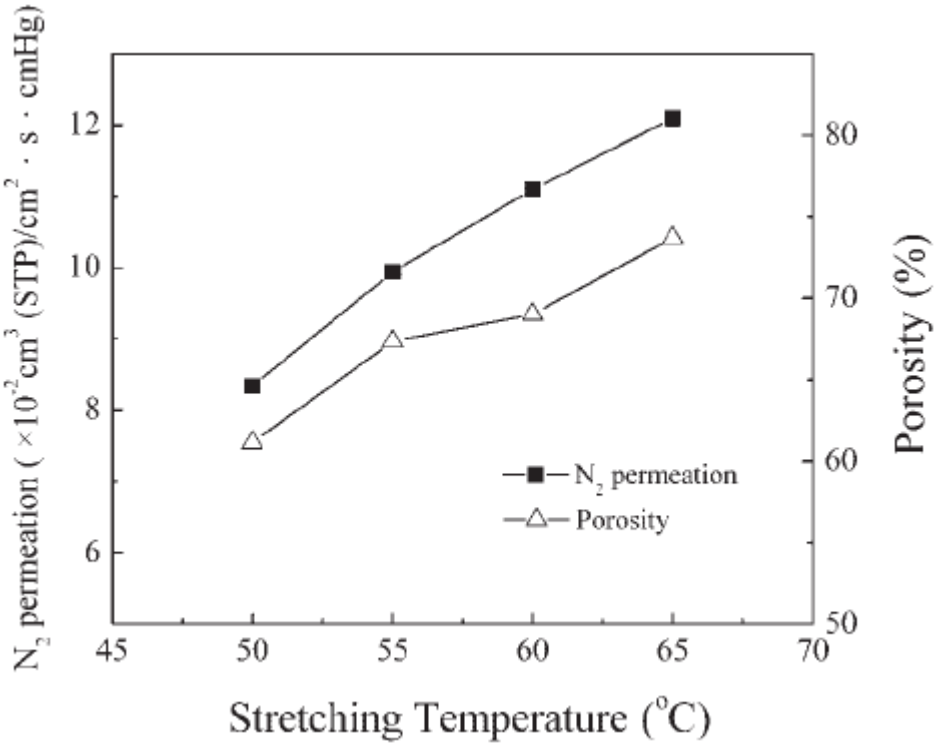

Figure 1.11. Effect of stretching temperature on N_2 permeation flux and porosity of HDPE hollow fiber membranes (Xi et al., 2008).

Flexible molecular chains in the amorphous region of crystalline polymers have almost no regular arrangement compared to those in the crystalline region, thus less resistance improved the movement and orientation capability of molecular chains under external force and temperature. Below the melting point of PE, molecular chains of PE hollow fibers would be much easier to be drawn out from the amorphous region and orient along the stretching direction at a relatively high temperature. Therefore, more rearrangement of the amorphous region into fibrils which bridged the separated lamellae resulted in high porosity in the hollow fiber wall. Meanwhile, the improved capability of movement suppressed the evolution of microvoids into breaking. It had been concluded that the introduction of the second stretching process with a proper temperature was necessary to insure good mechanical properties (Xi et al., 2008).

1.1.6.2.2.2.2. Effect of stretching rate

It was reported that N_2 permeation flux was increased by increasing the stretching rate of PE hollow fibers. However, the pore size decreased from 0.62 μm at a stretching rate of 200 mm/min to 0.5 μm at 400 mm/min (Fig. 1.12) (Xi et al., 2008).

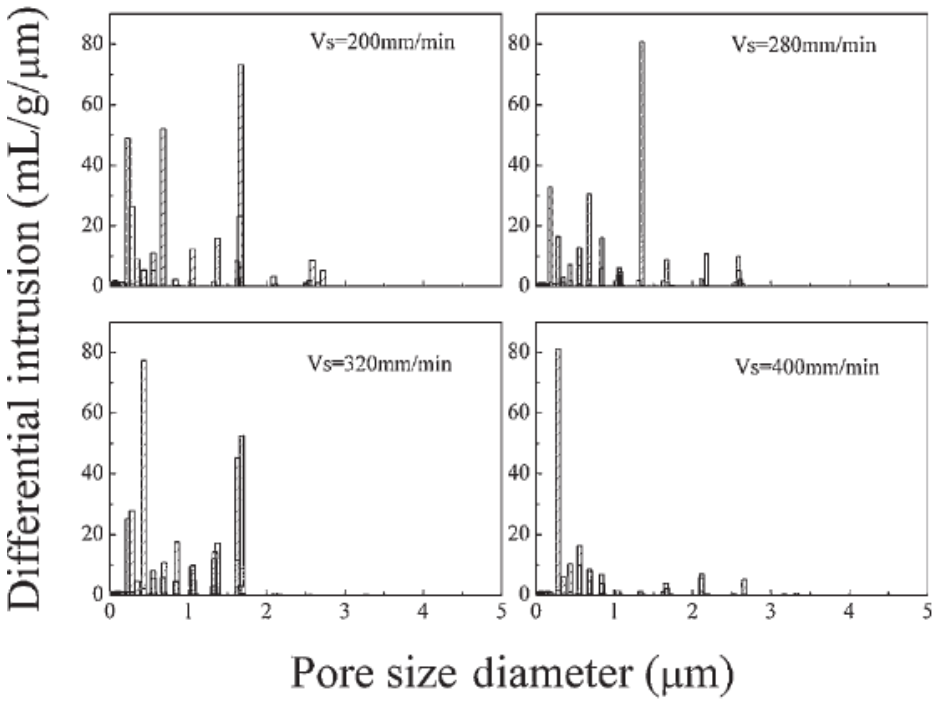

Figure 1.12. Effect of stretching rate on pore size distributions of HDPE hollow fiber membranes (Vs=stretching rate) (Xi et al., 2008).

This observation was explained by the reduction in the amorphous phase proportion under higher stress, resulting from higher stretching rates. While the amorphous region is responsible for micropore creation after stretching, smaller pores were created at higher stretching rates.

1.1.6.2.2.2.3. Effect of stretching ratio

Stretching ratio is the ratio of the final length to the initial length of the produced hollow fiber precursors. In the SEM photographs (Fig. 1.13) of PE hollow fiber membranes having different elongations, it was observed that the fibrils were elongated obviously when the stretching ratio increased.

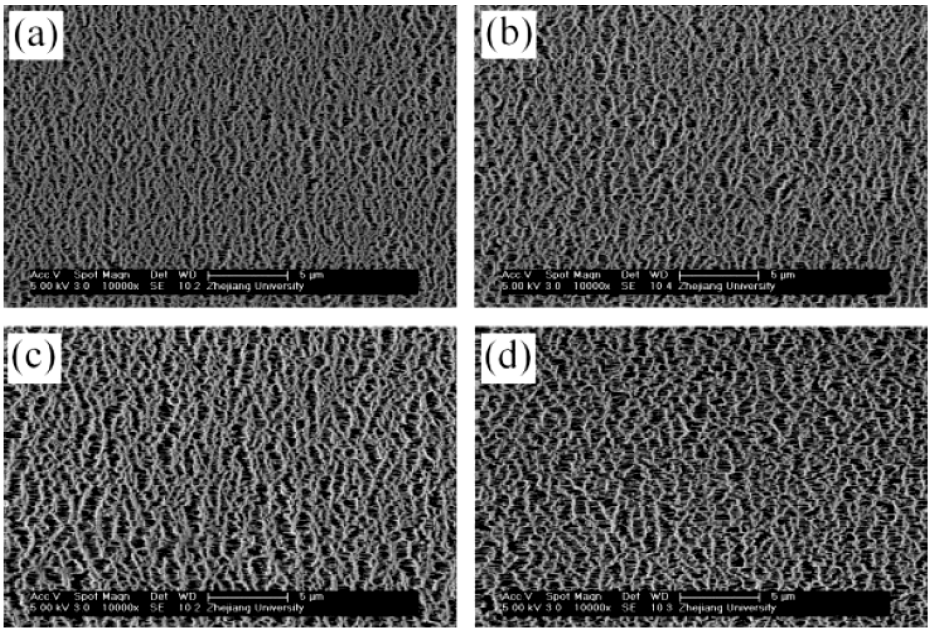

Figure 1.13. SEM photographs of the outer surface of HDPE hollow fiber membranes for different extensions: (a) 135%, (b) 159%, (c) 190%, and (d) 228% (Xi et al., 2008).

As shown in Fig. 1.14, the N_2 permeation flux was increased by increasing the stretching ratio and subsequently elongation.

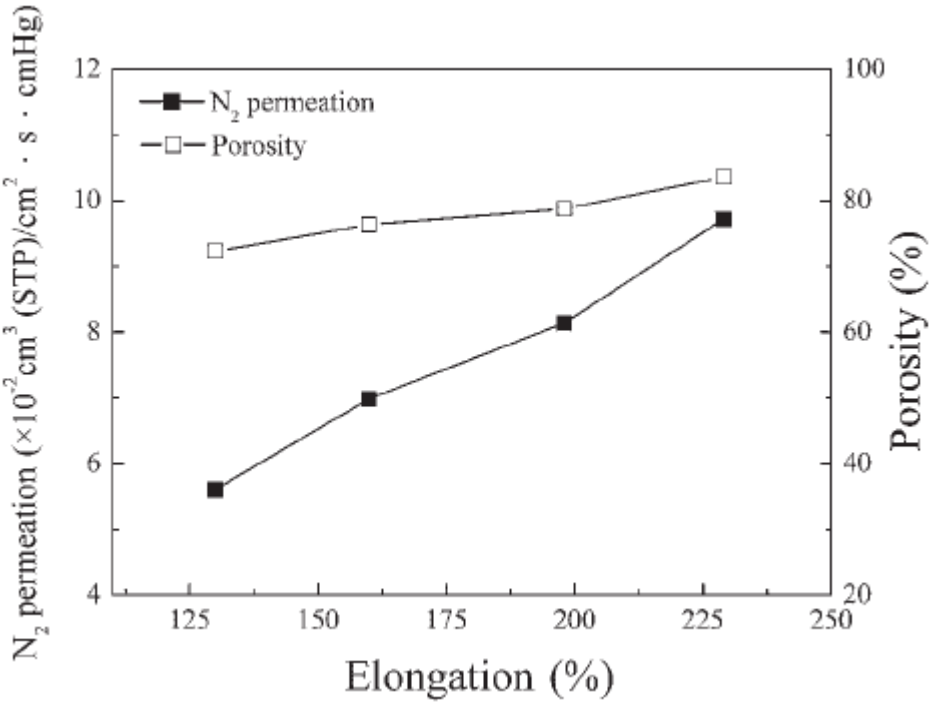

Figure 1.14. Effects of stretching ratio on N_2 permeation and porosity of HDPE hollow fiber membranes (Xi et al., 2008).

It can also be concluded that the space between separated lamellar crystals was enlarged by the external mechanical force. From the analysis of the results of a mercury porosimeter, the pore size distributions in Fig. 1.15 demonstrate that the amount of pores with a size smaller than 1 μm significantly increased when the stretching ratio increased from 2.3 to 3.3 μm. This was attributed to the fact that the fibrils, bridging the separated crystalline lamellae, may be broken under a high stretching ratio; at which point the stress concentration promoted the formation of cracks from destroyed micropores.

1.1.6.3. Solution spinning

Solution spinning of polymers is the main method for membrane fabrication and is based on the phase inversion process (Puri, 1990). This method uses polymer/organic solvent solutions. The solvent has to be removed after the formation of membrane. The pores are formed while evaporation of the solvent is taking place. However, these techniques are complex due to the high number of parameters to be controlled and intensive

steps like several washing and drying procedures. In addition, increasing demands on cost reduction and better environmental compatibility lead to the search for alternative solvent-free processes (Matsuyama, 2003).

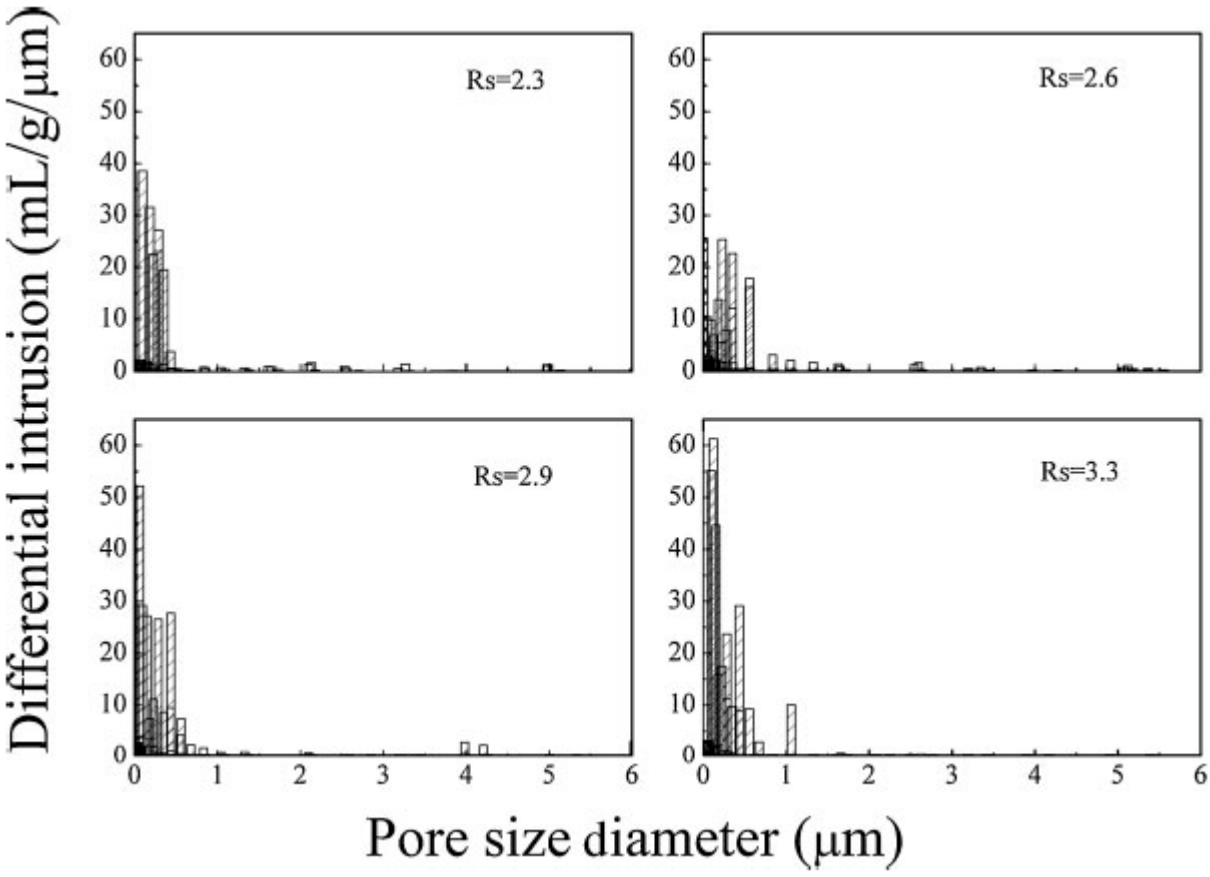

Figure 1.15. Effect of stretching ratio on pore size distributions of HDPE hollow fiber membranes (Rs=stretching ratio) (Xi et al., 2008).

1.1.6.4. Temperature induced phase separation method (TIPS) and non-solvent induced phase separation (NIPS)

Traditionally, polymer membranes shaped as porous hollow fibers were prepared using the diffusion induced phase separation technique or NIPS (Berghmans et al., 1996). In this process, a polymer solution and a solvent are placed in contact with a non-solvent for the polymer. Because of initial interdiffusion between the solvent and the non-solvent, the concentration of the polymer solution changes up to a point where phase separation occurs.

Thermally induced phase separation, or TIPS, is an alternative technique used for producing porous structures. In the TIPS process, a polymer is dissolved in a high boiling low molecular weight diluent at elevated temperatures and, after forming the solution to the desired shape (flat or hollow fiber membrane), it is cooled to induce phase separation. In the final stage of the membrane fabrication, the diluent is extracted by another solvent and then the solvent is removed to produce a membrane structure (LIoyd et al., 1991; Berghmans et al., 1996). The process uses the spinning of the polymer as well as the solvent through an extruder. In case of NIPS, a non-solvent is also added to the spinning mixture in the extruder. After spinning the polymer/solution mixture out of the extruder, the fibers are cooled via dry or wet-dry (air-gap) method. In dry cooling, the fiber is allowed to cool into the open air by convection and solvent evaporation, while in the wet-dry method a water bath is used (Berghmans et al., 1996). In the TIPS process, the spun sample is composed of a polymer and a diluent which form a homogeneous melt above its melting temperature, which undergoes a solid-liquid phase separation upon cooling. The sites occupied by the diluent become micropores after removal of the diluent. In this method, the pore size can be controlled by adjusting the cooling conditions and by selecting appropriate diluents. (Rajabzadeh et al., 2008).

Using TIPS and NIPS methods, membranes made of several different materials were reported to be fabricated, including PE (Matsuyama et al., 2004; Wang et al., 2010), PVDF (Ji et al., 2008; Rajabzadeh, 2008; Ghasem et al., 2012, Rajabzadeh, 2012), IPP (Yang et al., 2006; Yang et al., 2006), and PVDF/PMMA (Rajabzadeh, 2009).

1.1.7. Wetting phenomenon in membrane contactors - Causes and preventions

Abstract

Gas-liquid membrane contactors are promising alternatives to conventional absorption technologies. However, in spite of their important advantages, such systems suffer from gradual wetting of porous membranes with liquid absorbents. This review focuses on the wetting phenomenon, which is the main concern for long-term operation of CO_2 absorption in membrane contactors and has therefore an important impact on industrial applications. The impact of membrane wetting on mass transfer resistance and absorption efficiency, the effect of influencing parameters including absorbent (operational conditions, type and concentration) and membrane (hydrophobicity, pore size and porosity) properties on wetting phenomenon, as well as different methods to prevent membrane wetting, along with their advantages and drawbacks are discussed in detail.

1.1.7.1. Introduction

Capture of carbon dioxide (CO_2), the major greenhouse gas responsible for climate changes, has been a research focus in recent years (IPCC, 2005). A wide variety of CO_2 capture techniques have been proposed, including absorption, adsorption, cryogenic distillation and membrane techniques (Aaron et al., 2005; Lv et al., 2010; Luis et al., 2012). Among these, absorption in liquids (absorbent solutions) is the most well-established technology due to its highest CO_2 removal efficiency (up to 90%) (Gabelman and Hwang, 1999). However, absorption columns (bubble columns, packed columns and fluidized beds) suffer from several disadvantages such as large space occupancy, high capital cost, high tendency for corrosion and a variety of operational problems including liquid channeling, flooding, entrainment and foaming (Falk-Pedersen and Dannström, 1997; deMontigny et al., 2005; Karoor and Sirkar, 1993). To overcome the aforementioned problems, gas-liquid membrane contactors (GLMC) have been proposed as a promising alternative. GLMCs involve the transfer of CO_2 through a nonselective porous membrane, followed by its absorption into a liquid absorbent. This technology is integrated to exploit the benefits of both absorption (high selectivity) and membrane separation (modularity and compact structure) (Franco et al., 2008), and offers several advantages such as: operational

flexibility, independent gas and liquid flows, high surface area to volume ratio, compact size, easy scale-up and modularity (Gabelman, 1999). On the negative side, membranes introduce an additional resistance (the membrane resistance) to the overall mass transfer process, which becomes more significant when membrane pores are wetted with liquid absorbents (Dindore et al., 2004), leading to the deterioration of CO_2 absorption flux in long-term operation. Kreulen and Smolders (1993) were the first to suggest that the wetting of membrane pores significantly impacts mass transfer coefficients in the membrane module, leading to a sharp increase in membrane resistance and a rapid decline of absorption performance.

In order to have a good understanding of the wetting mechanism and its effects on CO_2 capture efficiency, this paper presents a comprehensive review on wetting phenomenon from two main aspects: i) wetting causes and ii) wetting preventions. These aspects embrace the wetting characteristics of membranes and the effect of influencing parameters on wetting tendency of membranes in GLMC, as well as the approaches to prevent membrane wetting.

1.1.7.2. Mass transfer resistance in GLMC and membrane wetting

According to the film theory, the overall mass transfer in a gas-liquid membrane contactor consists of three resistances in series: the resistance of the gaseous phase boundary layer ($1/k_G$), the membrane resistance ($1/k_m$) and the resistance of the liquid the phase boundary layer ($1/k_L$) (Fig. 1.16) (Rangwala, 1996; Khaisiri et al., 2009). The overall mass transfer resistance, based on the gas phase ($1/K_{OG}$) in a hollow fiber GLMC is given by:

$$\frac{1}{K_{OG}} = \frac{d_O}{k_G d_i} + \frac{d_O}{k_m d_{lm}} + \frac{1}{m k_L} \tag{1.1}$$

where k_G is the gas phase mass transfer coefficient (m/s); k_m is the membrane mass transfer coefficient (m/s); k_L is the liquid phase mass transfer coefficient (m/s); d_O is the outer diameter of hollow fiber membrane (m); d_i is the inner diameter of hollow fiber membrane (m); d_{lm} is logarithmic mean diameter (m) and m is the distribution coefficient between gas

and liquid phase (–). The individual mass transfer coefficients, k_G and k_L, are mainly determined by the geometry and flow conditions in the membrane contactor and various correlations are available in the literature to calculate them (Yang and Cussler, 1986; Dindore et al., 2005).

The membrane mass transfer resistance, as an additional resistance, should be taken into account, as it is significantly affected by wetting. Since convection in the membrane pores can be neglected, the mass transfer resistance of the membrane is entirely determined by solute diffusion in membrane pores that are filled with either gas or liquid. In ideal conditions, membrane pores are filled only with gas and the membrane mass transfer resistance of the gas-filled membrane pores can be estimated from (Kreulene and Smolders, 1993):

$$\frac{1}{k_{mg}} = \frac{\delta}{D_O}\frac{\tau}{\varepsilon} \tag{1.2}$$

where k_{mg} is the mass transfer coefficient through the gas-filled pores (m/s), while δ, τ and ε are the membrane thickness (which can also be assumed as the total pore length) (m), tortuosity (-) and porosity (-), respectively.

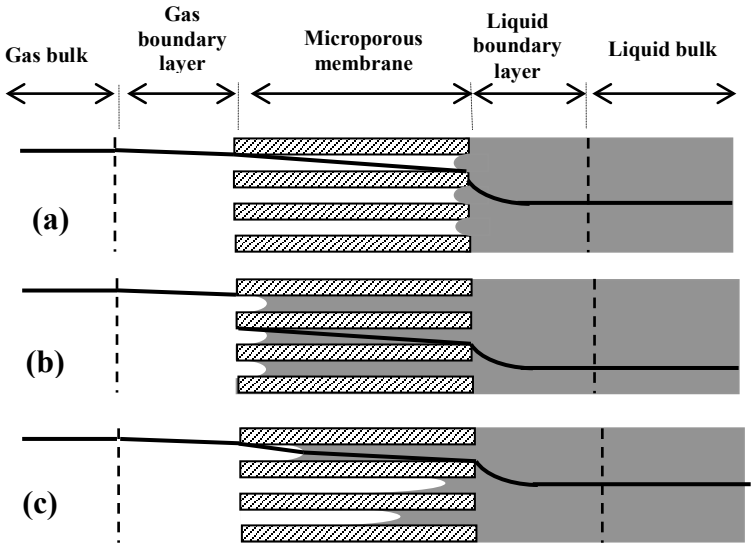

Figure 1.16. Operation modes and corresponding mass transfer resistances in a hydrophobic microporous membrane: (a) non-wetting patterns, (b) overall wetting mode and (c) partial-wetting mode.

D_o is the overall diffusion coefficient through membrane pores and is given by:

$$\frac{1}{D_O} = \frac{1}{D_{ij}} + \frac{1}{D_{kj}} \tag{1.3}$$

where D_{ij} and D_{kj} are diffusion coefficients respectively for molecular and Knudsen diffusion through membrane pores (m^2/s), and can be estimated using membrane and gas properties (Dindore et al., 2004; Mansourizadeh and Ismail, 2009).

However, ideal conditions (gas-filled pores) never happen. In real conditions, membrane pores are partially filled with liquid absorbent. In the worst case, i.e. when membrane pores are thoroughly filled with liquid, Knudsen diffusion can be neglected, owing to the higher density of molecules inside the pores. The membrane mass transfer resistance is then given by (Dindore et al., 2004; Mavroudi et al., 2006):

$$\frac{1}{k_{ml}} = \frac{\delta}{D_L}\frac{\tau}{\varepsilon} \tag{1.4}$$

where k_{ml} is the mass transfer coefficient in liquid filled pores (m/s), D_L is the diffusion coefficient of the solute in the liquid phase. In this case, the solute has to diffuse through the liquid-filled pores, resulting in a very low membrane mass transfer coefficient. Thus, care must be taken to avoid membrane pores filling with the absorbent liquid.

However, in practice, none of the above mentioned conditions (gas-filled and liquid-filled pores) happen in membrane contactors. In real conditions, membrane pores are partially wetted by liquid absorbent and therefore, a parameter must be added in both gas-filled and liquid-filled equations to show the partial penetration of liquid in pores. This parameter is called the wetting ratio (x^*) (Lin et al., 2008; Boributh et al., 2012). For partially wetted pores, the membrane resistance comprises both gas-filled and liquid-filled pores and can be expressed by (Mavroudi et al., 2006):

$$\frac{1}{k_m} = \frac{x^*}{k_{ml}} + \frac{1-x^*}{k_{mg}} \tag{1.5}$$

where the wetting ratio (x^*) is the ratio of pore length wetted with liquid (x) to the overall pore length (δ), as shown schematically in Fig. 1.17.

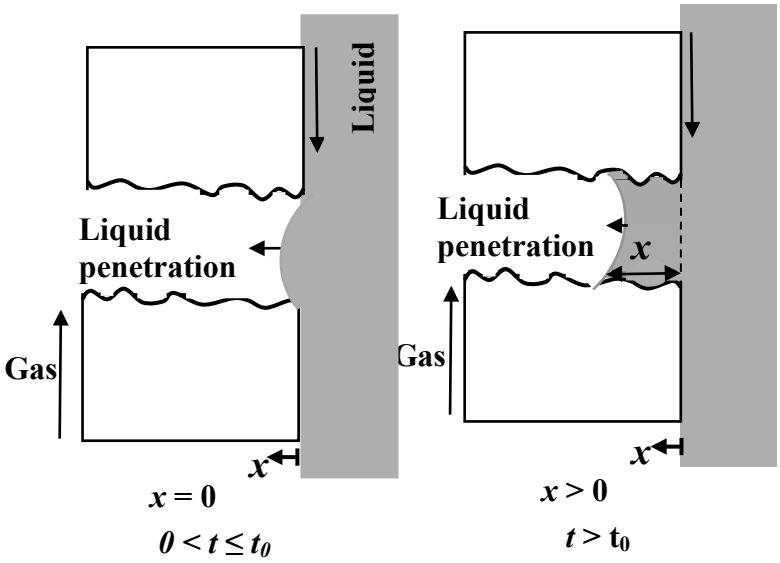

Figure 1.17. Membrane pore partial wetting by liquid.

Different parameters including membrane hydrophobicity, absorbent surface tension and viscosity were reported in the literature to influence the wetting ratio (Li and Chen, 2005; Wang et al., 2005; Mansourizadeh et al., 2009). These parameters are discussed in sections 1.1.7.4 and 1.1.7.5.

1.1.7.3. Wetting characteristics of membranes

Depending on membrane and absorbent properties, as well as operating conditions, three modes of operation including non-wetted, fully wetted and partially wetted conditions can occur in GLMC over prolonged periods of operation. For highly hydrophobic membranes, the non-wetting mode where the membrane pores are completely filled with gas can theoretically occur (Fig. 1.16a). For membranes presenting low hydrophobicity, membrane pores become completely liquid-filled and overall-wetting conditions occur (Fig. 1.16b) (Li and Chen, 2005; Wang et al., 2005; Zhang and Wang, 2005; Mansourizadeh, 2009). As discussed in the previous section, the non-wetting mode of operation is highly preferred, as it leads to minimal diffusion resistance in membrane pores (Dindore et al., 2004; Mavroudi et al., 2006; Rangwala, 1996). However, this condition cannot be achieved in practice. Even for hydrophobic membranes, aqueous solutions of

organic absorbent (especially alkanolamines) can partially penetrate into membrane pores and cause partial wetting (Fig. 1.16c) (Wang et al., 2005; Mansourizadeh et al., 2009). Membrane pores become gradually wetted over prolonged periods of operation and the membrane mass transfer resistance increases rapidly (Malek et al., 1997; Mavroudi et al., 2003; Zhang et al., 2005). Malek et al. (2005) were the first to study the effect of membrane wetting on the performance of a GLMC. It was concluded that partial wetting of the membrane can reduce the overall mass transfer coefficient in the membrane gas absorption process. Furthermore, the reduction of CO_2 capture performance in GLMC as a result of wetting was reported several times in the literature, (Keshavarz et al., 2008; Mansourizadeh et al., 2010; Mansourizadeh and Mousavian, 2013). like for example: (i) an important drop of the overall mass transfer coefficient in the first hours of operation in a GLMC using polypropylene (PP) membranes with monoethanolamine (MEA) absorbent (Falk-Pedersen and Dannström, 1997); (ii) 26% reduction of the absorption flux after 10 h of operation in a PVDF-DEA membrane contactor (Mansourizadeh and Mousavian, 2013).; (iii) reduction of 30% and 23% of the CO_2 absorption flux in the case of physical (water) and chemical (NaOH) absorption, respectively, after 150 hours of operation in a PVDF hollow fiber membrane contactor (Mansourizadeh et al., 2010). In addition, both theoretical and experimental results in the literature show a significant decrease in absorption flux as the result of a small increase in wetting ratio (Keshavarz et al., 2008). However, the rate of such a reduction was reported to be more important for low wetting ratios ($x^* \approx$ 0-1%). This was attributed to the fact that a very fast reduction in flux for such small wetting fractions causes lower CO_2 sequestration from the gas phase: the concentration of CO_2 in the gas phase increased, which increases the overall driving force of the system and slows down the future reduction of the absorption flux.

Various wetting mechanisms have been proposed in the literature (Lu et al., 2008; Lv et al., 2010). For a given membrane material and structure, the degree of partial wetting of membrane pores is quantified by the critical entry pressure (breakthrough pressure), defined as the minimum pressure needed for the liquid to wet the membrane pores. A dry membrane is brought into contact with a liquid and the liquid pressure is gradually increased in order to determine the value at which the liquid penetrates into the pores,

which represents the breakthrough pressure. It can be measured by observing the formation of the first liquid drop on the other side of the membrane (Kumar et al., 2002). For small uniform pores with cylindrical geometry, the breakthrough pressure (ΔP_c) can be determined by the Laplace-Young equation (Kim and Harriot, 1987):

$$\Delta P_c = \frac{2\gamma_L \cos\theta}{r_p} \tag{1.6}$$

where γ_L, θ and r_P represent the surface tension of the liquid (mN/m), the contact angle between the liquid phase and the membrane (°) and the maximum membrane pore radius (m), respectively. However, most membranes do not have cylindrical pores. To account for irregular pore structures, Franken et al. (1987) introduced a geometric pore coefficient *B* in the Laplace-Young equation as:

$$\Delta P_c = -\frac{2B\gamma_L \cos\theta}{r_p} \tag{1.7}$$

where $B = 1$ for cylindrical pores and $0 < B < 1$ for non-cylindrical pores.

Kim and Harriott (1987) studied the critical entry pressure for liquids in hydrophobic membranes with non-cylindrical pores. They assumed a doughnut type pore structure and derived an equation similar to the Laplace-Young equation, in which the contact angle θ was replaced by the effective contact angle θ_{eff}. Using this effective contact angle, the mechanical equilibrium state of a gas-membrane-liquid system can be described as:

$$\gamma_L \cos\theta_{eff} = \gamma_S - \gamma_{SL} \tag{1.8}$$

where γ is the surface tension and the subscripts L, S and SL refer to liquid-vapor, solid-vapor and solid-liquid interfaces, respectively. For polar or hydrogen bonding liquids on non-polar low energy surfaces, it can be assumed that only van der Waals dispersion forces act between the liquid and solid phases. In this case, the interfacial tension between the solid and liquid phase is approximately given by (Bargeman and Van Voorst Vader, 1973; Franken et al., 1987; Dindore et al., 2004):

$$\gamma_{SL} = \gamma_S + \gamma_L - 2\sqrt{\gamma_S{}^d \gamma_L{}^d} \tag{1.9}$$

where γ_S^d and γ_L^d are the dispersion components of the surface tension for solid and liquid, respectively. The term $\sqrt{\gamma_S{}^d \gamma_L{}^d}$ accounts for the dispersion component of the work of adhesion of a liquid to a solid surface. Eqs. (1.6)-(1.9) can be used to relate the liquid critical entry pressure (ΔP_c) to the surface tension terms as:

$$\Delta P_c = \frac{2\left(\gamma_L - 2\sqrt{\gamma_S{}^d \gamma_L{}^d}\right)}{r_p} \tag{1.10}$$

The quantity $\sqrt{\gamma_S{}^d \gamma_L{}^d}$ is constant for low surface tension liquids such as aqueous solutions having high alcohol concentration. When $\sqrt{\gamma_S{}^d \gamma_L{}^d}$ is equal to $\gamma_L / 2$, the numerator of Eq. (1.10) becomes zero and no additional pressure is required for wetting the membrane pores. This value of surface tension is known as the critical surface tension (γ_{CL}). Thus, the critical surface tension is the value of surface tension when critical entry pressure is zero, and can be obtained by the x-axis intercept of the critical entry pressure versus surface tension plot. Any solution, having a surface tension lower than γ_{CL}, will therefore spontaneously wet the membrane surface (Bargeman and Van Voorst Vader, 1973).

In order to prevent wetting in gas-liquid membrane contactors, it is suitable to operate at a pressure lower than the breakthrough pressure. Since membrane wettability is influenced by both membrane and liquid characteristics, these parameters will be further discussed in detail.

1.1.7.4. Effect of the liquid phase characteristics on wetting

The absorbent plays an important role on membrane wetting in long-term operation. The effects of liquid phase characteristics including liquid operating conditions (Lu et al., 2008; Zheng et al., 2005; Boributh et al., 2011; Wang et al., 2004b; Rongwong et al., 2009; Dindore et al., 2005; Zhang et al., 2008; Mansourizadeh et al., 2010; Boributh et al., 2012; Lu et al., 2008), liquid type (Rangwala 1996; Dindore et al., 2004; Ma'mun et al., 2007;

Yan et al., 2007; Zhang et al., 2008; Lu et al., 2008; Portugal et al., 2009; Lin et al., 2009; Bougie and Iliuta 2009; Lu et al., 2010; Bougie and Iliuta, 2010, Bougie and Iliuta, 2010; Chen et al., 2011; Bougie and Iliuta, 2011; Mosadegh-Sedghi et al., 2012a,b) and concentration (Franken et al., 1987; Lu et al., 2008; Rongwong et al., 2009) have been considered in the literature.

1.1.7.4.1. Effect of liquid operating conditions

Liquid phase operating conditions that affect the wetting phenomenon are the absorbent flow rate and pressure. The influence of liquid flow rate on membrane wetting during CO_2 absorption process has been considered by several authors (Mavroudi et al., 2006, Zhang et al., 2008; Boributh, 2012). It was observed that pore wetting becomes much more significant at high liquid flow rates than at low liquid flow rates. For example, an increase in wetting ratio by a factor of approximately 8 was observed by increasing the liquid velocity from 0.1 m/s to 0.4 m/s (Boributh, 2012). This increase in wetting by raising liquid flow rates was reported to be attributed to a reduction in the liquid boundary resistance ($1/k_l$) with increasing liquid flow rate, which increases the contribution of the resistance of the liquid inside the membrane pores (the resistance of the membrane with partially wetted pores, Eq. 1.5) to the overall mass transfer resistance (Zheng et al., 2008). Mavroudi et al. (2006) studied the time variation of overall mass transfer resistance (Fig. 1.18) and absorption flux (Fig. 1.19) in a CO_2-water membrane contactor as a function of liquid flow rate. They observed that the total mass transfer resistance rises rapidly with time, leading to a significant drop in absorption flux during the operation period. However, such deterioration becomes more significant at higher liquid flow rates. This behavior was supposed to be caused by the inevitable increase in liquid pressure as a result of increasing liquid flow rate, which results in higher trans-membrane pressure and consequently, facilitates the liquid intrusion into membrane pores and increases membrane wetting. The liquid penetrates initially into the largest pores of the membrane and, as the trans-membrane pressure increases, smaller pores are then wetted at a lower rate.

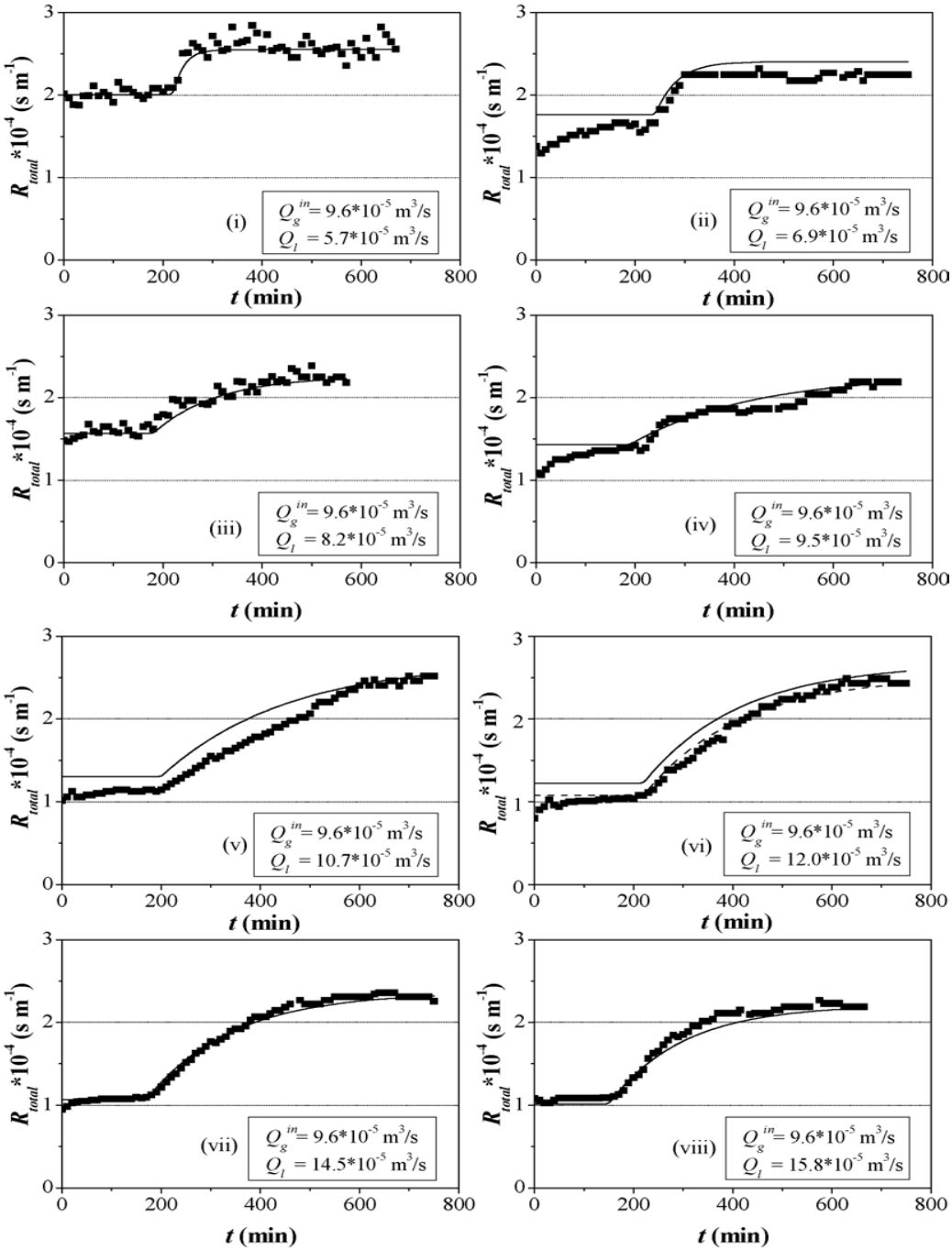

Figure 1.18. Variation of total resistance with time, at constant gas flow rate and different liquid flow for water-PP hollow fiber membrane contactor (–) theoretical, (■) experimental, (- - -) theoretical based on experimental liquid phase resistance at $Q_l = 12.0\times10^{-5}$ m^3/s (Mavroudi, 2006).

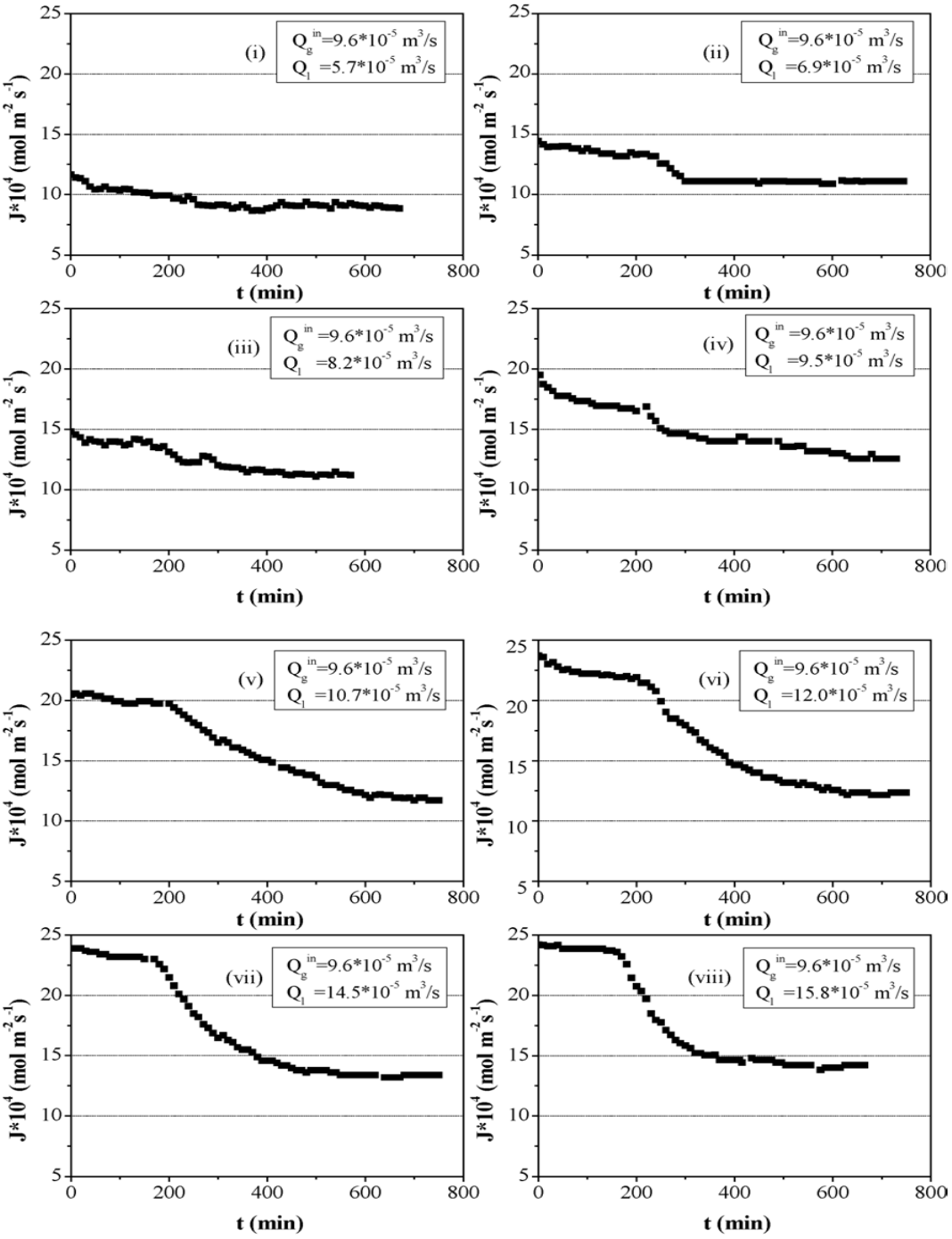

Figure 1.19. Variation of absorption flux with time, at constant gas flow rate and different liquid flow rates: (Mavroudi, 2006).

In addition to the flow rate, liquid side operating pressures can influence pore wetting and membrane phase mass transfer resistance (Lu et al., 2008; Zheng et al., 2005;

Boributh et al., 2011; Wang et al., 2004b). It is accepted that even fully-wetted condition can be transformed to partially wetted mode (or to non-wetted mode, in case of highly hydrophobic membranes) by reducing the liquid phase pressure below the critical entry pressure (Zheng et al., 2005). It was reported several times in the literature that the wetting ratio increases as the absorbent pressure rises (Boributh et al., 2011; Wang et al., 2004b, Rongwong et al., 2009). Lu et al. (2008) specified that, since the gas side operating pressure is constant, the increase in liquid inlet pressures would lead to an increase in trans-membrane pressures. Therefore, pore wetness increased in terms of the Laplace equation (Eq. 1.6), resulting in a deterioration in absorption flux.

1.1.7.4.2. Effect of absorbent type

For a given membrane material and operation conditions, the absorbent properties, including surface tension and viscosity, are the controlling parameters in membrane wetting. As indicated in Eq. 1.6, liquids with higher surface tensions have relatively little wetting potential in comparison to those with lower surface tensions. It was observed that when liquid surface tension decreased from about 33 mN/m to 30 mN/m, the potential of membrane wetting increased rapidly (Dindore et al., 2004). Commonly used absorbents for CO_2 capture are aqueous solutions of alkanolamines, which are weak bases which can react with CO_2 to form complexes having weak chemical bonds. These chemical bonds are easily broken upon mild heating, leading to absorbent regeneration. However, it has been reported that aqueous solutions of single (Rangwala, 1996; Dindore et al., 2004; Wang et al., 2004a; Zhang et al., 2008) and mixed (Rongwong et al., 2009) alkanolamine solutions have high wetting potential since their surface tensions are lower than that of water (Table 1.3). For example, the wetting potential of absorbents including MEA, DEA, MDEA (methyl diethanolamine) and DMEA (dimethylethanolamine) were investigated via measuring their surface tensions (Kumar et al., 2002). It was observed that from primary to tertiary amines, the surface tension of absorbents progressively decreases. Among tertiary amines, the surface tension of aqueous MDEA solution is higher than that of aqueous DMEA solution, due to the presence of an additional polar OH group in MDEA. The lower the surface tension of the solution, the lower is its contact angle with the membrane surface. This

indicates that solutions with lower surface tensions have a higher tendency to wet membranes (Dindore et al., 2004; Li and Chen, 2005; Lin et al., 2008).

On the other hand, absorbents with lower viscosity can penetrate more easily into membrane pores (Lin et al., 2008). Therefore, the wetting potential of an absorbent arises from the simultaneous effect of its surface tension and viscosity. The influence of different types of amine solutions used as liquid absorbent on CO_2 long-term absorption flux was investigated using 1 mol/l aqueous solutions of MEA, DEA, and AMP (2-amino-2-methyl-1-propanol) and water (for comparison) during 12 days of operation in GLMC (Rongwong et al., 2009). It was found that when pure water was used as absorbent, the CO_2 flux remained almost constant during the entire operating period. However, the CO_2 absorption flux continuously declined for amine solutions (Fig. 1.20).

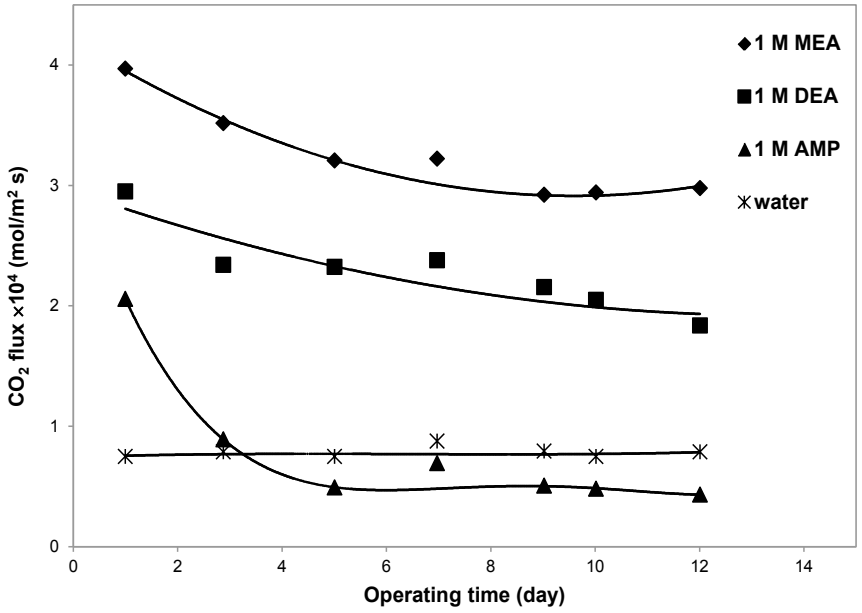

Figure 1.20. Effects of various types of amine solutions on long-term performance of membrane contacting process (Rongwong et al., 2009).

It was observed that the reduction in the absorption flux varied in the following order: DEA > AMP > MEA. This behavior was explained on the basis of the combined effect of absorbent surface tension and viscosity (Table 1.3).

Table 1.3. Properties of single and mixed CO_2 amine absorbents and contact angle corresponding to PVDF membranes at 20ºC (Kumar et al., 2002).

Absorbent	Surface tension (mN/m)	Viscosity (mPa.s)	Contact angle (º)
Water	71.0	0.91	91.8
MEA 0.25 mol/l	64.3	0.95	-
MEA 0.5 mol/l	64.0	1.00	91.3
MEA 1 mol/l	61.5	1.11	90.1
MEA 0.1 mol/l	70.6	0.92	91.5
DEA 1 mol/l	59.1	1.22	87.9
AMP 1 mol/l	58.8	1.42	86.9
MEA 0.25 mol/l + AMP 0.25 mol/l	61.0	1.05	87.6
MEA 0.25 mol/l + DEA 0.25 mol/l	62.0	1.04	89.6
DEA 0.25 mol/l + AMP 0.25 mol/l	58.3	1.11	85.2

The decrease in CO_2 flux for MEA was the lowest, since it has the highest surface tension among the studied amine solutions. However, the reduction of CO_2 flux for DEA was higher than that for AMP. Nevertheless, the measured surface tension and contact angle of AMP were slightly lower than DEA. The result may be explained by the viscosity effect. The viscosity of 1 mol/l AMP is about 0.2 mPa·s higher than that of 1 mol/l DEA and therefore, it is more difficult for AMP to penetrate into the membrane pores, leading to less membrane wetting. Aiming to reduce membrane wetting problems encountered by the use of alkanolamine solutions, the challenge is to propose alternative absorbents with lower wetting tendency. Several reports introduced amino acid salts as good alternatives to alkanolamines (Kumar et al., 2002; Ma'mun et al., 2007; Lu et al., 2008; Portugal et al., 2009; Lu et al., 2010). The investigations show that the breakthrough pressure of aqueous amino acid salt solutions are about 2-6 kPa higher than that of water and unlike aqueous alkanolamines solutions, the surface tension and consequently the breakthrough pressure increase with increasing salt concentration (Kumar et al., 2002). A pilot-scale hollow fiber membrane contactor including PP membranes in contact with potassium glycinate (PG) absorbent successfully operated over 40 h, while maintaining a CO_2 removal efficiency of

about 80% in this period (Fig. 1.21) (Yan et al., 2007). In addition, it was observed that PG acted as an inactive substance and the surface tension of aqueous PG solution increases with PG concentration, decreasing therefore the wetting tendency.

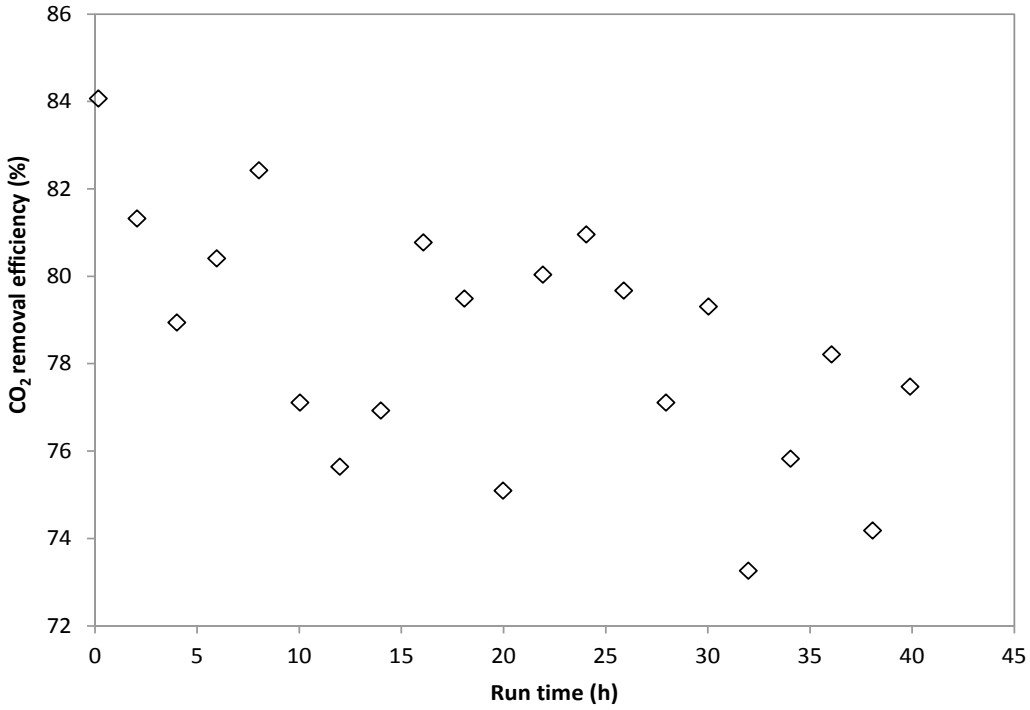

Figure 1.21. Long-term performance of the PP hollow fiber membrane contactor over 40 h at ambient temperature using PG as CO_2 absorbent (Yan et al., 2007).

Mixed piperazine (PZ)/amine absorbents have also been considered as alternatives to pure alkanolamine solutions (Lin et al., 2009a; Lin et al., 2009b; Chen et al., 2011; Bougie and Iliuta, 2009; Bougie and Iliuta, 2010; Bougie and Iliuta, 2010; Bougie and Iliuta, 2011; Mosadegh-Sedghi et al., 2012a). It was found that increasing PZ concentration, in mixed AMP/PZ absorbent, increases absorbent viscosity, leading to a decrease in membrane wetting ratio (Lin et al., 2009a). Besides the influence of viscosity, the reduced wetting potential of PZ containing absorbents arised from the fact that in this case, PZ acts as a surface inactive substance, increasing therefore the solution mixture surface tension and inhibiting pore intrusion by the liquid meniscus (Mosadegh-Sedghi et al., 2012a).

The mixed aqueous absorbent containing MEA and triethanolamine (TEA) was reported by Yeon et al. (2005) as another alternative to single alkanolamine solutions. In addition to the high absorption efficiency, the use of this mixed solution in a PVDF hollow fiber membrane contactor showed stable absorption flux during 80 hours of operation.

1.1.7.4.3. Effect of absorbent concentration

In addition to the absorbent type, membrane wettability is also influenced by absorbent concentration (Franken et al., 1987; Lin et al., 2008; Lu et al., 2008; Rongwong et al, 2009; Boributh et al., 2012). Depending on the absorbent type, the increase in absorbent concentration can either raise or reduce the surface tension of the absorbent solution, resulting in changes in the absorbent wetting potential. If the absorbent contains organic compounds, its surface tension drops rapidly with increasing concentration of the organic compound, leading to enhanced membrane wetting (Franken et al., 1987). Moreover, when the concentration of the organic compound exceeds a critical value, the contact angle between membrane and absorbent decreases below 90°. Consequently, the liquid will wet the membrane surface and penetrate into the pores. The concentration of the organic component at which this occurs is called the "maximum allowable concentration" (MAC) and can be determined by the penetration drop method. At this concentration, the liquid surface tension is equal to its critical surface tension γ_{CL} and the breakthrough pressure equals zero (Franken et al., 1987).

Rongwong et al. (2009) studied the effect of MEA concentration on CO_2 flux during 12 days of operation using PVDF hollow fiber membranes. It was found that the decline in CO_2 flux increased with increasing MEA concentration. The CO_2 flux continuously decreased when using MEA aqueous solution of 0.25, 0.5, and 1 mol/l, by about 19, 23, and 26% of the initial flux, respectively. This reflects the increase in membrane mass transfer resistance due to membrane wetting (Fig. 1.22).

The absorbent/membrane contact angle and absorbent surface tension decreases with increasing MEA concentration (Table 1.3). Lu et al. (2008) also reported that membrane wetting was higher for 1 M MEA than for 0.5 M MEA. Boributh et al. (2012) estimated the wetting ratio as a function of absorbent concentration and velocity. The

wetting ratio increases with liquid velocity as well as with MEA concentration (Fig. 1.23). The increase in MEA concentration leads to a significant reduction in solution surface tension and can increase membrane wetting.

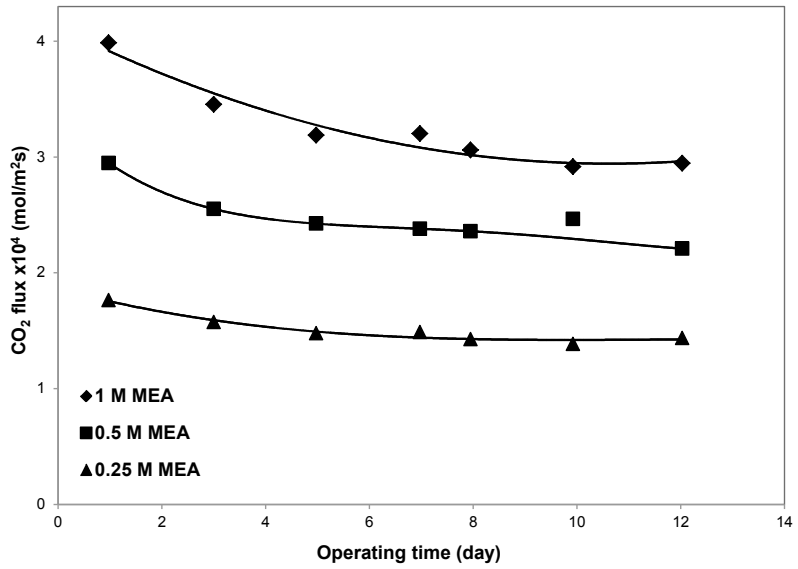

Figure 1.22. Effect of MEA concentration on long-performance of the membrane contacting process (Rongwong et al., 2009).

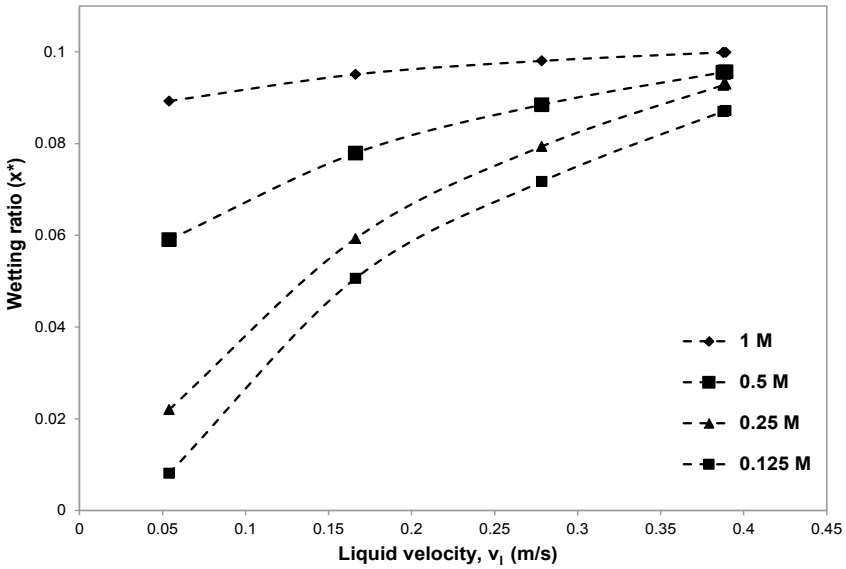

Figure 1.23. Simulation results of the effect of liquid velocity and MEA concentration on wetting ratio of PTFE hollow fiber membrane (Boributh, 2012).

1.1.7.5. Effect of membrane characteristics on wetting

For a given absorbent, the wetting tendency of a membrane is influenced by membrane characteristics, including chemical properties of the membrane surface (membrane surface energy) and membrane structure (pore size and porosity). Generally, membranes having lower surface energies have less wettability than those having higher surface energies. Membrane surface energy is closely associated with its surface hydrophobicity. The level of surface hydrophobicity can be predicted via the contact angle formed by a liquid drop on the membrane surface. An angle greater than 90° indicates that the liquid tends to shrink away from the solid surface and exhibits non-wetting tendencies. On the contrary, an angle smaller than 90° corresponds to a high membrane wettability.

In addition to surface hydrophobicity, membrane wettability is influenced by pore size and porosity. As indicated by Eq. 1-6, critical entry pressures for membranes with smaller pores are higher than those for membranes with larger pores. Several reports in the literature indicate that pore wetting occurs more easily in membranes with bigger pore sizes and high porosities (Malek et al., 1997; Keshavarz et al., 2008; Zheng et al., 2008; Mansourizadeh et al., 2012). However, in order to characterize the wettability of a membrane, surface pore size, porosity and hydrophobicity must be taken into account.

One can assume a membrane with ultra-hydrophobic properties, while it can be subjected to the pore intrusion by absorbents at low liquid pressures. For example, based on contact angle measurements, Khaisiri et al. (2009) reported the following order of membrane wettability: PTFE > PP > PVDF, while, based on the breakthrough pressure measurements, Yeon et al. (2003) reported that PVDF membranes have higher wetting resistance compared to PTFE membranes. On the other hand, some reports indicated that PVDF membranes are wetted after several hours of operation in membrane contactors (Zhang et al., 2008; Atchariyawut et al., 2009, Chen et al., 2009). These contradictory results can be seen in Table 1.4.

Recently, Rahbari-Sisakht (2012) analyzed two kinds of PVDF membranes, fabricated (i) using pure PVDF and (ii) via the addition of a surface modifying macromolecule (SMM) to the PVDF during extrusion. During the phase inversion, SMM migrates to the membrane surface and acts as both a pore former and surface modifier to

increase membrane surface hydrophobicity. The authors observed that in comparison to pure PVDF membrane, the PVDF/SMM membrane shows higher contact angle, but lower critical entry pressure due to its larger pore diameters. However, during 150 h operation in a CO_2-water membrane contactor, the PVDF/SMM membranes were reported to have much higher wetting resistances than those of pure PVDF.

In case of a definite absorbent, unlike the contact angle, which is affected only by membrane surface properties, membrane breakthrough pressure is also influenced by bulk properties (Kumar et al., 2002). Therefore, in order to have a good understanding of membrane wettability, a comprehensive study comprising contact angle and breakthrough measurements, as well as long-term operation in membrane contactors, should be performed.

Table 1.4. Wettability of commonly used membranes.

Membrane	Absorbent	Operation time[1]	Wettability[2]	Reference
PTFE	MEA	6600 h	-	Nishikawa et al., 1995
	AMP	-	-	Kim and Yang, 2000
	MEA	-	-	
	MDEA	-	-	
	NaOH	-	-	Matsumoto et al., 1995
	MEA	-	-	
	MEA	>7 days	-	Falk-Pedersen and Dannström , 1997
	MEA/AMP/PZ	60 h	-	Chen et al., 2011
	MEA	40 h	-	deMontigny et al.,
	MEA	-	+	Marzouk et al., 2012
	DEA	-	+	
	DETA	-	+	
PP	NaOH	-	+	Rangwala, 1999
	DEA	-	+	

Table 1.4. Wettability of commonly used membranes (Continued).

Membrane	Absorbent	Operation time[1]	Wettability[2]	Reference
	MEA	-	+	
	DEA	-	+	Kumar et al., 2002
	MDEA	-	+	
	Activated amino acid salts	-	-	
	NaOH	-	+	Matsumoto et al.,
	MEA	-	+	
	Activated amino acid salts	40 h	-	Yan et al., 2007
	MEA	A few hours	+	Falk Pedersen and Dannström , 1997
	Propylene carbonate	-	+	Dindore et al., 2004
	Water	-	-	
	Water	-	+	Zhang et al., 2008
	DEA	-	+	
	Activated amino acid salts	-	-	Lu et al., 2009
	MEA	-	+	Lv et al., 2010
	MDEA	-	+	
	MEA	40 h	+	deMontigny et al., 2006
	MEA	6600 h	+	Nishikawa et al., 1995
	PE+F	NaOH	-	-
		MEA	-	-
	PP+F	Alkanolamine/PZ	30 days	-
	PE+F	NaOH	-	-

Table 1.4. Wettability of commonly used membranes (Continued).

	Absorbent	Operation time[1]	Wettability[2]	Reference
PVDF	Water	40 h	+	Zhang et al., 2008
	DEA	40 h	+	
	Water	-	-	Dindore et al., 2004
	AMP	-	+	Lin et al., 2008
	AMP/PZ	-	+	
	MDEA	-	+	
	MDEA/PZ	-	+	
	MEA	12 days	+	Rongwong et al., 2009
	MEA/SG	-	-	
	MEA/NaCl	-	-	
PP/PDMS	MEA	6 days	+	Falk-Pedersen and Dannström , 1997
PFA	MEA	-	-	Marzouk et al., 2012
	DEA	-	-	
	DETA	-	-	

[1] either the operating time was not indicated, or the absorption operation was not performed; [2] + : wetted, - : non-wetted;

In addition, in order to compare the wettability of different membranes, only one parameter should be modified at a time; i.e. either membranes with the same structure (pore size and porosity) and different level of hydrophobicity, or membranes with the same hydrophobicity and different structures should be studied. Such systematic studies have not been reported in the literature yet.

1.1.7.6. Membrane stability and its effect on wetting

Long-term deterioration in membrane stability can strongly affect their performance and efficiency, mainly due to morphological and chemical changes on the membrane

surface that can affect membranes wettability. Reduction in membrane stability, which can be either morphological or chemical, has been reported in several investigations.

1.1.7.6.1. Morphological changes

Membrane morphological changes were first reported by Kamo et al. (1992). PP hollow fiber membranes were immersed for 30 min in different liquids and then characterized in terms of their pore shape and porosity. SEM micrographs before and after the solvent treatment showed that the slit-like pores apparently changed to an elliptical shape by this treatment and consequently, the width between the adjacent microfibrils expanded and the pore size enlarged. It was mentioned that the solvent forms a liquid bridge between two microfibrils during the evaporation process and makes the pore enlargement irreversible. Similar morphological changes were reported by Barbe et al. (2000). The authors reported surface morphological changes of microporous polypropylene (PP) membranes after 72 h contact with water. The results showed an increase in the size of larger pores and a decrease in the size of the smaller ones. The authors suggested that this behavior can be attributed to the effect of pore intrusion by the liquid meniscus. In the case of large pores, the fibrils that link the crystalline lamellae and form boundaries between pores are forced apart as the result of water intrusion below the membrane surface. This pushes away the fibrils at the boundary of small pores, causing smaller pores to decrease in size, while larger ones increase. In addition, it was reported that PP membrane surface morphologies suffered from significant changes when fibers were immersed in MEA solution (Lv et al., 2010). Some slit-like membrane pores in the fresh sample (blank PP membrane) shrank longitudinally and became elliptical or even circular (Fig. 1.24). The calculated equivalent diameter distribution of membrane pores showed that, with an increase in immersion time, the distribution profile flattens and moves towards the larger pore side. The same observation was recently reported in the case of PP hollow fiber membranes used for stripping CO_2 from MEA via a vacuum regeneration process (Fang et al., 2012). After 480 h operation, it was observed that some slit-like pores shrank longitudinally and became elliptical after long term running. The pore equivalent diameter

shifted from 0.082 μm for fresh membranes to 0.105 μm after 480 h use in CO_2 stripping in the GLMC.

There are several reports in the literature showing that morphological changes strongly depend on liquid surface tension and become more significant with the decrease in liquid surface tension. Barbe et al. (2000) observed no morphological change for PP membranes after 72 h contact with 30 wt% $CaCl_2$ solution whose surface tension is higher than that of water. In addition, it was reported that when PP membranes are immersed in 30 wt% DEA solutions with 4 wt% CO_2 loading, pore deformation becomes less significant as compared to PP membranes immersed in 30 wt% DEA solutions without CO_2 loading. Since the surface tension of a 30 wt% DEA solution with 4 wt% CO_2 loading is higher (65.6 mN/m) than that of a 30 wt% DEA solution (63.7 mN/m), the loaded amine solution tends to spread less on the material surface as compared to the corresponding pure amine aqueous solution (Wang et al., 2004). Mosadegh-Sedghi et al. (2012) studied the morphological degradation of low density polyethylene (LDPE) hollow fibers in contact with different amine solutions including 30 wt% MEA, 11 wt% 2-amino-2-hydroxymethyl-1,3- propanediol (AHPD), 25 wt% MEA + 5 wt% PZ and 10.11 wt% AHPD + 0.89 wt% PZ. They reported that the structural stability of membrane pores (morphological stability) is strongly associated with the surface tension of the contact solution (absorbent). Solutions with lower surface tension can penetrate more easily into the pores. Therefore, pore enlargement became more significant after 30 days immersion in 30 wt% MEA, which had the lowest surface tension among the studied solutions (64 mN/m), and pore enlargement was less significant after 30 days immersion in the AHPD + PZ solution which had the highest surface tension (72 mN/m).

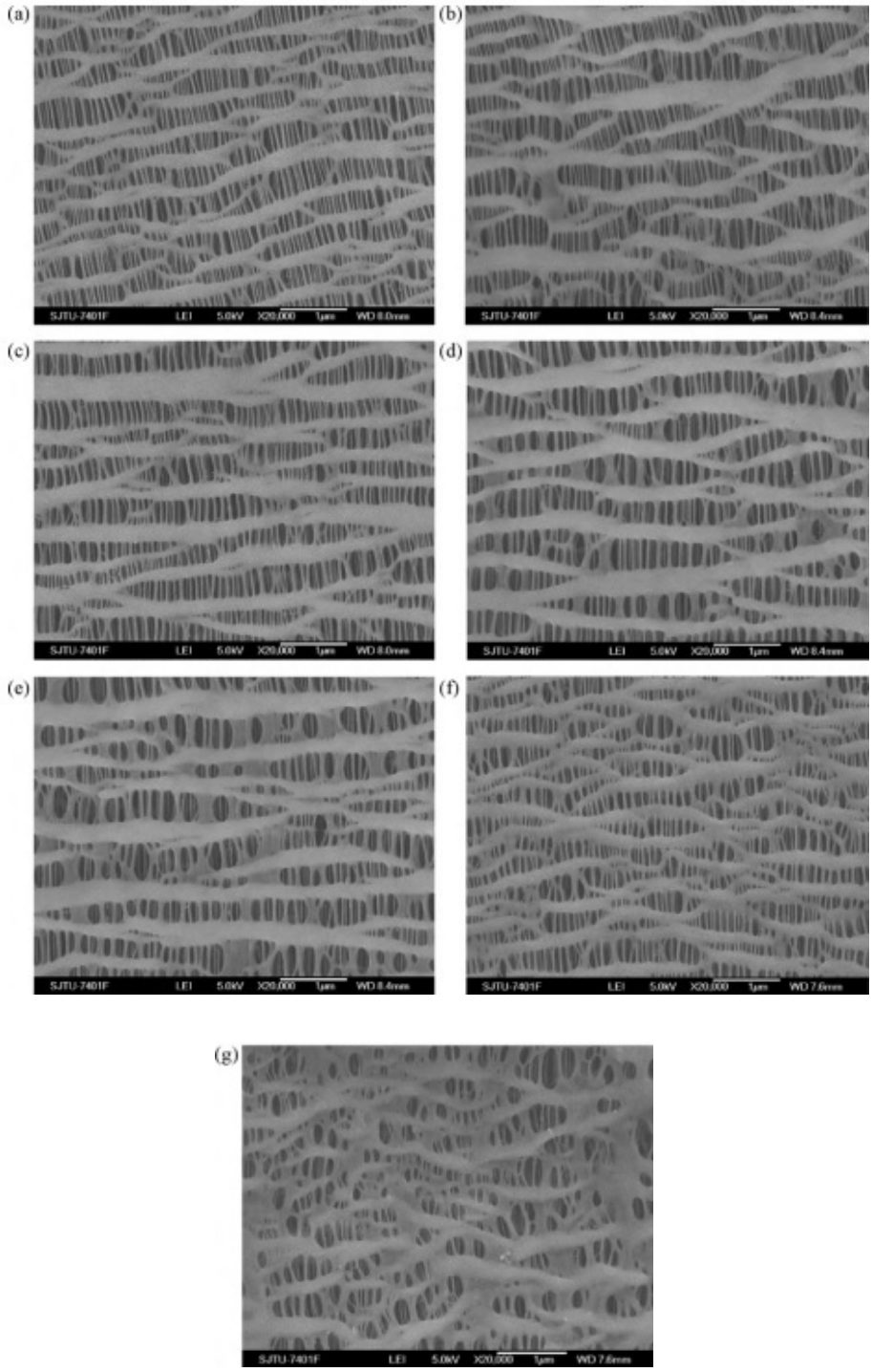

Figure 1.24. Field emission scanning electron micrographs (magnification: 20,000) for: (a) non-immersed PP fibers, PP fibers immersed in (b) 30 wt% MEA for 10 days, (c) 30 wt% MEA for 30 days, (d) 30 wt% MEA for 60 days, (e) 30 wt% MEA for 90 days, (f) deionized water for 60 days, and (g) 30 wt% MDEA for 60 days (Lv et al., 2010).

Morphological degradation of membranes, attributed to membrane pore enlargement, can affect the membrane wettability. According to Eq. 1.6, the increase in membrane pore size leads to a decrease in membrane breakthrough pressure, which results in an increase in membrane wetting tendency. The effect of immersion time of PP hollow fiber membrane in MEA solution on the membrane breakthrough pressure was investigated by Lv et al. (2010). For PP fibers immersed in 30 wt% MEA at different immersion times, the increase in immersion time from 0 to 90 days led to an increase in pore diameter and a decrease in breakthrough pressure (Fig. 1.25). For example, for a pore diameter of 0.1 μm, the breakthrough pressure decreased from 2500 kPa to around 125 kPa after 90 days immersion in 30 wt% MEA. A PP hollow fiber GLMC is therefore expected to be wetted during the CO_2 capture process due to the dramatic decrease in membrane breakthrough pressure. Kamo et al. (1992) also reported a decrease in breakthrough pressure of PE hollow fiber membranes after 30 min immersion in several liquids. The breakthrough pressure was reduced from 216 kPa (before immersion) to 186 kPa, 156 kPa and 137 kPa, respectively, after immersion in ethyl alcohol, p-xylene and dimethylformamide (DMF). This reduction in breakthrough pressure was attributed to membrane pore enlargement.

1.1.7.6.2. Chemical changes

In addition to morphological changes, some chemical changes also occur on the membrane surface due to oxidative degradation of membrane material or chemical reactions of membrane material with alkanolamine solutions. Franco et al. (2008) reported the possibility of oxidation of PP hollow fiber membranes after 68 h use in CO_2 absorption process in the presence of 20 wt% MEA solution as the chemical absorbent. X–ray photoelectron spectroscopy (XPS) analysis of the inside surface of both fresh and used PP hollow fibers showed an increase in elemental oxygen on the surface from 0.78 to 1.49%, which was proposed to be related to the oxidation of the PP membrane (Table 1.5).

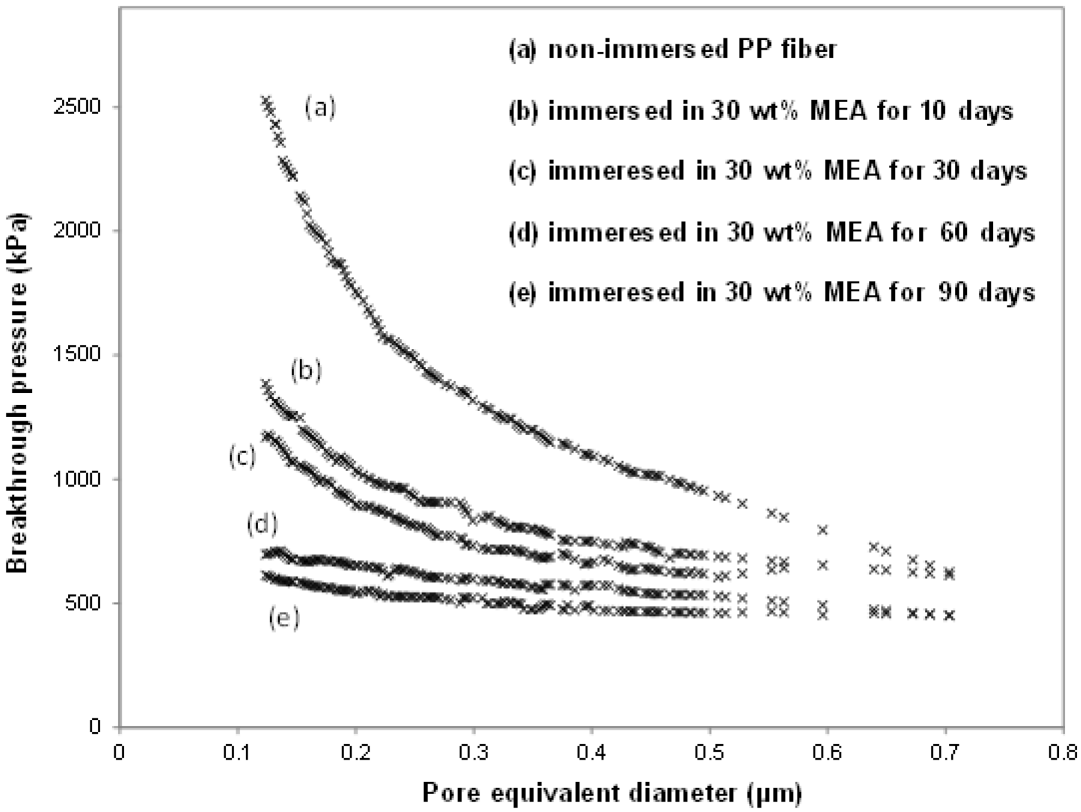

Figure 1.25. Breakthrough pressures of PP membranes as a function of pore equivalent diameter for fibers immersed in 30 wt% MEA for different periods (Lv et al., 2010).

Table 1.5. XPS results for surface elemental composition of PP hollow fiber membranes (Franco et al., 2008).

Atom	PP	PP-used[1]
O	0.78	1.49
C	99.22	98.51

[1]PP subjected to CO_2 absorption experiments with 20 wt% MEA solution for 68 hours

Massey et al. (2007) reported that the oxidative degradation of polyolefins was promoted in the presence of water. The mechanism proposed for this hydrolytic degradation involves the formation of alcohol (C-OH) and ketone (C=O) functions (Fig. 1.26). The authors observed that such degradation was slightly slowed down by adding to the polymer a small amount (4 wt%) of hindered amine light stabilizers (HALS).

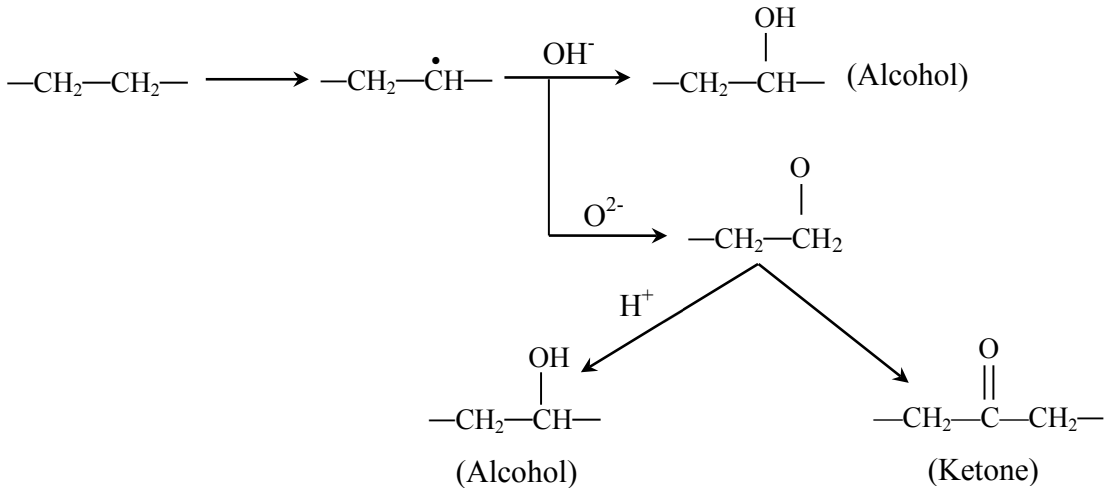

Figure 1.26. Proposed mechanisms for the hydrolytic degradation of LDPE (Massey et al., 2007).

The origin of the above mentioned chemical degradations lies in the auto-oxidation of membrane material. Polyolefins, like PP and PE, can undergo auto-oxidation through the following pathway (Rychly et al., 1997).

$$2PEOOH \longrightarrow PE^{\bullet} + PEOO^{\bullet} + \alpha V \quad (1.11)$$

$$PEOO^{\bullet} + PE \rightarrow PEOOH + PE^{\bullet} \quad (1.12)$$

$$PE^{\bullet} + O_2 \rightarrow PEOO^{\bullet} \quad (1.13)$$

$$2PEOO^{\bullet} \rightarrow ketones, acids, aldehydes \quad (1.14)$$

where $PEOOH$, $PEOO^{\bullet}$ and $PE^{\bullet}$ represent, polyethylene hydroperoxide, polyethylene peroxy radical, and polyethylene alkyl radical, respectively. α and V represent, respectively, the number and type of volatile species generated by $PEOOH$ decomposition. Carbonyl group (C=O) containing products (aldehydes, ketones and carboxylic acids) are formed during termination reactions (Eq. 1.14). Auto-oxidation of polyolefins occurs in the presence of air where oxygen exists in abundance and accelerates in the presence of water (Massey et al., 2007) and basic media (Mosadegh-Sedghi et al., 2012).

Another possible cause for membrane surface property changes is a chemical reaction between polymeric membranes and amines, as suggested by Wang et al. (2004). The generation of new peaks possibly related to C-N bonds (XPS spectrum), observed after

a 10 days contact of the PP membrane with a DEA solution showed possible chemical interactions between the membrane and the alkanolamine solution. Based on XPS analysis, the formation of such new peaks was also reported for a 10 day contact between PP membranes and MEA solutions (Lv et al., 2010). In addition, Mosadegh Sedghi et al. (2011,2012) performed a comprehensive investigation on chemical alteration of low density polyethylene (LDPE) hollow fibers in contact with MEA and 2-amino-2-hydroxymethyl-1,3-propanediol (AHPD) solutions by combining FT-IR spectroscopy, XPS analysis, surface tension and contact angle measurements. A two-step mechanism of membrane chemical degradation was proposed, comprising the auto-oxidation of polyethylene (PE) material in aqueous solution of amines which generated carbonyl groups (C=O), followed by the interaction between PE and amines which led to the formation of amide groups (Mosadegh-Sedghi et al., 2011). Such degradation was shown to be hindered to a great extent by the addition of PZ in amine solutions, due to the steric hindrance effect of PZ (Mosadegh-Sedghi et al., 2012).

Despite the crucial role of membrane chemical stability on its wetting tendency, very few investigations have been performed on this subject. Both types of membrane chemical alteration (oxidative degradation and chemical reaction between membrane material and amines) result in the formation of hydrophilic C-O, C=O or C-N containing products, including alcohols, aldehydes, ketones and amides, which cover the membrane surface and therefore influence its wettability. Contact angle measurements were carried out for PP membranes immersed in water, 30 wt% MEA and 30 wt% MDEA solutions for periods up to 90 days (Lv et al., 2010). At the end of the immersion period, fibers were rinsed several times with deionized water and dried in vacuum at 70 °C for 10 h to completely remove the remaining amine solution on the fiber surface. It was observed that the contact angle significantly decreased during this period. A 25% decrease (from 121.6^{o} to 90.8^{o}) for PP immersed in 30 wt% MDEA for 60 days indicated that the membrane surface hydrophobicity was significantly reduced due to the immersion in an alkanolamine solution. Further increase in the immersion time to 90 days resulted in a smaller decrease in contact angle (about 0.7%). Mosadegh-Sedghi et al. (2012) also reported that the contact angle of PE hollow fiber membranes decreased from 128.4° to 112.2° for a 30 day

immersion in 30 wt% MEA and to 118.6° for a 30 day immersion in 10.11 wt% AHPD solution. However, the addition of 5 wt% PZ in the same amine solutions led to a smaller decrease in contact angle to values of 116.5° and 121.4°, respectively. The smaller decrease in contact angle after the addition of 5 wt% PZ to 30 wt% MEA and 0.89 wt% to 11 wt% AHPD was attributed to the role of PZ as a surface inactive substance (it increases the surface tension of MEA and AHPD solutions). PZ-containing amine solutions therefore seem to be good alternatives to single amine solutions as absorbents in GLMC, due to their effect in reduction of membrane wettability.

1.1.7.7. Wetting prevention

In order to avoid membrane wetting, different methods have been suggested in the literature including: i) effective selection of membrane-absorbent, ii) optimization of operation conditions, iii) use of composites, iv) selection of asymmetric membranes, and v) surface modification of membranes.

1.1.7.7.1. Membrane/absorbent compatibility

Compatibility between the membrane type (material) and the liquid absorbent in membrane contactors is an effective parameter in wettability determination. Generally, compatibility depends on absorbent surface tension as well as membrane surface energy (Dindore et al., 2004; Bougie and Iliuta, 2013). Liquids with lower surface tension have greater tendency to wet the surface, while membranes with higher surface energy are more vulnerable to wetting. Molecular structure and composition have been found to strongly influence the liquid surface tension. As example, AHPD, a sterically hindered alkanolamine with 4 hydrophilic groups and a carbon number of 4, has remarkably higher surface tension, compared with alkanolamines and seems, therefore, an appropriate absorbents to be used in GLMC (Bougie and Iliuta, 2013). Wettability of commonly used membranes with different liquid absorbents is summarized in Table 1.4. The only membrane material which was recently reported to be more hydrophobic than PTFE is PFA (poly(tetrafluoroethylene-co-perfluorinated alkyl vinyl ether)) (Marzouk et al., 2012). Except for PFA, it can be seen that polytetrafluoroethylene (PTFE) is the most resistant material to wetting by different aqueous solutions, owing to its relatively low surface

energy (17-22 mN/m) (Fu et al., 2004; Shojaie and Gholamalipour, 2011) and thus, it has been extensively used in GLMC systems. However, several important drawbacks (Lee et al., 2004; deMontigny et al., 2006; Khaisiri et al., 2009) including: i) complicated and high cost of fabrication, ii) environmentally malignant method of fabrication, and iii) small specific interfacial area leading to a reduction in absorption efficiency and iv) non recyclability, limit large scale use of PTFE materials. Table 1.6 presents the characteristics (pore size and porosity) and price for commercial PTFE in comparison to commercial PP and PVDF (hollow fiber membranes). The price of commercial PTFE hollow fiber membranes are about 100-200 times higher than that of PP. In addition, PP hollow fiber membranes provide higher surface area (deMontigny et al., 2006; Khaisiri et al., 2011). Therefore, polyolefin based membranes represent a good alternative to PTFE.

Table 1.6. General properties of some types of commercial PP, PVDF and PTFE hollow fiber membranes.

Description	**PP**	**PVDF**	**PTFE**	Reference
Max. available pore size (µm)	0.25	0.03	1.0	Lee et al., 2004
Max. void fraction (%)	75.2	82.2	70.1	Khaisiri et al., 2009
	82.2	-	59.2	deMontigny et al., 2006
Max. specific area (m^2/m^3)	2855	1488	1340	Lee et al., 2004
	2752	-	429	deMontigny et al., 2006
Cost (US $/m)	0.01	-	23	deMontigny et al., 2006
	0.01	0.36	11.5	Khaisiri et al., 2009

However, as indicated in Table 1.4, they have large wettability and are wetted by alkanolamine solutions in short term operation. Also, laminated membranes combining two layers, one representing a typical porous membrane and the other being made of microfibers used as support to stiffen the whole assembly to offer a better mechanical resistance, can be another interesting alternative (Bougie and Iliuta, 2013). This can be attributed to the fact that the lamination process seems to increase surface roughness, leading to higher contact values. Moreover, the fabrication of laminated membranes, like PP/PTFE, requires less amount of PTFE, which can reduces the cost (Bougie and Iliuta, 2010; Bougie and Iliuta, 2013).

1.1.7.7.2. Optimizing operating conditions

Operating conditions such as temperature and pressure can affect the wettability of membranes in membrane contactors. As liquid surface tension decreases with increasing temperature (Bougie and Iliuta, 2013), operating temperature should not exceed a certain value, so that absorbent surface tension remains above the critical value. This critical surface tension can be determined by a Zisman Plot (Fox and Zisman, 2006). For a specific membrane this value is equivalent to the surface energy of the membrane. The Zisman plot for a low density polyethylene film is shown in Fig. 1.27. Only few investigations have been reported for the effect of operating temperature on membrane wetting (Malek et al., 1997; Garcia-Payo, 2000; Lu et al., 2008). Lu et al. (Lu et al., 2008) reported a reduction of total mass transfer to about 59% with increasing operating temperature from 288 K to 308 K This was attributed to the alteration of both membrane and absorbent physical properties (absorbent viscosity, absorbent surface tension, membrane surface energy and membrane-absorbent contact angle) by temperature.

On the other hand, liquid side operating pressure plays a crucial role in long-term absorption performance. The operating pressure of the liquid phase should be higher than that of the gas phase in order to prevent bubble formation, which can result in significant loss of valuable gas components and reduction in absorption efficiency (Kreulen and Smolders, 1993). However, high liquid pressure can gradually cause liquid penetration into

membrane pores, which leads to partial wetting of the membrane. It is therefore advisable to work at pressures lower than the breakthrough pressure (Dindore et al., 2004).

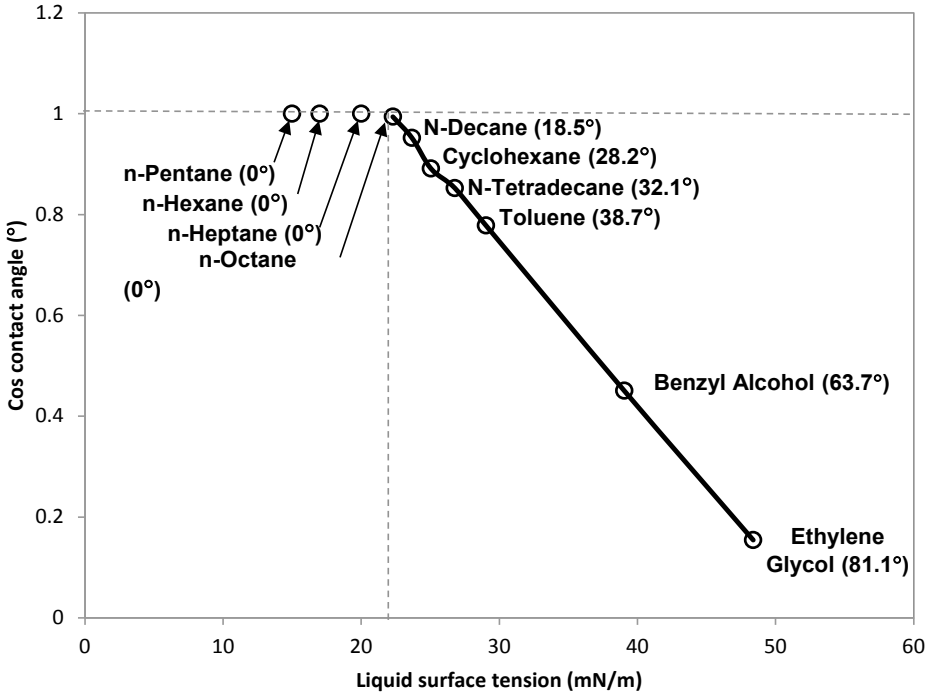

Figure 1.27. Zisman plot representing the critical surface tension of several liquids for LDPE films (Fox and Zisman, 2006).

1.1.7.7.3. Composite membranes

Using composite membranes comprising a microporous support coated by a dense top layer is another effective method for membrane wetting prevention (Nymeijer et al., 2004). The dense top layer is in contact with the liquid phase and serves as a stabilization layer, by not permitting the liquid to penetrate inside the pores. The material for this layer should be highly permeable to the targeted gas components and hydrophobic enough to prevent wetting. Chabanon et al. (2011a,b) studied the wetting resistance of a composite membrane consisting of a PP porous membrane coated with a dense top layer of poly(1-trimethylsilyl-1-propyne) (PTMSP), in a long period operation (10 h) in GLMC using MEA and a blend of MDEA and triethylenetetramine (TETA) as absorbents. The system was reported to operate without wetting problems, so that the CO_2 removal efficiency remained

higher than 90% at the end of the operating period. Similar behaviour was reported by Nguyen et al. (2011) in the case of a composite hollow fiber membrane with a thin top skin of Teflon coated on a PP porous support. Fig. 1.28 shows a schematic representation of the resistance of a gas-liquid membrane contactor with a composite membrane as interface between gas and liquid phases. The overall mass transfer resistance ($1/K_{OG}$) comprises four consecutive resistances in series and can be written as:

$$\frac{1}{K_{OG}} = \frac{1}{k_g} + \frac{1}{k_S} + \frac{1}{k_C} + \frac{1}{mk_L} \tag{1.15}$$

where $1/k_g$, $1/k_S$, $1/k_C$ and $1/k_L$ represent resistances of the gas boundary layer, porous support, dense coating layer and liquid phase boundary layer, respectively. The presence of the dense layer introduces an additional resistance. This additional resistance can sometimes be as high as 10^4 s/m, which is comparable to the resistance of liquid phase boundary layer and 10^2 times higher than that of the gas boundary layer. It can therefore become the limiting step in the absorption process (Nymeijer et al., 2004).

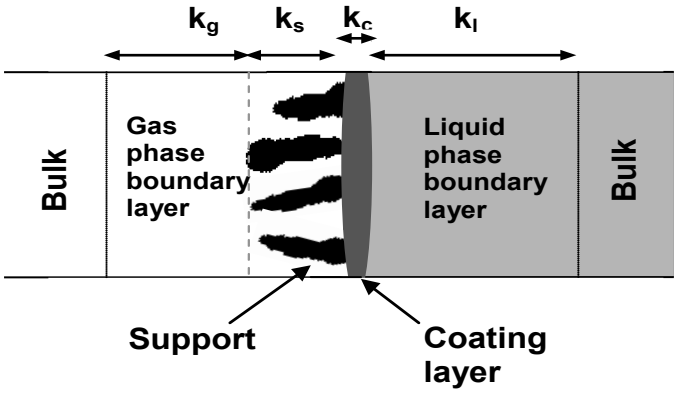

Figure 1.28. Schematic presentation of the resistances of a gas-liquid membrane contactor with a composite membrane as interface between gas and liquid phases (Nymeijer et al., 2004).

1.1.7.7.4. Asymmetric membranes

Asymmetric membranes having a dense top layer (Fig. 1.29) are considered in the literature for their lower wetting tendency (Kreulen and Smolders, 1993; Wang et al., 2000; Ismail and Yaacob, 2006; Choi et al., 2010; Chen et al., 2011). Using wet-spinning method, different porous asymmetric membranes such as PVDF (Wang et al., 2000; Choi et al.,

2010; Mansourizadeh et al., 2010; Mansourizadeh et al., 2012; Mansourizadeh and Mousavian, 2013), polyimide (PI) (Kawakami et al., 1997; Mikawa et al., 2002), polysolfune (PS) (Ismail et al, 2004; Torres-Trueba, et al., 2008) and polyamide (PA) (Kazama and Sakashita et al., 2004) were fabricated in the literature. Chen et al. (2011) studied the wetting resistance of both symmetric and asymmetric PTFE membranes in contact with a mixed amine absorbent (AMP/MEA/PZ solution). They observed that the asymmetric PTFE membrane shows lower wettability in comparison to the symmetric one, mainly because the dense top layer of the asymmetric membrane, having small porosity and pore diameters, hardly tends to be intruded by the absorbents. However, asymmetric membranes introduce higher mass transfer resistance due to the existence of a dense skin on the membrane surface, leading to a reduction in CO_2 absorption flux (Kreulen and Smolders, 1993).

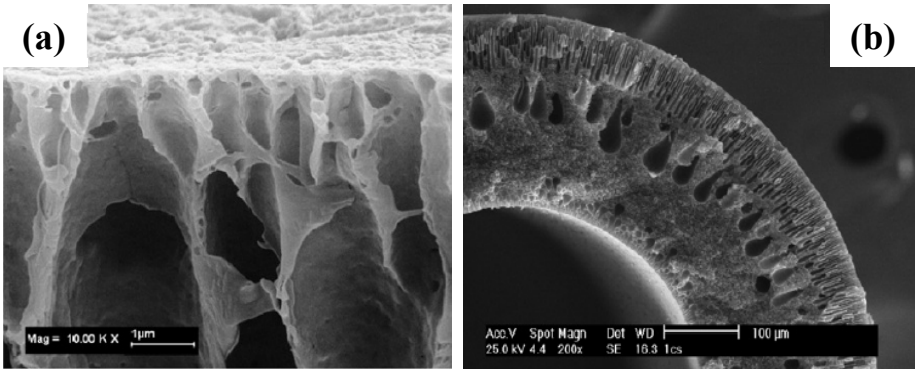

Figure 1.29. Pore structures of asymmetric a) PVDF (Mansourizadeh et al., 2012) and b) PSF (Ismail et al., 2004) hollow fiber membranes.

1.1.7.7.5. Surface modification

Several hydrophobic surface modification techniques have been developed to reduce surface wettability of polymers. However, among such techniques, only a few were employed to decrease wettability of porous polymeric membranes. The following section reviews the approaches to hydrophobic surface modification of *polymeric films*, as well as *polymeric porous membranes*.

1.1.7.7.5.1. Hydrophobic surface modification of polymeric surfaces

Table 1.7 summarizes the methods developed for hydrophobic treatment of polymeric surfaces including: i) roughening and ii) fluorination of the polymeric surfaces. Most of the treatments have been performed to produce self-cleaning surfaces, without focusing on a specific application. As indicated in Table 1.8, only few hydrophobic treatments in the literature have been applied on membrane surfaces (Kim et al., 1994; Franco et al., 2008; Kim et al., 2008; Lv et al., 2012).

Table 1.7. Summary of available hydrophobic surface modification methods performed on polymeric surfaces.

Method		Surface material	Water contact angle (^{o})	Application in membrane	Reference
Surface roughening	Template (nano casting/replication)	PDMS	160	No	Sun et al., 2005
		HDPE	159	No	Lee and Park, 2007
		PSF	Adv[1]: 155	No	Lee et al., 2004
			Rec: 147	No	
		polyvinyl alcohol (PVA)	171	No	Feng et al., 2003
		perfluoropolyether (PFPE)	152	No	Lee et al., 2012
	Solution casting	LDPE	173	No	Lu et al., 2004
		LLDPE	153	No	Yuan et al., 2008
		Poly-styrene (PS)	154	No	Fan et al., 2011
		PP	**169**	**Yes**	Franco et al., 2008
		PP	**158**	**Yes**	Lv et al., 2012
		PAMS	152	No	Fan et al., 2011
		LDPE	152	No	Yuan et al., 2012
	Stretching	**PTFE**	**171**	**Yes**	Xi et al., 2008
		PE	**131**	**Yes**	Lee et al., 2006
Fluorination	Etching Laser	PDMS	160	No	Jin et al., 2005
	Plasma	PET	153	No	Teshima et al., 2005
		PS	170	No	Shui et al., 2005

Table 1.7. Summary of available hydrophobic surface modification methods performed on polymeric surfaces (Continued).

Method		Surface material	Water contact angle (^{o})	Application in membrane	Reference
Fluorination	Peramanent grafting	PET	140	No	Ramaratnam et al., 2007
		PET	130	No	Boguslavsky et al., 2011
	Melt blending	PP+F	130	No	Ebbens and Badyal., 2001
		HDPE+PFPE	106	No	Puukilainen and Tapani, 2005
	Plasma fluorination	**PP + CF_4**	**143**	**Yes**	Lin et al., 2009a
		PVDF + CF_4	**155**	**Yes**	Lin et al., 2009b
		Poly-butadiene + CF_4	157	No	Woodward et al., 2003
		LDPE + F_2	Adv:150 Rec:85	No	Kirk et al., 2010
		PTFE + SF_6	145	No	Rangel et al., 2003

[1] Adv: Advancing contact angle; Rec: Receding contact angle

1.1.7.7.5.1.1. Surface roughening

Superhydrophobic surfaces, having water contact angles over 150°, have attracted much attention due to their high water repellence and self-cleaning properties. The most known superhydrophobic surface in nature is the lotus plant leaf. Scanning electron microscopy images show that lotus leaf surfaces are a combination of micro and nano-scale hierarchical structures which make them extraordinarily water repellent and keep them spotless (Fig. 1.30) (Cassie and Boxter, 1944; Feng et al., 2002; Ma and Hill, 2006). Water cannot spread out on the leaves, but rolls as droplets and remove grime and soil as they move. In order to obtain a superhydrophobic surface, a combination of a low surface energy material and surface roughness is required.

According to the Cassie and Baxter theory (Cassie and Baxter, 1944), the contact angle of a hydrophobic rough surface comprising solid and air can be determined using the following relation:

$$\cos\theta_r = f_1 \cos\theta - f_2 \quad (1.6)$$

where θ refers to the contact angle of the smooth surface, θ_r defines the contact angle of the rough surface, while f_1 and f_2 are the fractions of solid and air on the composite surface, respectively. This equation predicts that increasing the fraction of air (f_2) would lead to an increase in contact angle (the fraction of air increases by increasing the surface roughness, leading therefore to an increase in contact angle).

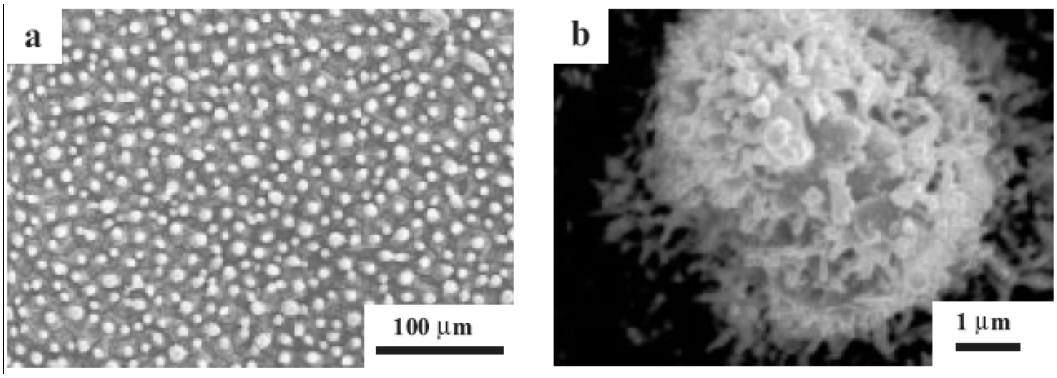

Figure 1.30. SEM of the surface of a lotus leaf: a) large area, every epidermal cell forms a papilla covered with a dense layer of paraffin wax; b) enlarged view of a single papilla (Feng et al., 2002).

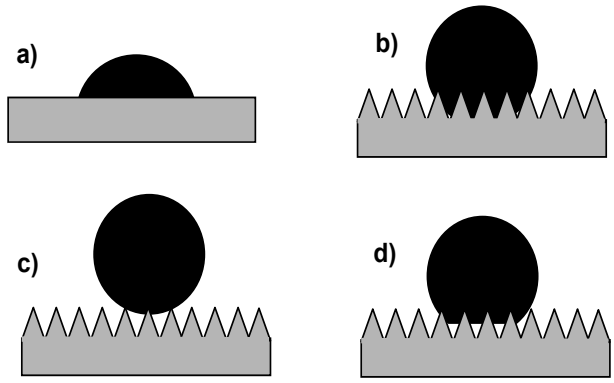

Figure 1.31. Effect of surface roughness on wetting behavior of solid substrates: a) smooth surface, b) rough surface with micron structures, c) rough surface with micron and nano structures in ideal condition and d) rough surface in real condition (Feng et al., 2002).

This remarkable rise of contact angles by increasing surface roughness is called the "lotus effect", which can be mimicked in artificial highly hydrophobic surfaces (Fig. 1.31) (Cassie

and Baxter, 1944; Feng et al., 2002; Woodward et al., 2003; Erbil et al., 2003; Ma and Hill, 2006; Yan et al., 2008).

1.1.7.7.5.1.1.1. Permanent grafting

As an alternative to the above mentioned techniques, an interesting modification technique was proposed by Ramaratnam et al. (2007), which eliminate the need for using solvents and diluents. In this work, ultrahydrophobic textiles were fabricated via surface roughening using permanent grafting of nanoparticles on polymeric surfaces. A primary reactive layer was formed on the surface of a substrate using nanoparticles functionalized by poly(glycidylmethacrylate) (PGMA), an epoxy containing polymer. Being highly reactive, the formed layer can adhere to various kinds of polymers with different functional groups (carboxyl, anhydride, hydroxyl). Using this technique, the authors fabricated a superhydrophobic surface of poly(ethylene terephthalate) (PET) polyester fabric by grafting functionalized silica nanoparticles, as shown in Fig. 1.32. First, PGMA and NaOH were used to functionalize silica nanoparticles and PET surface, respectively. Then, functionalized silica nanoparticles were grafted into the reactive surface of NaOH treated PET substrate. Finally, a hydrophobic and reactive copolymer (styrene-ethylene-butadiene-styrene, SEBS) was used to generate an ultra-thin hydrophobic coating on the PET surface, roughened by functionalized silica nanoparticles. The resulting textile possesses superhydrophobic properties (low surface energy and surface roughness), and shows water contact angles higher than 150°. Using the same method, ultrahydrophobic PET surfaces were also fabricated by grafting functionalized multi-walled carbon nanotubes (MWCNT) on PET treated surfaces (Boguslavski et al., 2011). Although permanent grafting seems not to be restricted to be applied on membrane surfaces, no report has been found in the literature on the application of this technique on hydrophobic modification of membranes.

1.1.7.7.5.1.1.2. Template method

This method, also known as the replication or nanocasting method, is an efficient technique for roughening flat surfaces during molding. Anodized aluminum oxide molds are usually used as replication templates. This technique comprises three steps (Fig. 1.33): i) photolithography, to form microstructure pattern on the Al surface, using UV irradiation,

ii) Al etching, to generate hemispherical concaves (holes) on the Al surface, and iii) anodization and polymer replication to form various nanostructures on the Al surface. There are several reports in the literature concerning the fabrication of rough surfaces with superhydrophobic characteristics using the template method (Table 1.7) (Lee et al., 2004; Lu et al., 2004; Lee et al., 2007). It is obvious that this technique is effective for products fabricated via injection molding, but cannot be applied to films or fibers that are continuously produced through an extrusion process.

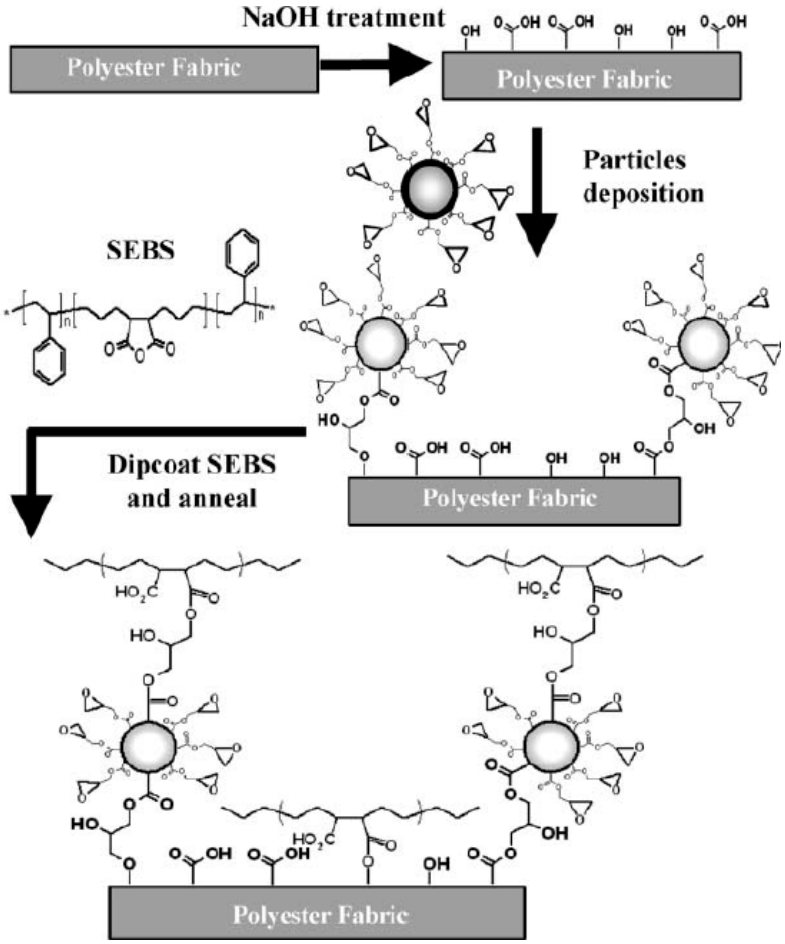

Figure 1.32. Attachment of silica nanoparticles and hydrophobic polymer to polyester fabric (Ramaratma, 2007).

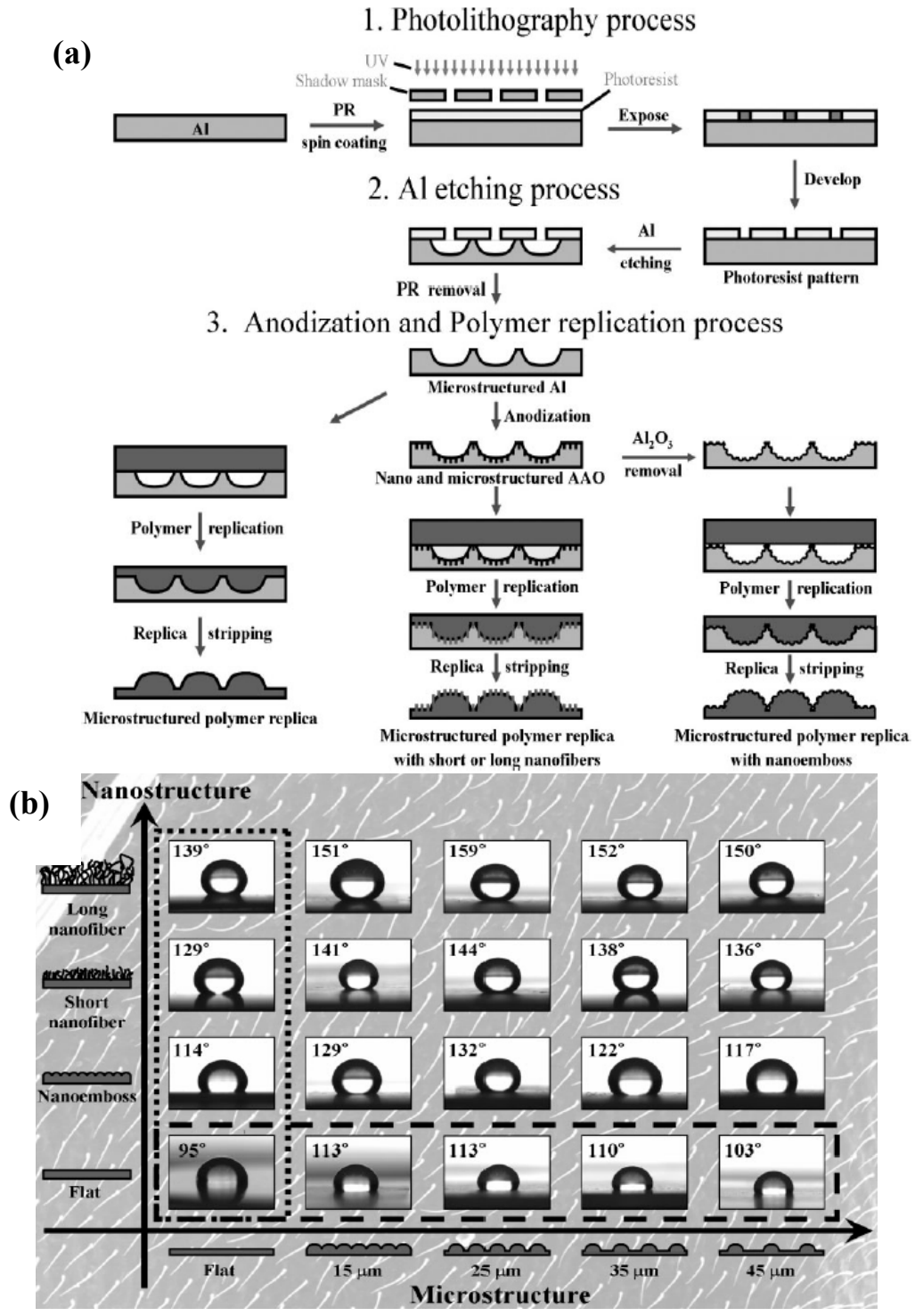

Figure 1.33. a) HDPE replicas with various shapes of nanometer- and micrometer-structured surfaces prepared by template method: a) process steps and b) water contact angles of HDPE replicas compared to that of the flat HDPE surface (Lee et al., 2007).

1.1.7.7.5.1.1.3. Solution casting method

In this technique, the phase separation of a polymer solution is responsible for roughness creation. The process consists of polymer dissolution in a proper solvent followed by phase separation of the solution, which is triggered either by the addition of a non-solvent (NIPS) or by decreasing the solution temperature (TIPS). Eventually, a spongy coating with a rough structure (Fig. 1.34) is formed by casting of a few drops of polymer solution on a substrate, followed by slow evaporation of the solvent (Choi et al., 2010). This method has extensively been used in fabricating superhydrophobic coatings (Table 1.7) (Erbil et al., 2003; Jin et al., 2005; Yang et al., 2011; Lv et al., 2012; Yuan et al., 2012). However, the need for using toxic and expensive solvents (mainly xylene) to form polymer solutions restricts the large scale productivity of this technique.

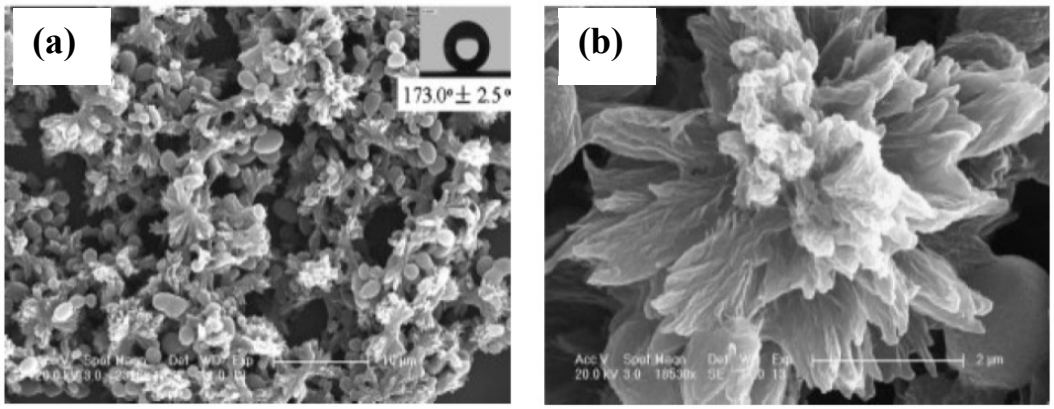

Figure 1.34. Hierarchical structure on LDPE surface prepared by solvent-non solvent method, b) enlarged view of a single floral structure (Lu et al., 2004).

1.1.7.7.5.1.2. Fluorination methods

Fluorinated polymer surfaces have widely been considered for their low surface energies and subsequently, their lower wetting tendencies (Pike and Ho, 1996; Iyengar et al., 1996). Most reported fluorination techniques in the literature include melt blending of polymers with fluorochemicals and plasma surface treatments.

1.1.7.7.5.1.2.1. Melt blending

Sargent and Alender (Sarget and Alender, 1996) proposed a straightforward approach for surface fluorination of polymers, including mixing a small amount of fluorine-containing material with a polymer melt through the injection molding process. The segregation of the dopant towards the surface occurs during the film formation as a consequence of its lower surface energy. Using this method, several fluorinated polymeric surfaces were fabricated (Table 1-4). Since no solvent or diluent is used, this method is safe and environmentally friendly, while its simplicity makes it practical and applicable to a wide range of polymer/fluorochemical blends.

1.1.7.7.5.1.2.2. Plasma treatment

Plasma is a partially or fully ionized gas containing electrons, ions and neutral atoms or molecules (Chang, 1998). Plasma-induced fluorination techniques are mostly used to initiate surface fluorination via the excitation and dissociation of feed gases, including CF_4 (Cordeiro et al., 2008), SF_6 (Rangel et al., 2003), F_2 (Kirk et al., 2010) and XeF_2 (Wheale et al., 2011). Fluor atoms produced in the plasma abstract hydrogen atoms from hydrocarbons on polymeric surfaces and passivate the resulting alkyl sites to produce $C\text{-}F_n$ sites (Yang et al., 2010). This technique targets only a thin layer of the surface and can thus alter surface properties of the polymer, while bulk properties remain unchanged. Different plasma processes such as plasma surface activation followed by grafting of functional groups (Lin et al., 2009) and pulsed plasma (Khorasani et al., 2005) have been investigated to deposit fluorochemicals on polymer surfaces. Since plasma surface treatments can be performed near ambient temperature, they have low energy consumption. However, operation cost is still high due to the necessity of having a vacuum environment during the process.

1.1.7.7.5.2. Hydrophobic surface modification of membranes

Only few investigations have been performed in the literature concerning hydrophobic surface modification of porous membranes (Occhiello et al., 1989; Iyengar et al., 1996; Sargent and Alender, 1996; Pike and Ho, 1996; Chang, 1998; Kim et al., 2002; Rangel et al., 2003; Khorasani et al., 2005; Franco et al., 2008; Jian et al., 2009; Lin et al.,

2009; Kirk et al., 2010; Lv et al., 2010; Franco et al., 2011; Wheale et al., 2011; Yang et al., 2011; Wei et al., 2012).

1.1.7.7.5.2.1. Solution casting

In this method, a rough and spongy coating is prepared by the solution casting method and is deposited on a membrane surface. Using this method, superhydrophobic flat (Franco et al., 2008) and hollow fiber (Lv et al., 2012) PP membranes were fabricated via the deposition of a porous crystalline polypropylene coating on top of commercial PP membranes. Rough coating layers were prepared by dissolving polypropylene granules in a solvent (xylene) at high temperatures (about 120°C), followed by the addition of a few droplets of a miscible liquid (non-solvent). Solutions were then cast on top of polypropylene flat and hollow fiber membranes via spin coating. In this technique, the surface roughness and porosity are influenced by the nature of the non-solvent and its concentration. The commonly used non-solvents are methyl ethyl ketone (MEK) and cyclohexanone. It was observed that, under the same conditions, the use of methyl ethyl ketone (MEK) resulted in higher average water contact angle (138°) compared to cyclohexanone (127°). However, cyclohexanone provides a higher number of spherulites of small diameter, attributed to the more homogeneous surface formed by cyclohexanone compared to that with MEK (Fig. 1.35) (Lv et al., 2012). By optimizing the non-solvent nature and concentration, a high water contact angle of 169° was achieved. In comparison to pure MEK and cyclohexanone, the MEK/cyclohexanone mixture combining both advantages of homogeneity and high surface roughness, can be considered as a more efficient non-solvent (Lv et al., 2010). In this case, by optimizing the MEK/cyclohexanone mixture concentration, an average water contact angle of 158° was obtained for PP membranes (Lv et al., 2012).

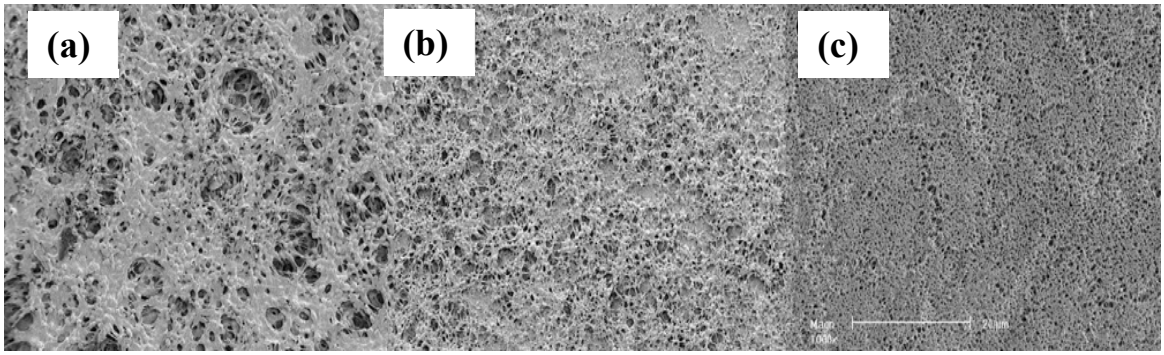

Figure 1.35. SEM images depicting the change in surface morphology with the type of non-solvent used which include (a) MEK at a magnification of 750x, (b) cyclohexanone at a magnification of 750x and (c) the untreated polypropylene membrane at a magnification of 1000x (Franco et al., 2008).

As shown in Fig. 1.36, for long-term CO_2 absorption using 1 mol/l MEA as absorbent, it is clear that modified PP membranes show a higher wetting resistance than untreated ones (Lv et al., 2012). Before 7 days, the reduction in absorption flux was not notable. After 7 days, a slight decreased of about 14% was found, and the value remained constant for 20 days.

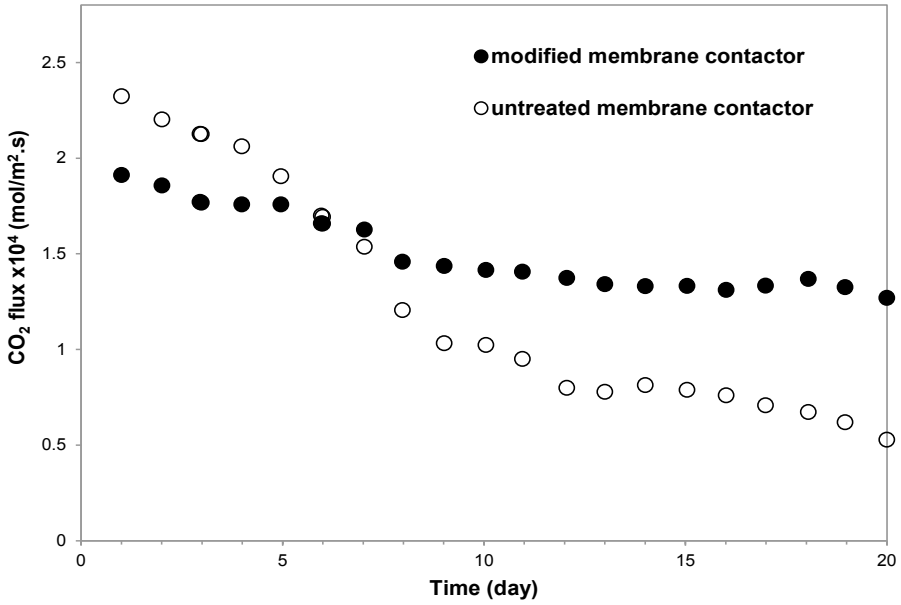

Figure 1.36. Influences of surface modification of the PP membrane, via the solution casting technique on CO_2 mass transfer rate during long-time operation (Lv et al., 2012).

However, as depicted in Fig. 1.37, CO_2 flux value of modified membranes was lower than that of untreated membranes for the first 6 days. This was attributed to the fact that, along with the desired hydrophobicity enhancement effect, the deposition of a coating layer resulted in decreasing membrane porosity and increasing mass transfer resistance, which are unfavorable for CO_2 absorption process.

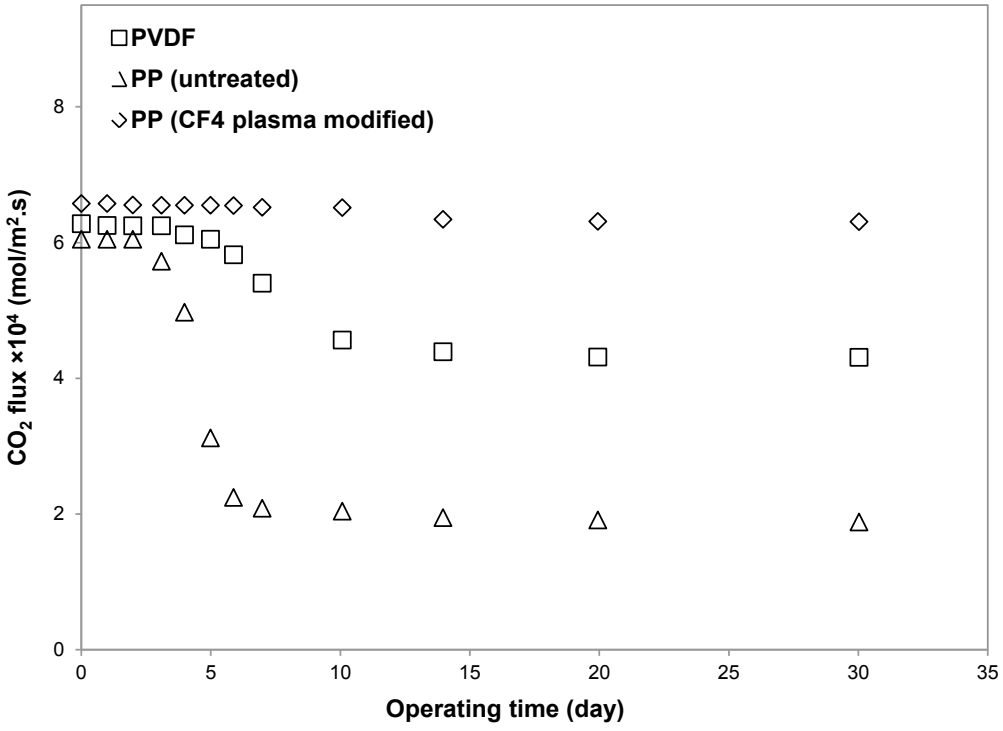

Figure 1.37. Comparison of CO_2 absorption fluxes of plasma modified and unmodified membranes at long-term operation in a hollow fiber membrane contactor (Lin et al., 2009).

1.1.7.5.2.2. Plasma treatment

Hydrophobic plasma treatments have been employed for surface fluorination of different membranes such as, PVDF (Jian et al., 2009), polysulfone (PSF) (Kim et al., 2002), polycarbonate (PC) (Occhiello et al., 1989), polyethersulfone (PES) (Wei et al., 2012) and PP (Lin et al., 2009; Franco et al., 2011). The influence of plasma treatment on membrane wettability was studied in the case of CF_4 plasma surface modification of PP hollow fiber membranes (Lin et al., 2009; Franco et al., 2011). The CO_2 absorption performance of the treated membrane was investigated in membrane contacting system

using aqueous solutions of PZ/MDEA and PZ/AMP. Furthermore, the modified membranes showed a remarkably higher wetting resistance during 20 h of operation compared to untreated PP and PVDF membranes (Fig. 1.37). In addition, the effect of plasma sputtering of PP flat membranes by PTFE on membrane wettability was investigated (Franco et al., 2011). It was observed that the water contact angle and breakthrough pressure increased, respectively, from 127° and 29 kPa for untreated PP membranes to 151° and 71 kPa after PTFE sputtering, due to increasing membrane surface roughness and decreasing membrane surface energy, as well as the decrease in membrane surface pore size after treatment. Moreover, the estimated wetting degree after 25 days of CO_2 absorption was reduced from 100% for untreated PP membranes to 60% for treated ones.

1.1.7.7.5.2.3. Stretching method

Melt spinning of semi-crystalline polymers (comprising crystalline and amorphous regions) results in the formation of a precursor with lamellar structure (Fig. 1.38a). These precursors are then annealed to improve crystallinity (Keller and Marchin, 1967; Shen et al., 2002). Afterwards, during the axial stretching process, such well-crystallized precursors form a membrane structure comprising lamellae stacks (obtained from the crystalline region), microvoids (formed in the amorphous region) and microfibrils (connecting lamellae stacks), as shown in Fig. 1.38b,c (Zhang et al., 2004). Such a rough and porous structure can result in a decrease in membrane surface energy (Xi et al., 2008). Ultrahydrophobic HDPE hollow fiber membranes with a water contact angle of 131° was fabricated by stretching HDPE hollow fiber precursors (Lee et al., 2006). Therefore, stretching, as a post treatment process (performed on membrane precursors, fabricated via the melt-spinning process (Lee et al., 2006; Xi et al., 2008; Mosadegh Sedghi et al., 2012b), can simultaneously form a porous structure and improve membrane surface hydrophobicity.

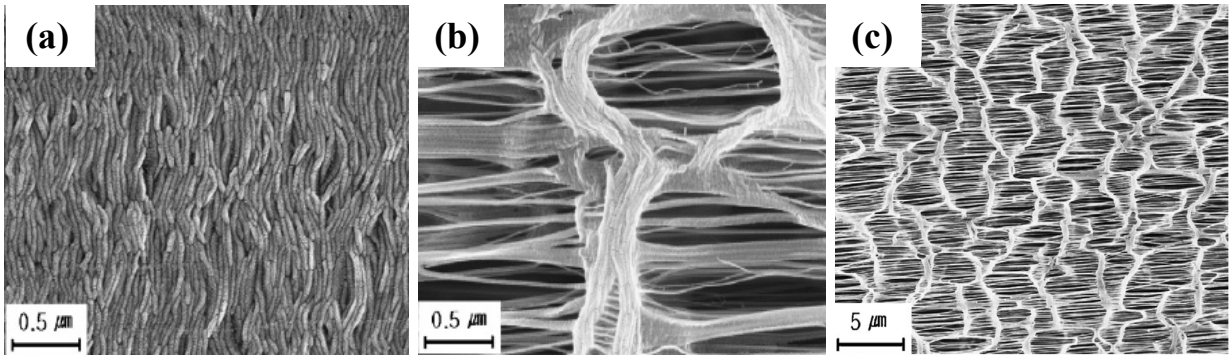

Figure 1.38. SEM images of a) inner surface of polyethylene hollow fiber precursors after annealing, b) inner surface of membranes prepared from annealed hollow fiber precursors by hot stretching and c) microfibrils and lamellar stacks of membranes prepared from annealed hollow fiber precursors by hot stretching (Chen et al., 2011).

1.1.7.7.5.2.4. Template leaching

Recently, a hybrid process combining melt extrusion and continuous template-leaching techniques was proposed as a novel solvent-free method to improve membrane surface hydrophobicity during fabrication (Nishikawa et al., 1995; Mosadegh-Sedghi et al., 2013). This method provides effective roughness on membrane surface which can significantly decrease membrane wettability. As a solvent-free method, melt-extrusion and template leaching technique overcome the environmental impacts of the solution casting method. In addition, unlike the stretching method which requires several annealing and mechanical stretching treatments after the membrane fabrication, in this method no post-treatments are employed and therefore, it is expected to be industrially applicable for different kinds of polymers. Using this method, highly hydrophobic LDPE hollow fiber membranes with water contact angle of 130° were produced. Fig. 1.39 reports scanning electron images of the surface of these fibers, for which the surface roughness is clearly seen.

Plasma treatment, stretching and template leaching method are solvent-free techniques which are considered as clean and environmentally friendly membrane hydrophobic modification methods. However, plasma required vacuum which is really costly (Lin et al., 2009). Stretching method is considered as a post-treatment, which is applied on membranes after fabrication and required several thermal and mechanical steps.

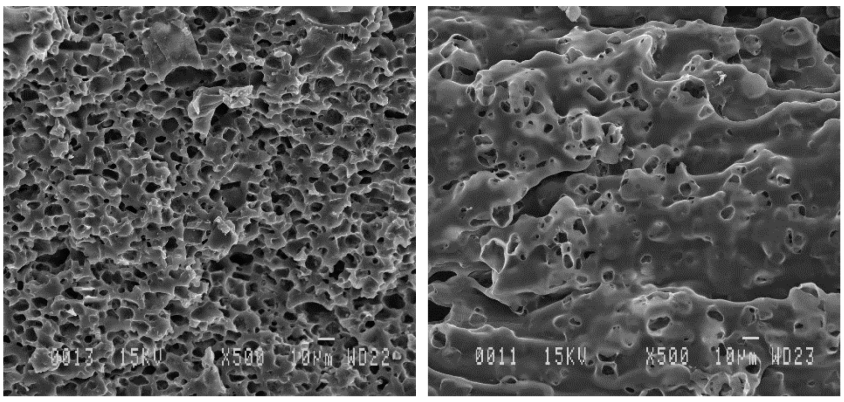

Figure 1.39. SEM images of a) cross-section and b) outer surface of LDPE hollow fiber membrane fabricated by template leaching method (Mosadegh-Sedghi et al., 2013).

On the other hands, this method is only applicable for semi-crystalline polymers (Shen et al., 2002). Template leaching, as the only continuous solvent-free method which does not employ any after-treatments, is considered as an attractive method. However, membrane pore size is determined by salt particle size used to produce porous structure. Therefore, since limited sizes of salt particles are commercially available, controlling pore size is restricted in this technique (Mosadegh-Sedghi et al., 2013).

1.2. Conclusions

Microporous polymeric membranes used for gas separation in gas-liquid membrane contactors are commonly prepared via phase inversion methods involving toxic and expensive solvents and diluents. Even for hydrophobic membranes, the wetting phenomenon of porous membranes by liquid absorbents, which leads to the increase in total mass transfer resistance and thus, to a reduction in absorption efficiency, is still a major problem in membrane contactors. The impacts of various parameters on membrane wetting and the main approaches to prevent such phenomenon make the object of several articles in the literature.

The type of liquid absorbent has a significant impact on membrane wetting. The higher the absorbent surface tension and viscosity, the lower its tendency to wet the membrane pores. In addition, liquid-side operating conditions have an important effect on membrane wetting. Liquid pressure should be lower than membrane breakthrough pressure to avoid wetting. The operating temperature influences the absorbent physical properties

(viscosity and surface tension). Liquid surface tension and viscosity decrease with the increase in temperature and therefore, in real conditions (absorption temperatures around 50-60°C), the absorbent has more facility to penetrate inside the membrane pores.

Table 1.8. Comparison of available hydrophobic surface modification methods performed on porous polymeric membranes.

Method	Advantages	Disadvantages
Solution casting	• Uniform thickness of cast layer	• Environmentally malignant • Uneconomical (expensive
Plasma treatment	• Safe and environmentally friendly • Applicable at low temperatures (near ambient temperature)	• High cost (vacuum environment) • Applicable only to flat membranes (extremely
Stretching method	• Environmentally friendly (solvent-free method)	• Restricted to semi-crystalline polymers • Limited applicability for large scale production
Template leaching	• Environmentally friendly (solvent-free method) • Applicable to all types of polymers • Merged with the fabrication process	• Limited membrane pore size control (depends on available particle template size)

PTFE is currently the most resistant material to wetting, mainly due to its high hydrophobicity. However, its use for gas separation by GLMC in industrial large-scale applications is limited due to several important drawbacks like high fabrication cost and environmental impacts. Replacing PTFE with other kinds of polymeric membranes (like PP) requires the use of suitable hydrophobic surface treatments to increase membrane wetting resistance to values comparable to PTFE. Membrane surface roughening

techniques, including the template method, solution casting and permanent grafting methods, have been proposed to increase membrane surface hydrophobicity. Stretching methods include several thermal and mechanical treatments and are only applicable to semi-crystalline polymers. Solution casting methods use toxic and inflammable solvents and diluents which are expensive and environmentally malignant. Membrane surface fluorination technologies, an alternative to surface roughening, have a high cost and potential environmental impacts.

1.3. Objectives of work

Polymeric membranes used for gas separation in gas-liquid membrane contactors are usually prepared via a phase inversion methods involving toxic and expensive solvents and diluents, making the fabrication process uneconomic and environmentally malignant. The melt-spinning and stretching method, the only solvent-free technique proposed to produce hollow fiber membranes, requires several post-treatments which make the process industrially non-applicable. The development of efficient solvent-free techniques for membrane fabrication is still a challenge for industrial implementation of GLMC.

1.3.1. General objective

The main objective of the present doctoral project was to fabricate efficient (microporous and highly hydrophobic) hollow fiber membranes for CO_2 separation in GLMC via a solvent-free method, as a clean, economical, and environmentally friendly alternative to the commonly used ones (namely, PTFE).

1.3.2. Specific objectives

To achieve this goal, the following specific objectives were defined:

- Optimisation of operating conditions for membrane fabrication.
- Investigation of morphological, chemical and thermal stability of membranes in contact with different absorbent solutions.
- Determination of membrane wetting behaviour in contact with different absorbent solutions.

The principal aim of this thesis was to develop highly hydrophobic microporous membranes for CO_2 capture in GLMC, by an economic and environmentally friendly method that does not require the use of solvents or diluents. In the first paper (Chapter 2), a comprehensive description of the fabrication and characterisation of new LDPE hollow fiber membranes is presented. LDPE was selected for its low price which makes the fabrication process industrially economical, for its better chemical stability compared to other polyolefins, as well as for the easiness of the fabrication process.

Chapter 2

Highly hydrophobic microporous LDPE hollow fiber membranes by melt-extrusion coupled with salt-leaching technique

Résumé

Des membranes microporeuses et hautement hydrophobes à fibres creuses en polyéthylène de basse densité (LDPE) ont été préparées par un procédé sans solvant, en combinant les techniques d'extrusion et le lavage de sel. Des particules de NaCl (5 à 10 μm) ont été mélangées avec le LDPE pour produire un mélange contenant 35, 40, 50, 60, 65 et 68 wt% de sel. La structure microporeuse a été produite par le lavage des particules de sel emprisonées dans la matrice polymère par immersion dans l'eau à 60°C. Les membranes fabriquées ont été ensuite caractérisées en termes de morphologie, porosité et distribution de la taille des pores, rugosité de la surface et hydrophobicité, ainsi que des propriétés mécaniques. L'augmentation remarquable de l'angle de contact eau/membrane de 98° pour des fibres creuses fabriquées sans ajout de sel (échantillon témoin) à 130° pour les membranes fabriquées avec une teneur en sel initiale de 68 wt% est essentiellement attribuée à la structure rugeuse de la surface qui contient un grand nombre de micropapilles produites par l'élimination du sel. L'augmentation de la rugosité de la surface et de la porosité des membranes avec l'augmentation de la teneur initiale en sel a été confirmée par microscopie électronique à balayage (SEM) et force atomique (AFM).

Abstract

Microporous and highly hydrophobic low density polyethylene (LDPE) hollow fiber membranes were successfully prepared via a solvent-free method, combining melt extrusion and salt-leaching techniques. NaCl particles with particle size of 5-10 μm were mixed with LDPE pellets to produce a blend of 35, 40, 50, 60, 65 and 68 wt% of salt. A microporous structure was produced by leaching the salt particles from the hollow fiber matrix via immersion in water at 60°C. The fabricated membranes were then characterized in terms of morphology, porosity and pore size distribution, surface roughness and hydrophobicity, as well as mechanical properties. The remarkable increase in the water contact angles from 98° for LDPE hollow fibers fabricated without the addition of salt (blank sample) to 130° for membranes fabricated with initial salt content of 68 wt% is mainly attributed to the rough surface structure, comprising a large number of micropapillas produced by removing the imbedded salt crystals. The increase in surface roughness and porosity of hollow fiber membranes with increasing initial salt content was confirmed by SEM and AFM microscopy.

2.1. Introduction

Wetting of porous polymeric membranes by liquid absorbents has been considered as the major problem in membrane gas liquid contactors (GLMC). In non-wetted conditions, membrane pores are filled only with the gas. However, partial wetting of membrane pores by the liquid absorbent can result in a significant increase in membrane mass transfer resistance, a gradual reduction of the gas flux through the membranes, and therefore a decrease in membrane efficiency and long-term performance of membrane contactors (Nishikawa et al., 1995; Dindore et al., 2004).

The wetting tendency of a membrane by a specific liquid is determined by membrane chemical and morphological properties and is related to its surface energy (hydrophobicity) and pore size. In order to avoid wetting phenomena, highly hydrophobic membranes are required. The wettability of commonly used polymeric membranes with different solutions is summarized in Table 2.1. It can be seen that, due to its lowest surface energy, polytetrafluoroethylene (PTFE) is the most resistant polymer to wetting and therefore, it has been extensively used in GLMC systems, despite several serious drawbacks which limit its large scale applicability (complex, costly, and environmentally malignant method of fabrication, small specific interfacial area, difficult pore size control, non-recyclability).

Table 2.1. Wettability of commonly used membranes

Reference	Wettability	Absorbent	Membrane
Nishikawa et al. (1995)	-	MEA	PTFE
Falk-Pedersen and Dannström (1997)	-	Amine solution (AMP, MEA, MDEA)	
Kim et al. (2000)	-		
Matsumoto et al. (1995)	-	NaOH solution, MEA solution	
deMontigny et al. (2006)	-	MEA, AMP	
Khaisri et al. (2009)	-	Water, MEA	
Rangwala (1996)	+	NaOH solution	PP
Falk-Pedersen and Dannström (1997)	+	Alkanolamine solution	
Kumar et al. (2002)	+		
Kumar et al. (2002)	-	Amino acid salts (Potassium taurate)	
Matsumoto et al. (1995)	+	NaOH solution, MEA solution	
Dindore et al. (2004)	+	Propylene carbonate	
Khaisri et al. (2009)	+	Water, MEA	
deMontigny et al. (2006)	+	MEA , AMP	
Lu et al. (2009)	-	Activated absorbent	
Matsumoto et al. (1995)	+	NaOH solution, MEA solution	PE
Nishikawa et al. (1995)	+	MEA	
Yeon et al. (2003)	-	5% MEA +5% TEA	PVDF
Khaisri et al. (2009)	+	Water, MEA	

General characteristics of some kinds of commercial polytetrafluoroethylene (PTFE), polypropylene (PP) and polyvinylidene fluoride (PVDF) hollow fiber membranes are presented in Table 2.2. Polypropylene, an inexpensive and frequently available alternative, has been intensely studied in the literature. However, due to its higher surface energy (around 35 mN/m) compared to PTFE (around 19 mN/m), PP has a large wettability and consequently, it has been reported to be wetted by alkanolamine solutions (the most used

absorbent in GLMC) during short term operation (Nishikawa et al., 1995). Polyethylene (PE), having the same wetting tendency as PP, is also an alternative material but has been little studied in this context. Nevertheless, it has several advantages including recyclability, flexibility of operation, simplicity of transformation to flat and hollow fiber membranes through different methods, good availability and low cost, and chemical stability higher than that of PP (Xi et al., 2008). Methods used for hydrophobic treatment of polyolefins such as laser etching (Jin et al., 2005), plasma treatment (Shui et al., 2004) and solution casting (Lu et al., 2004) are mostly uneconomic or use toxic solvents. In addition, most of them cannot be applied on non-flat surfaces and thus are not appropriate for hollow fiber membranes.

Table 2.2. Commercial hollow fiber membrane characteristics.

Description	**PP**	**PVDF**	**PTFE**	**Reference**
Max. available pore size (μm)	0.25	0.03	1.0	Lee et al. (2004)
Max. void fraction (%)	75.2	82.2	70.1	Khaisri et al. (2009)
	82.2	-	59.2	deMontigny et al. (2006)
Max. specific area (m^2/m^3)	2855	1488	1340	Lee et al. (2004)
	2752	-	429	deMontigny et al. (2006)
Cost (US $/m)	0.01	-	23	deMontigny et al. (2006)
	0.01	0.36	11.5	Khaisri et al. (2009)

It has been shown that effective roughening of a specific surface can significantly increase its hydrophobicity (Lu et al., 2004; Lee et al., 2007; Franco et al., 2008; Yuan et al., 2008). Many natural plant leaves have superhydrophobic properties due to their rough structure (Blossey, 2003). There have been several reports in the literature on fabrication of artificial superhydrophobic surfaces via roughening low surface energy materials (Ma et al., 2005; Yuan et al., 2008). However, despite its important role in reduction of membrane wettability, increasing the hydrophobicity of porous polymeric membranes via creating

rough structures remains considerably untouched. To the best of our knowledge, the only report was that of Lv et al. (2012), who performed a solvent-based treatment (cyclohexanone and methyl ethyl ketone mixture) of polypropylene (PP) membrane fibers by depositing a rough layer on the surface in order to improve its hydrophobicity and consequently, to reduce the wetting phenomenon.

Porous polymeric membranes are usually fabricated via conventional wet-phase inversion methods through thermally induced phase separation (TIPS) (Kim and LIoyd, 1991) or non-solvent induced phase separation (NIPS) (Pinnau and Koros, 1993) processes, which involve the dissolution of polymer in toxic organic compounds. The porous structure forms during phase separation, induced either by thermally cooling of polymer solution or by adding a non-solvent. A serious drawback of these processes is the use of large amounts of expensive, harmful and partly flammable compounds (solvents) which have to be removed after membrane formation via several intense washing procedures, making the process uneconomic and not environmentally benign. Besides the above mentioned disadvantages, these processes suffer from low production rate due to the slow liquid-liquid phase separation phenomenon (Krause et al., 2001).

Taking into consideration the drawbacks mentioned above, it seems worth using solvent-free alternative methods for the fabrication of porous polymeric membranes. Only a few solvent-free methods for preparation of porous polymeric membranes have been proposed in the literature (Gore, 1976; Lin et al., 2009; Xi et al., 2008) the most important of which is the melt-spinning and stretching method. It is based on the melt extrusion of pure semi-crystalline polymers to form flat or hollow fiber precursors, followed by axial stretching of such precursors to form a porous structure. This technique is only applicable to semi-crystalline polymers, and in addition to the mechanical stretching process, it requires several thermal post-treatments to promote crystallinity and avoid membrane shrinkage (Kim et al., 1994).

There are few studies in the literature on the fabrication of open-cell foams containing polymer/filler composites using leachable salts with PP (Chu et al., 2009) polymethylmetacrylate (PMMA), polysulfone (PSF) and polystyrene (PS) (Narkis and Joseph, 1978), LDPE (Dangtungee and Supapol, 2010) and polyurethane rigid (PU) foams

(Verdolotti et al., 2011). Despite the importance of porous polymeric materials, little attention was given to the use of open-cellular foams prepared via salt leaching from polymer/salt composite matrix for membrane applications. However, the leaching process, which is the most important part of this technique, still remains noticeably untouched. Long leaching times (around 90 h) and batch-wise leaching process as post-treatment, make this process industrially inapplicable. Moreover, none of the abovementioned studies concentrate on the control of salt particle size, salt content and the final product shape (only film products were prepared). On the other hand, inhomogeneity and large particle size of salts (45-850 μm) make these foams inappropriate for membrane applications.

This work proposes to exploit a hybrid process which combines *melt extrusion* with *continuous template-leaching* techniques, as a novel solvent-free method for hollow fiber membrane fabrication (Mosadegh Sedghi et al., 2012b). In addition to a porous structure, this method provides an effective roughness on membrane surface and therefore, a significant decrease of membrane wettability. Compared to the methods mentioned above, the proposed method is simple, does not require post treatments, and is cheap and gentle for the environment. The fabricated membranes were characterized in terms of morphology, porosity and pore size distribution, surface roughness and hydrophobicity, as well as mechanical properties.

2.2. Experimental

2.2.1. Material

LDPE used in this work was Novapol LA 0219-A (Nova Chemicals) with a density of 919 kg/m^3 (ASTM D792) and a melt index of 2.3 g/10 min (ASTM D1238). NaCl (SODA-LO 20) with particle size of 5-10 μm was supplied by Main Street Ingredients.

2.2.2. LDPE hollow fiber fabrication

The melt-extrusion system used for LDPE hollow fibers fabrication is shown in Fig. 2.1 (detailed information about the extrusion process is given in Appendix A). LDPE hollow fiber membranes were produced using a Haake Rheomix TW-100 co-rotating twin-screw extruder. LDPE pellets were mixed thoroughly with NaCl particles to form blends

containing 35, 40, 50, 60, 65 and 68 wt% salt. For comparison, a nonporous LDPE hollow fiber sample (blank) was also prepared without the addition of salt. The mixture was then fed into the extruder in two steps using a hopper. In the first step, the mixture was melt blended above the melting temperature of LDPE to obtain a uniform polymer/salt blend. The temperature profile was controlled at 115°C for zone 1, 135°C for zone 2 and 140°C for zone 3 and the die zone (zone 4). After cooling down through a water bath at room temperature, the extrudate was pelletized using a PELL 2 pelletizer supplied by Berlyn Company (not shown). For the nonporous (blank) LDPE hollow fiber sample, the first extrusion step was skipped. In the second step, the prepared pellets were fed into the extruder using the hopper at a temperature of 115°C for zone 1, 135°C for zone 2 and 140°C for zones 3 and 4. The extruder was operated at a constant mass flow rate of 0.4 kg/h and a screw speed of 60 rpm. To produce a stable hollow fiber structure, the inside air pressure was controlled to prevent collapse. The extrudate was taken out of the hollow fiber die with an inside and outside diameters of 5 and 7 mm, respectively, and cooled down through a water bath fed by a fresh water spray and emptied by salt-rich water drains at 60°C. Finally, a take-up unit was used to control drawing speed at 250 cm/min. Detailed specifications of microporous LDPE hollow fiber membranes fabricated by this method are given in Table 2.3.

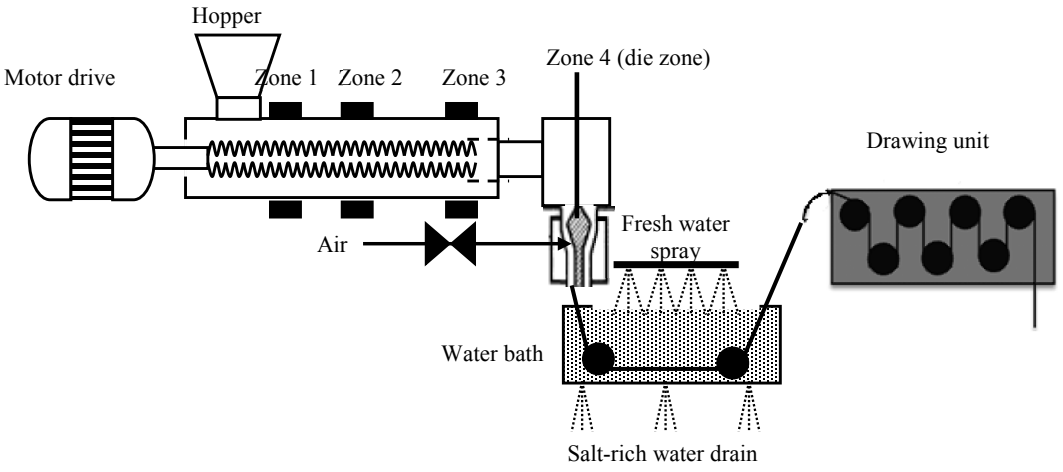

Figure 2.1. Melt-extrusion, cooling and drawing system for hollow fiber precursor fabrication.

Alternatively, in a batch-wise leaching process, 30 mm of prepared hollow fiber samples were placed in small vials, fully filled with water. The vials were sealed thoroughly and kept for 160 min in an oven at 60°C to enhance the leaching process. Water was changed every 20 min to avoid saturation.

Table 2.3. General specifications of LDPE hollow fibers.

Fiber characteristics	Blank LDPE	LDPE-35 wt% NaCl	LDPE-40 wt% NaCl	LDPE-50 wt% NaCl	LDPE-60 wt% NaCl	LDPE-65 wt% NaCl	LDPE-68 wt% NaCl
Outer diameter (mm)	2.66	2.75	2.79	2.62	2.45	2.62	2.60
Inner diameter (mm)	1.90	2.05	2.05	2.11	1.88	2.01	1.99
Thickness (mm)	0.38	0.34	0.37	0.25	0.28	0.30	0.30

2.2.3. Membrane characterization

2.2.3.1. Salt removal and formation of porous structure

The porous structure of the LDPE hollow fibers was formed by removal of salt particles using a water leaching technique. The amount of salt removal was determined by comparing the dry weight of each specimen before and after leaching, using a high-resolution Mettler AE 240 digital balance. In addition, the content of salt remained in/removed from LDPE hollow fiber membranes with different initial salt content was confirmed by thermogravimetric analysis (TGA) of fresh fibers (before leaching) and fibers leached with water for 160 min (after leaching), using a TA Instruments TGA model Q5000 IR from ambient temperature to 950°C at a heating rate of 10°C/min under air.

The porosity of the hollow fiber membranes (P) was determined via density measurements using Eq. (2.1):

$$P(\%) = \left(1 - \frac{\rho_1}{\rho_0}\right) \times 100 \tag{2.1}$$

where ρ_0 is the density of the nonporous LDPE hollow fiber (blank) and ρ_1 is the density of porous LDPE hollow fiber membranes with different initial salt contents. ρ_0 and ρ_1 were calculated by measuring the volume and the weight of hollow fiber samples as (the same relation is used for both ρ_0 and ρ_1):

$$\rho_1 = \frac{W}{\pi L\left(R^2 - r^2\right)} \tag{2.2}$$

where W is the weight of the hollow fiber, R and r are the outer and inner radius, respectively, and L is the length of the hollow fiber. The porous structure of hollow fiber membranes was investigated using a scanning electron microscope (SEM) (JEOL Ltd., JSM-840a). Pore diameter distributions were calculated by digitizing and analyzing the SEM images using Image-Pro Plus version 5.0 software (Media Cybernetics Inc.).

2.2.3.2. Roughness measurements

AFM studies were conducted in tapping mode on the interior surface of hollow fibers using a Nanoscope III equipped with a 1553D scanner (Veeco Instruments Inc.). Samples were prepared by cutting the membranes longitudinally in very narrow ribbons of less than 1 mm width and 5 mm length. Analysis was done on the membranes with 40 and 60 wt% of initial salt content, as well as on nonporous LDPE hollow fiber (blank) for comparison.

Mean surface roughness (R_a), maximum roughness (R_{max}) and RMS values (R_s) were determined using the Veeco NanoScope Software (version 5.30). R_a and R_s are calculated as:

$$R_a = \sqrt{\frac{\sum_{i=1}^{N}\left(Z_i - Z_{ave}\right)^2}{N}} \tag{2.3}$$

$$R_s = \frac{\sum_{i=1}^{N}\left|Z_i - Z_{cp}\right|^2}{N} \tag{2.4}$$

where N is the number of points in the measured surface area, Z_i is the vertical scanner tip

position at a given position of the image, Z_{ave} is the average Z value and Z_{cp} is the Z value of the center plane.

2.2.3.3. Contact angle measurements

The optical contact angle analyzer (OCA15 EC Plus, DataPhysics) was used to measure water contact angle of LDPE hollow fibers using the sessile drop method. The system included a high resolution camera and specific software developed to capture and analyze the contact angle on very small and curved surfaces. For very precise measurements, water droplets of 0.15 µl were dispensed on both inner and outer surfaces of hollow fiber samples via an ultra-thin needle with an internal diameter of 0.18 mm. For each experimental condition, measurements were performed on at least three samples and on three different portions of each sample in order to ensure the reproducibility of the results. The reported contact angle data represent the average of three experimental values.

2.2.3.4. Mechanical properties

Mechanical properties of LDPE hollow fiber membranes including tensile strength, Young's modulus, and elongation at break were measured using a universal mechanical analyzer from Instron model 5565. During the test, the hollow fiber membranes were stretched at a constant rate of 50 mm/min until break-up. The data reported for each property is the average of at least 4 measurements.

2.3. Results and discussion

2.3.1. Formation of porous structure

Fibers containing 35-68 wt% salt were produced using the system schematized in Fig. 2.1. 35 wt% was selected as the lower limit of salt content because lower content did not produce porous structures after salt leaching. On the other hand, 68 wt% was selected as the upper limit because of operational restrictions; for higher salt content, the mechanical/rheological properties were too weak for the fiber to be drawn via the drawing system. Before the fiber fabrication process, an additional extrusion step was carried out to assure good distribution of salt particles in the polymer melt. After fiber fabrication via the second extrusion step, salt particles were leached either through batch-wise or via the

continuous leaching process, as described before (§2.2). In order to accelerate the leaching, the process was performed at around 60°C. With the increase of temperature, NaCl solubility in water increases and the diffusion process is accelerated, reducing therefore the leaching time. However, the leaching temperature is limited by the polymer deformation that begins at around 85°C, as well as for economic considerations (energy required for heating water, water losses by evaporation). 60°C was found sufficiently high to reduce efficiently the leaching time and sufficiently far from causing modifications in the polymer structure. Except for increasing the temperature, the leaching time can also be reduced by a great extent by intensifying the mass transfer at the liquid/membrane interface, which can be achieved by creating turbulence in the water bath via a shower-like water distribution (Fig. 2.1).

Since the formation of a porous structure strongly depends on the amount of salt removed from the fiber matrix, it is essential to determine the level of salt removed from LDPE/salt fibers. The amount of salt removed from LDPE/salt hollow fibers was obtained by comparing the dry weight of each sample before and after leaching in water. The amount of salt removal (% salt removal) was calculated according to the following relation:

$$\%salt\ removal = 100\frac{\%weight\ loss}{\%initial\ salt\ content} \tag{2.5}$$

Fig. 2.2 shows the amount of salt removed from LDPE hollow fibers for each of the salt content used. The amount of salt removal was found to increase with increasing the initial salt content from 35 to 68 wt%. The values vary from around 3 to 5% for samples with initial salt contents of 35 and 40 wt% to about 100% for those containing 60 to 68 wt% NaCl. This can be attributed to the increasing number of pathways formed by the interconnections of salt particles, as they get closer together with the increase of salt content. These interconnecting pathways provide better access to water for leaching out the salt particles.

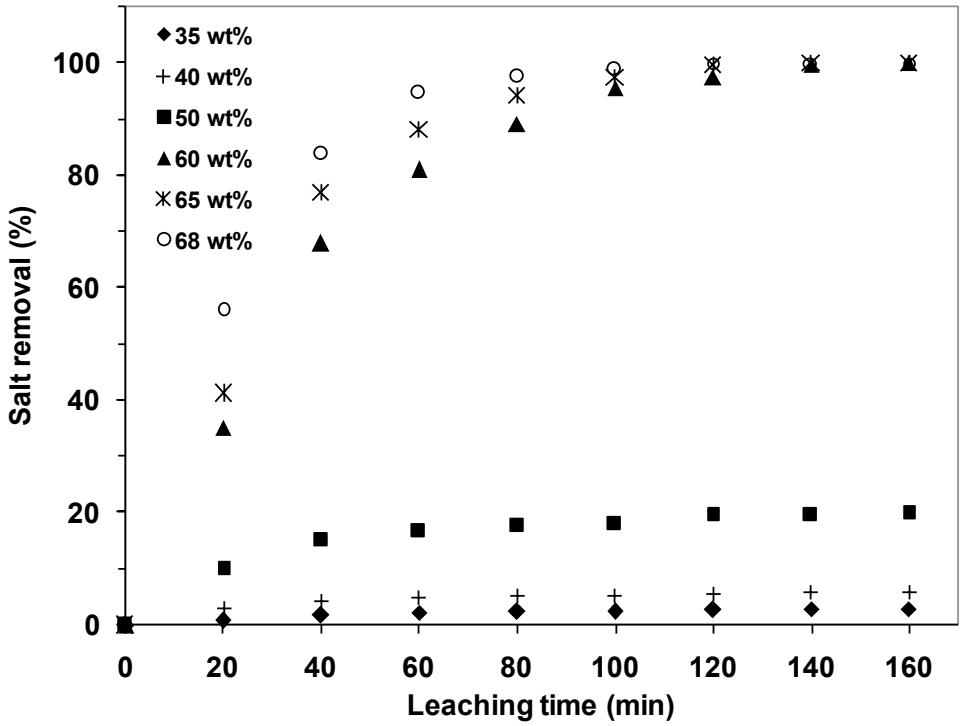

Figure 2.2. Amount of salt removal from hollow fiber membranes with different initial salt contents.

TGA curves of LDPE hollow fiber membranes with various initial salt contents are presented in Fig. 2.3. At a temperature range of around 300-500°C, a weight loss of about 70% was observed, due to the polymer thermal degradation.

After the complete degradation of the polymer matrix, the sample weight remains constant and the weight in this region (500-750°C) is equivalent to the salt content in the corresponding sample. The lower salt contents shown by TGA than those initially blended with the polymer can be attributed to losses during fabrication (Table 2.4). The second loss around 750°C can be associated to NaCl degradation.

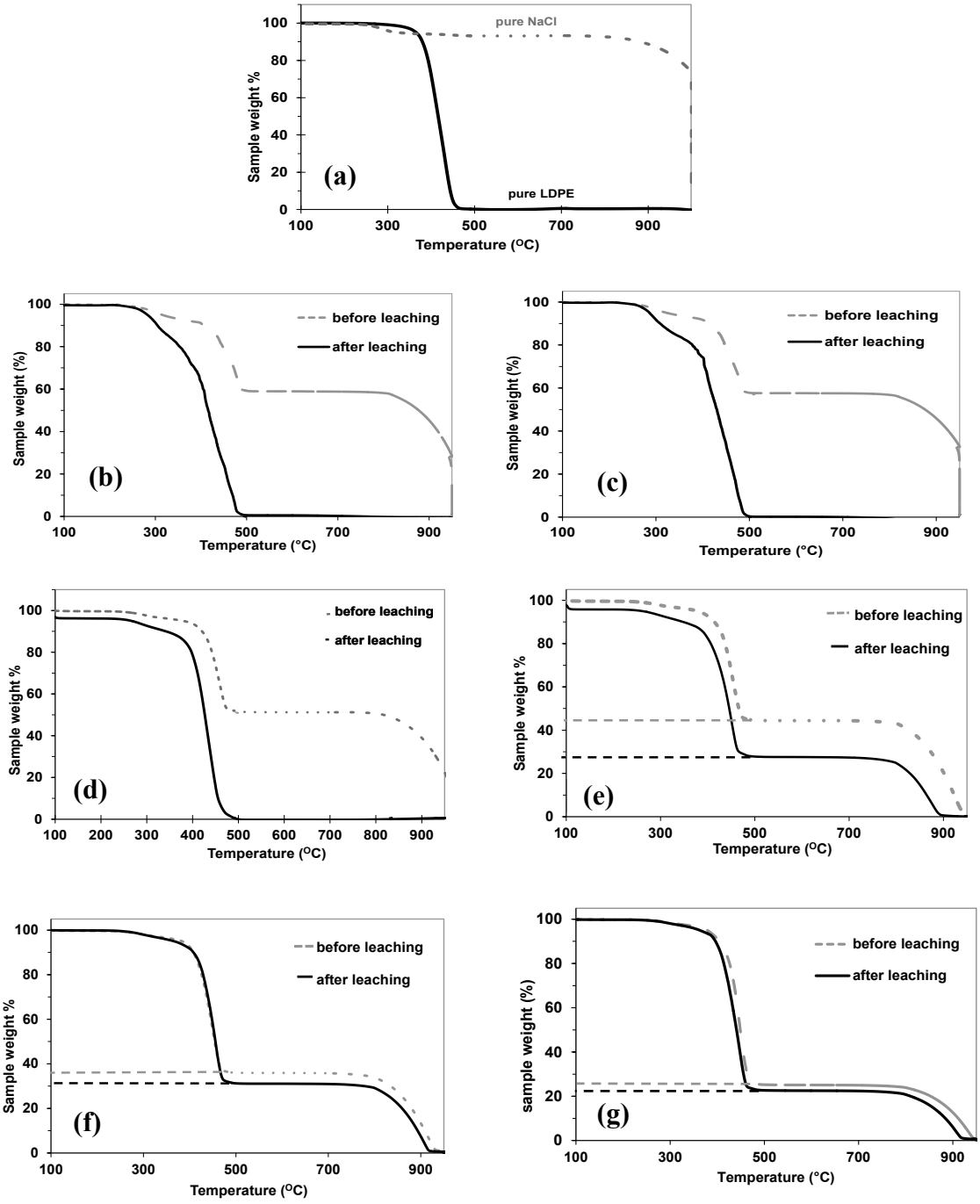

Figure 2.3. Thermogravimetric analysis (TGA) curves for a) pure LDPE and pure NaCl; and LDPE hollow fiber membranes with initial salt content of: b) 68 wt%, c) 65 wt%, d) 60 wt%, e) 50 wt%, f) 40 wt% and g) 35 wt%.

Table 2.4. Salt loss in the 1st and the 2nd extrusion steps.

wt% salt before extrusion (in polymer/salt blend)	wt% salt after 1st extrusion step (blending)	wt% salt after 2nd extrusion step (fiber fabrication)	% salt loss in the 1st extrusion step	% salt loss in the 2nd extrusion step
35	27	25	22	7.0
40	37	36	7.5	2.7
50	42	44	16	4.7
60	56	53	7.1	3.5
65	59	57	9.2	3.3
68	61	59	10.2	3.3

From the TGA analysis, several conclusions can be drawn. The real initial salt content for all samples was found to be lower than that initially mixed with PE. This can arise either from the loss of ultra-fine salt particles from the hopper or due to their sticking inside the extruder. Moreover, for samples with an initial salt content lower than 60 wt%, leaching was never complete, even after 160 min of continuous leaching. This demonstrates that the amount of salt removal increases with increasing initial salt content and was confirmed by comparing the SEM micrographs of LDPE hollow fibers with 0-68 wt% initial NaCl content (Figs. 2.4 and 2.5). It can be clearly observed that the structure of hollow fibers changed from dense and nonporous (Fig. 2.4), to porous and highly rough with a large number of micropapillas on the surface, as the salt content increased up to a maximum of 68% (Fig. 2.5).

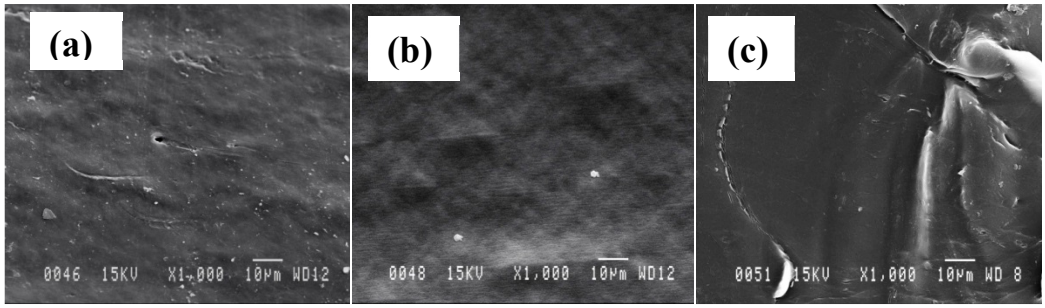

Figure 2.4. SEM micrographs of blank LDPE hollow fiber: a) exterior surface, b) interior surface and c) cross-sectional edge.

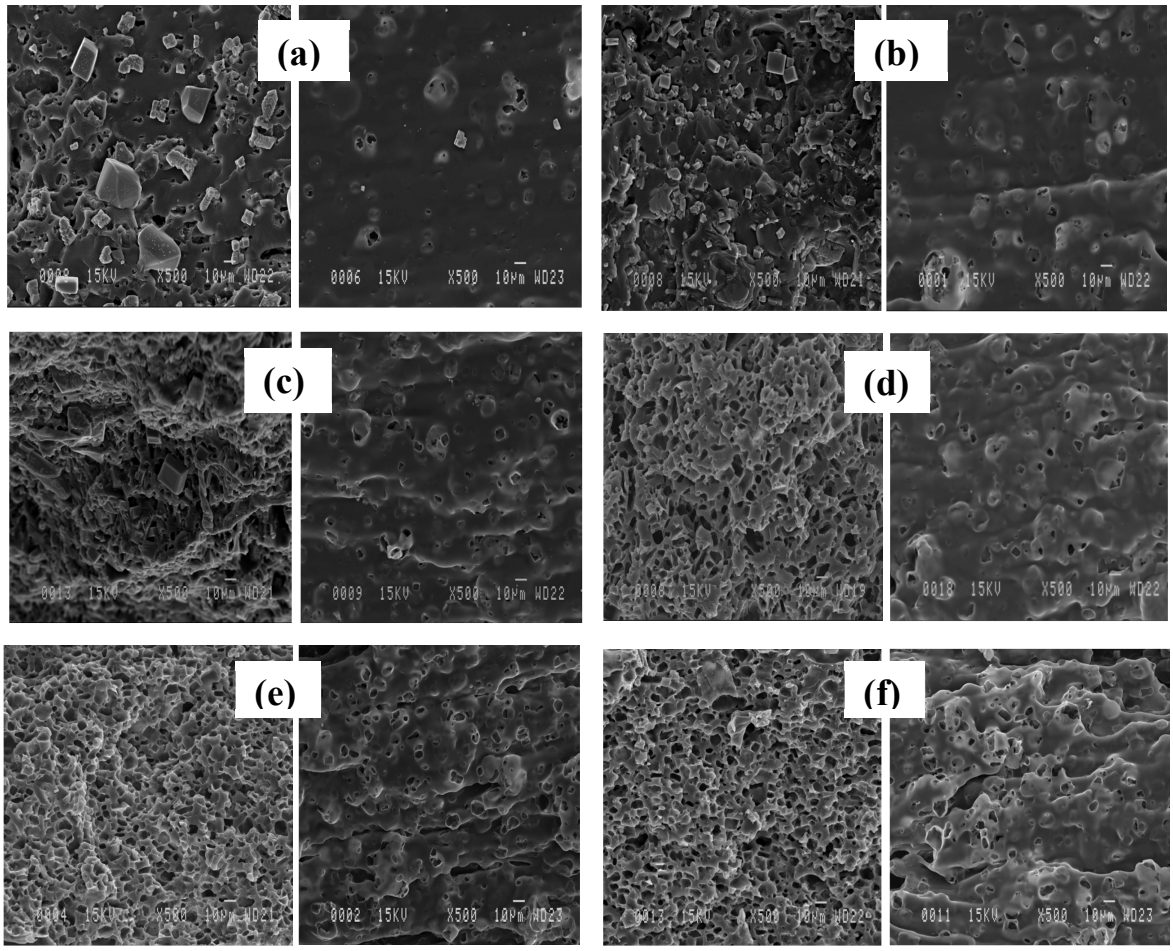

Figure 2.5. SEM micrograph of cross-sectional (left side) and internal surfaces (right side) of LDPE hollow fiber membranes with initial salt contents of: a) 35 wt%, b) 40 wt%, c) 50 wt%, d) 60 wt%, e) 65 wt% and f) 68 wt %.

In addition, the SEM micrographs of the hollow fiber cross-sections (Fig. 2.5) show that the porous structure becomes more interconnected through the thickness, as the initial salt content increases from 35 to 68 wt%. On the other hand, the cross-section images of samples with initial salt contents of 35-50 wt% (Fig. 2.5a-c, left hand side), show square NaCl crystals which are close to the fiber surface, but do not touch the crystals at the surface and therefore, remained unleached even after 160 min of washing. The number of crystals present on the fiber surface (Fig. 2.5a-c, right hand side) is much smaller than those remaining in the center of the fiber (Fig. 2.5a-c, left hand side), which is probably related to the higher interconnection needed to reach crystals in the center of the sample as compared to those close to the surface. The remaining salt crystals amount decreases as the initial salt

content increases from 35 to 50 wt% and becomes totally absent for initial salt content of 60-68 wt%.

Density and porosity of LDPE hollow fiber membranes are presented in Table 2.5.

Table 2.5. Density and porosity of LDPE hollow fiber membranes.

Fibers	**Density (g/cm^3)**	**Porosity (%)**
Blank (neat)	0.92	-
35 wt% NaCl	1.17	9
40 wt% NaCl	1.04	13
50 wt% NaCl	0.93	26
60 wt% NaCl	0.72	49
65 wt% NaCl	0.72	49
68 wt% NaCl	0.70	51

In accordance with SEM micrographs, the porosity of hollow fiber samples increases from 0% for blank LDPE hollow fibers to about 51% for LDPE hollow fiber membranes with 68 wt% initial salt content. Furthermore, the density of hollow fiber samples is inversely proportional to the initial salt content and fiber porosity.

Fig. 2.6 shows the pore size distribution of LDPE hollow fiber membranes after complete salt removal (samples prepared using 60-68 wt% salt). For all membranes, the maximum pore diameter is in the 2-5 μm range. In addition, the pore diameter slightly decreases with increasing the initial salt content.

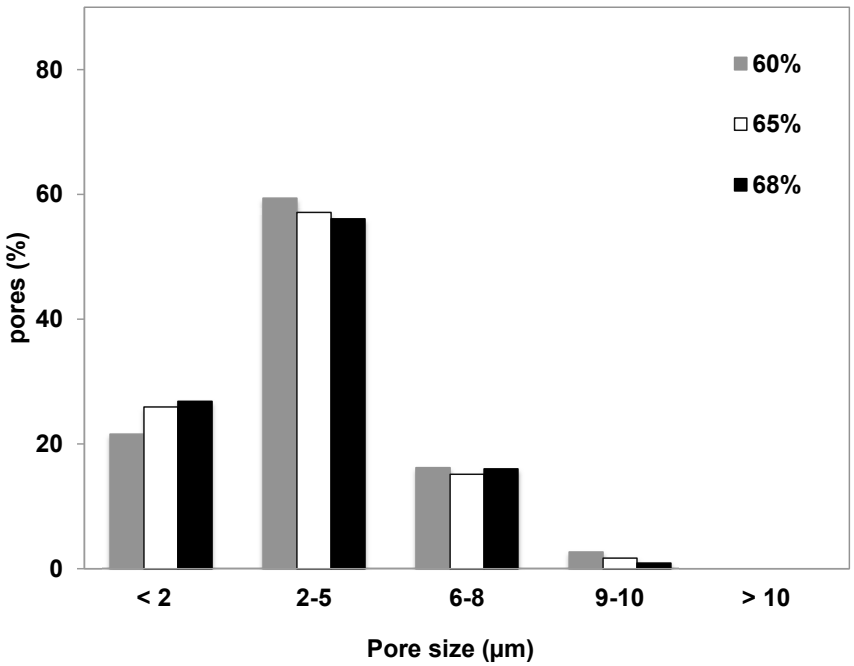

Figure 2.6. Pore size distribution of LDPE hollow fiber membranes with different initial salt contents (35-68 wt%).

2.3.2. Roughness

AFM micrographs of LDPE fibers and the roughness parameters are shown in Fig. 2.7 and Table 2.6 for blank LDPE hollow fibers and membranes with initial salt content of 40 and 60 wt%. The Z scanning scale corresponding to changes in sample height rises from 600 nm for the blank sample to 7.1 µm for the sample with initial salt content of 60 wt% (Fig. 2.7). This important increase is due to the formation of micropapillas; it clearly shows the significant increase of the surface roughness using this microporous membrane manufacturing technique.

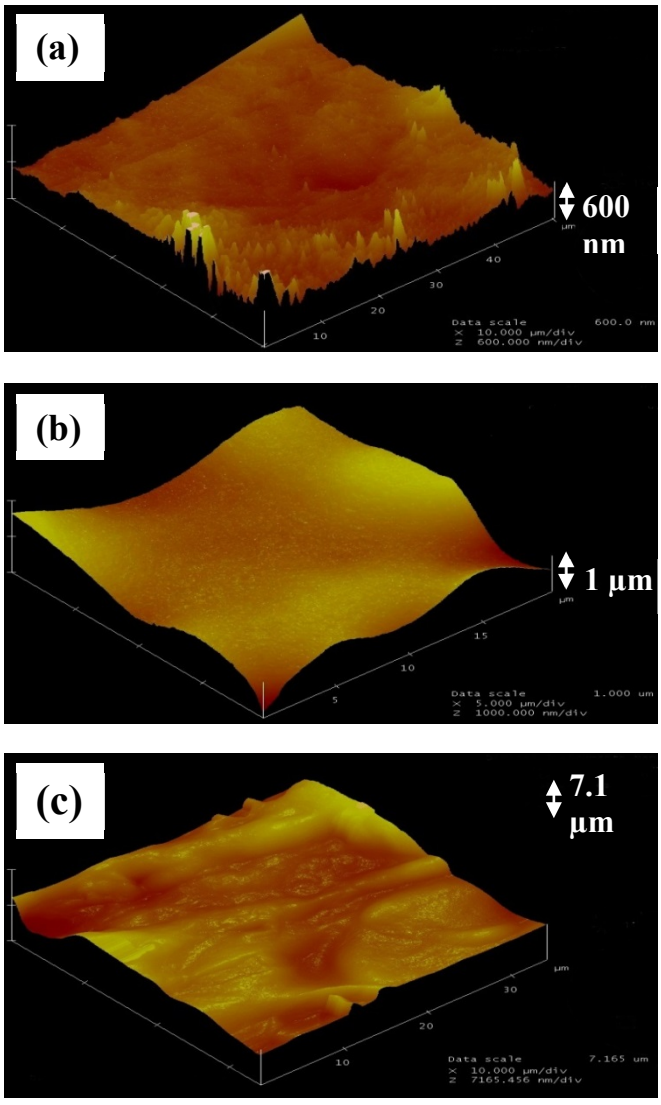

Figure 2.7. AFM analysis of a) blank LDPE hollow fibers, b) LDPE hollow fiber membrane with initial salt content of 40 wt% and c) LDPE hollow fiber membrane with initial salt content of 60 wt%.

Moreover, the increase in the salt content leads to the formation of higher micropapillas. In addition, as shown in Table 2.6, the mean roughness (R_a) increases with increasing the salt content, from 70.3 nm for the smooth surface of the blank LDPE hollow

fiber to about 157 and 681.2 nm for membranes with 40 and 60 wt% initial salt content, respectively.

Table 2.6. Roughness parameters of LDPE fibers (scan size = 5 μm × 5 μm).

Hollow fibers	R_a (nm)	R_s (nm)	R_{max} (μm)
blank	70.3	99.0	1.4
40 wt%	157.0	195.3	1.5
60 wt%	681.2	825.1	6.1

2.3.3. Contact angle

The static water contact angle of LDPE hollow fiber samples is presented in Table 2.7. It can be clearly observed that the contact angles, for both inner and outer surfaces, increase with increasing the initial salt content.

Table 2.7. Water contact angle of inner and outer surfaces of LDPE hollow fibers.

Membrane	Contact angle (°)		Uncertainty (°)	
	Inner surface	Outer surface	Inner surface	Outer surface
Blank (neat)	98.6	98.2	0.6	0.5
35 wt% NaCl	100.0	98.6	0.6	0.9
40 wt% NaCl	100.9	98.6	0.7	1.2
50 wt% NaCl	105.1	100.3	1.2	0.8
60 wt% NaCl	120.2	117.1	2.4	1.3
65 wt% NaCl	128.5	120.0	1.0	1.2
68 wt% NaCl	129.9	121.4	1.9	0.9

In all cases, the contact angles of inner surfaces are higher than those for outer ones. For the sample with 68 wt% initial salt content, the inner surface contact angle reaches to about 130°. This is attributed to the higher surface roughness caused by the increase in the

number of micropapillas and the high porosity membrane structure, as a result of the increase of the initial salt content. The surface of microporous LDPE hollow fibers can be considered as a composite comprising trapped air and rough LDPE. According to the Cassie and Baxter theory (Cassie and Baxter, 1944), the contact angle of a hydrophobic rough surface comprising solid and air can be determined using the following relation:

$$\cos\theta_r = f_1 \cos\theta - f_2 \tag{2.6}$$

where θ and θ_r represent, respectively, the contact angle of smooth and rough surface, and f_1 and f_2 are, respectively, the fractions of solid and air in the composite surface. This equation predicts that increasing the fraction of air (f_2) would lead to the increase in the contact angle. Since roughness and porosity increase with increasing initial salt content, more air can be trapped in the pores and surface valleys leading to higher contact angles. This remarkable increase in contact angles with initial salt content can arise from the lower tendency of the surface to wetting and is considered as the "lotus effect" which can be mimicked in artificial highly hydrophobic surfaces (Lu et al., 2004, Franco et al., 2008; Yuan et al., 2008). By increasing the initial salt content, much rougher surfaces are obtained (Fig. 2.7 and Table 2.6), resulting in a lower contact between the sample surface and the testing liquid.

2.3.4. Tensile properties

The tensile properties of LDPE hollow fiber samples (neat LDPE and fibers with 40-68 wt% initial salt contents), in terms of Young's modulus, tensile strength and elongation at break are presented in Table 2.8. It can be seen that Young's modulus increases with increasing the initial salt content, reaches a maximum around 50 wt% salt and then decreases. The increase of Young's modulus from 135 MPa for neat LDPE to 154 and 164 MPa, respectively for samples with 40 and 50 wt% initial salt is attributed to the large amount of salt remaining in the samples after leaching (Fig. 2.3e-f) which increases the fiber rigidity. However, the reduction of modulus with further increase in initial salt content is related to the formation of the porous structure. In this case, the porous fibers can be considered as a composite material, comprising voids as the dispersed phase (trapped gas in

the membrane pores) and the LDPE matrix as the continuous phase. By increasing the initial salt content, the volume fraction of voids increases after leaching, leading to a lower amount of material able to sustain the applied stresses. The same trend can be seen for the tensile strength results. These results are in agreement with the micrographs presented in Fig. 2.3e-f; the reduction of tensile strength with increasing the initial salt content can be related to the combined effects of residual salt particles inside the LDPE structure and those removed by leaching to form the porous LDPE structures (Dangtungee and Supapol, 2010). The slight increase in the stress at break for the sample with 68 wt% initial salt content compared to the one at 60 wt% could be attributed to a change in the volume fraction of open/close pores as the porosity increases. This effect was observed earlier by Narkis et al. (1978) Finally, elongation at break was found to drop sharply initially (0-50 wt% NaCl), but less at higher salt contents (60-68 wt%) as the materials are already brittle (low elongation at break). Such observations are in good agreement with tensile properties reported in the literature for porous polymeric membranes and rigid particle filled polymeric composites (Cassie and Baxter, 1994; Childress et al., 2005; Dangtungee and Supapol., 2010; Verdolotti et al., 2011; Mosadegh Sedghi et al, 2012b).

Table 2.8. Tensile properties of LDPE hollow fibers with different initial salt contents.

Salt content (wt%)	Young's modulus (MPa)	SD (MPa)	Tensile strength (MPa)	SD (MPa)	Elongation at break (%)	SD (%)
0	135.3	0.8	11.2	1.5	807.2	6.5
40	154.1	0.2	6.5	0.3	106.0	6.6
50	164.0	5.5	5.6	0.1	20.5	4.2
60	38.4	0.7	3.6	0.1	51.9	7.3
68	31.7	0.3	4.0	0.2	74.7	6.9

SD: standard deviation

2.4. Conclusions

Highly hydrophobic microporous LDPE hollow fiber membranes were prepared using melt extrusion of LDPE/NaCl blends followed by salt leaching in water. Membrane

porosity, which is strongly dependent on the amount of salt removed from the hollow fiber structure, increased with increasing initial salt content. Due to the presence of micropapillas, the roughness created on the membranes surface led in a remarkable increase in hydrophobicity from 98^{o} for neat LDPE to 130^{o} for hollow fibers prepared with 68 wt% NaCl. The mechanical properties reported (Young's modulus, tensile strength and strain at break) were shown to be highly dependent on initial salt content, but can be directly related to the final structure of the hollow fiber through the porous structure produced.

The compatibility between membranes and absorption solutions is crucial for efficient application in gas separations using GLMC. The chemical stability of the membrane material (LDPE) in contact with aqueous MEA solution (the most used absorbent for acid gas separation in industry but also the most corrosive one), before and after the contact with CO_2, was first investigated in detail and is the object of the following paper (Chapter 3). To better understand whether LDPE undergoes chemical degradation in contact with MEA and to eliminate the possible interference of pore structure, non-porous LDPE fibers were used.

Chapter 3

Chemical alteration of LDPE hollow fibers exposed to monoethanolamine solutions used as absorbent for CO_2 capture process

Résumé

L'effet de la monoéthanolamine (MEA) sur la surface des fibres non poreuses en polyéthylène de basse densité (LDPE), destinées à être utilisées dans les contacteurs à membrane, a été étudié. Les fibres creuses en LDPE ont été maintenues en contact avec une solution de MEA (fraiche et après absorption du CO_2) pour des durées variant de 8 à 45 jours à différentes températures et pH de la solution. Les analyses d'angle de contact, Spectroscopie Infrarouge à Transformée de Fourier (FT-IR) et Spectrométrie Photoélectronique X (XPS) ont été effectuées afin de contrôler les changements chimiques sur la surface de la membrane.

Après contact entre les fibres et les solutions fraiches de MEA pendant une durée prolongée (plus de 8 jours) suivi par le lavage des échantillons avec de l'eau, l'analyse XPS a montré une augmentation du contenu d'oxygène et d'azote dans les fibres. De plus, les spectres FT-IR ont montré la présence de groupements carbonyle et amide à la surface de la fibre. Ces groupements ont été trouvés en quantité plus importante à des températures plus élevées. Il est suggéré que les fibres creuses en LDPE subissent une dégradation oxydative. La réaction entre la MEA et les groupements carbonyle générés par oxydation sur la surface du LDPE peut conduire à la formation des groupements amide. D'autre part, les mesures d'angles de contact ont montré que l'hydrophobicité des fibres creuses a diminuée suite à l'augmentation de leur énergie de surface, ce qui peut conduire à la réduction de la stabilité à long terme des membranes dans les contacteurs à membrane. Toutefois, sur la base des analyses FT-IR et des mesures d'angle de contact, la dégradation chimique du LDPE a été moins importante en présence de CO_2 due à la réduction du pH des solutions de MEA suite à l'absorption du CO_2, ce qui a conduit à une altération beaucoup plus lente de l'hydrophobicité de la membrane.

Abstract

The effect of monoethanolamine (MEA) on the surface of non-porous low density polyethylene (LDPE) hollow fibers aimed to be used in membrane contactors was investigated. LDPE hollow fibers were kept in contact with MEA solution (fresh (unloaded) or after CO_2 loading) for lengths of time varying from 8 to 45 days, at different temperatures and solution pH. FT-IR, XPS and contact angle were performed in order to monitor chemical changes on the membrane surface.

After keeping the fibers in contact with unloaded MEA solutions for prolonged time (more than 8 days) and thoroughly washing the samples with water, XPS analysis showed an increase in oxygen and nitrogen content of hollow fibers. In addition, FT-IR spectra showed the presence of carbonyl and amide groups on the LDPE hollow fiber surface. These groups were found to be in more significant quantity at higher temperatures. It is suggested that the LDPE hollow fibers undergo oxidative degradation. The reaction between MEA and carbonyl groups generated by oxidation on the LDPE surface might lead to the formation of amide groups. On the other hand, contact angle measurements showed that the hydrophobicity of hollow fibers decreased as the result of the increase in their surface energy, which can reduce the long-term stability of membranes in membrane contactors. However, based on both FT-IR and contact angle measurements, LDPE chemical degradation was found to be less important in the presence of CO_2 due to the reduction of the pH of loaded MEA solutions, leading to a much slower alteration of the membrane hydrophobic properties.

3.1. Introduction

Carbon dioxide (CO_2) is one of the major greenhouse gases and thus is believed to be the main responsible factor for increasing the earth's surface temperature. CO_2 is mainly produced in large amounts by different industrial processes connected to oil refineries, cement works, and steel and iron production (IPCC, 2005). Conforming to the *Canadian Environmental Protection Act* (CEPA, 1999), Canadian companies are pushed to reduce their greenhouse gas emissions. Various separation processes for CO_2 removal have been developed such as absorption, adsorption, membrane and cryogenics (Rao and Rubin, 2002). Among them, absorption (especially using amine-based absorbents) is the most common industrial process mainly due to its highest CO_2 removal efficiency (Yang et al., 2008). Conventionally, the gas absorption process is carried out in different units such as bubble columns, sieve trays or packed towers. Due to the direct contact of the two fluid phases (G and L), the use of conventional gas-liquid contactors often leads to several technical problems such as foaming, emulsions, unloading and flooding. An alternative technology that overcomes operational problem of conventional contactors and also offers substantially more interfacial area than conventional approaches is non-dispersive contact via a microporous membrane. The use of membrane contactors has various advantages over the traditional gas absorption processes: (i) large contact area for promoting an efficient gas-liquid mass transfer, (ii) high modularity and compatibility for an easy scale-up, (iii) the possibility of varying stream flow rates independently and without the occurrence of loading or flooding (Gabelman, 1999; Li and Chen, 2005). The contact between the gas and the liquid is made after the gas diffuses through the membrane pores. In non-wetting conditions, the gas-liquid interface is then formed at the pore openings adjacent to the liquid (Falk-Pedersen et al., 1997).

One of the potential problems associated with membrane contactors is the reduction in membrane morphological and chemical stability, resulting in a decrease in their performance and efficiency. Few works available in the open literature concern *morphological changes* of polyolefin membranes in contact with different solutions. Barbe et al. (2000) reported surface morphological changes of microporous polypropylene flat membranes after 72 h contact with water, which was attributed to the effect of pore

intrusion by the liquid meniscus. Similar behaviour was observed in the case of polypropylene (PP), polyvinilydene fluoride (PVDF), polyethersulfone (PES) and polystyrene (PS) membranes exposed to various liquid absorbents such as alkanolamine solutions, selexol and dimethyl formamide (Kumar et al., 2002; Dindore et al., 2004; Wang et al., 2004a). Porcheron and Drozds (2009) attributed the partial wetting of membrane pores wetting to a possible plasticizing effect of CO_2 in membranes inside the contactors. *Chemical degradation of polyolefin materials* was investigated by different groups (Bevilacqua, 1964; George and Chaemy, 1991; Henry et al., 1992; Gugumus, 2001; Massey et al., 2007). It was shown to be mainly due to the well-known auto-oxidation phenomenon in air (Bevilacqua et al., 1964; George and Chaemy, 1991; Gugumus, 2001). Bevilacqua et al. (1964) proposed a mechanism for polyethylene oxidation by nucleophilic attack of peroxy anions on hydroperoxides. In this mechanism, acetic acid, formic acid and acetone were reported to be the main polyethylene oxidation products. Messey et al. (2007) showed that, at room temperature, LDPE oxidation is accelerated in the presence of water due to a "hydrolytic degradation" mechanism, leading to the generation of ketone and alcohol groups. In addition, the impact of carbonyl group (main polyolefin oxidation product) concentration on oxidation rate of polyolefins in aqueous media was monitored by Henry et al. (1992). The authors showed that alkaline and neutral aqueous environments accelerate the thermal oxidation of polyolefins in comparison to that in air, whereas acidic solutions can significantly retard this phenomenon.

To our knowledge, only few studies concern *chemical degradation of polyolefin based membranes* (Wang et al., 2004a; Franco et al., 2008; Lv et al., 2010). Wang et al. (2004a) studied the influence of diethanolamine (DEA) on polypropylene hollow fiber membranes. Based on XPS analysis results, they reported the possibility of chemical reaction between polypropylene and DEA, which may be responsible for the membranes surface energy changes, leading to a deterioration of membrane hydrophobicity. Franco et al. (2008) analysed the interaction between polypropylene hollow fiber membranes and MEA solution after 68 h use for CO_2 capture in membrane contactors. The authors observed an increase in elemental oxygen of polypropylene membrane surface from 0.78 to 1.49%, which could be attributed to the oxidation of polypropylene. Lv et al. (2010)

investigated the changes in surface hydrophobicity of polypropylene hollow fiber membranes in contact with amine solutions. The authors mentioned that improving surface hydrophobicity of membranes may be an effective way of overcoming wetting problem.

In our laboratory, extensive studies concerning the CO_2 capture in membrane contactors are in progress. As the performances of membrane contactors strongly depend on the properties of both absorption liquid and membrane and on the compatibility between them, the proper choice of the membrane/absorption liquid combination is a crucial step in developing CO_2 absorption modules. The present study focuses on the chemical stability of hollow fiber membranes fabricated from LDPE upon exposure to MEA aqueous solutions used as absorbent for CO_2 capture in membrane contactors. MEA based absorbents have a considerable interest in the CO_2 absorption process due to the fast reactivity with CO_2 through the formation of stable carbamates. This work aims to shed light upon whether LDPE membranes undergo chemical changes in presence of MEA solutions (with and without CO_2 loading), and if so, how different parameters including temperature, contact time, washing duration and solution pH can influence such changes. In order to provide a better understanding of the chemical degradation in LDPE hollow fibers upon exposure to MEA based absorbent in the absence and in the presence of absorbed CO_2, a combination of FT-IR spectroscopy, XPS analysis, surface tension and contact angle measurements was considered. To our knowledge, no similar study is available in the open literature.

3.2. Experimental methods

3.2.1. Chemicals and materials

99% grade monoethanolamine (MEA) supplied by Sigma-Aldrich was dissolved in deionized water to prepare a 30 wt% MEA aqueous solution, which is the usual industrial operating concentration (Choi et al., 2009). CO_2 was of commercial grade with a minimum purity of 99.9 % (Praxair). For the polymer matrix, low density polyethylene (LDPE) was used: Novapol LA 0219-A (Nova Chemicals). This polymer has a density of 919 kg/m^3 (ASTM D792) and a melt index of 2.3 g/10 min (ASTM D1238).

3.2.2. Hollow fiber fabrication

The melt-extrusion system for LDPE hollow fibers fabrication is shown in Fig. 3.1. LDPE hollow fibers were produced using a Haake Rheomix TW-100 co-rotating twin-screw extruder with three heating elements in the extruder cylinder (zone 1-3) and more heating elements around the die (zone 4). The temperature profile was controlled at 135, 150 and 160°C for zones 1, 2 and 3, respectively (from the feeder), and the die temperature was fixed at 145°C. The die geometry has inside and outside diameters of 5 and 7 mm, respectively. The extruder was operated at a total flow rate of 1.2 kg/h and the screw speed was set at 85 rpm. To produce stable hollow fibers, inside air pressure was controlled to prevent collapse. The extrudate was cooled down through a water bath at room temperature. Finally, a take-up unit was used to control drawing speed (2.12 m/min) and stretching. The detailed specifications of non-porous LDPE hollow fibers fabricated by this method are given in Table 3.1.

Table 3.1. Specifications of fabricated LDPE non-porous hollow fibers.

Characteristics	
Fiber outer diameter (μm)	2100
Fiber inner diameter (μm)	2000
Fiber thickness (μm)	50
Effective fiber length (mm)	30

3.2.3. CO_2 loading and pH monitoring

CO_2 loading in 30 wt% MEA was performed in a 300 ml Pyrex Erlenmeyer connected to the CO_2 stream line. A calibrated glass pH meter probe (Mettler-Toledo S20 SevenEasy™) was immersed in the solution for pH measurements. The pH of the solution was monitored during CO_2 loading under continuous stirring. When the desired pH value was reached, the CO_2 flow was switched off and the solution was kept for about 10 minutes under stirring to allow the system to reach equilibrium (constant pH).

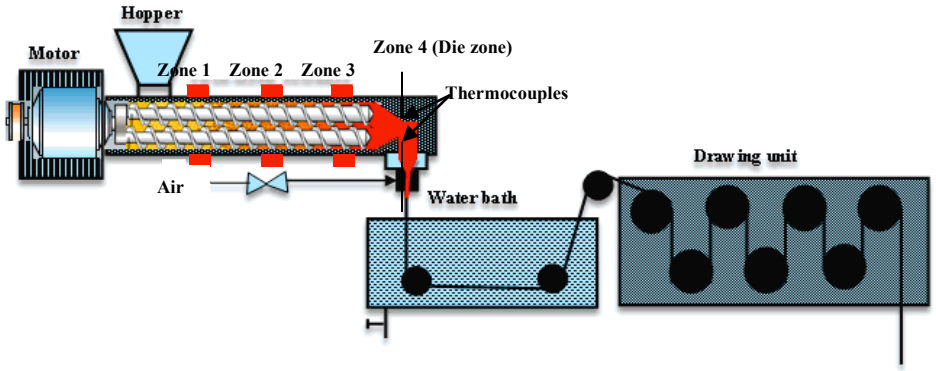

Figure 3.1. Melt-extrusion, cooling and drawing system for hollow fiber precursor fabrication.

3.2.4. Hollow fiber immersion in MEA solutions

Vials containing samples of 30 mm long LDPE hollow fibers which were cut longitudinally from the center line were completely filled with about 2 ml of MEA solution (loaded or unloaded). Various samples taken randomly from the fabricated fibers were completely immersed in the solution and the vials were sealed in order to prevent air penetration into the vials. Since the entire surface of each sample was in contact with the solution in well-defined conditions, each point on the surface was considered representative of the whole fiber. The samples were kept either at room temperature or at 65^{o}C, for different periods: 1 hour, 8 days, 2 weeks and 1 month. After a specified period of time, hollow fibers were first rinsed thoroughly in water and then kept in deionized water for 8 days. Water was daily changed to make sure that all molecules physically adsorbed on the surface were removed by diffusion in water.

Five kinds of samples were prepared: (1) blank LDPE hollow fiber before contact with solutions, (2) LDPE hollow fiber immersed in 30 wt% MEA solution without CO_2 loading (pH 12), (3) LDPE hollow fiber immersed in 30 wt% MEA solution after CO_2 loading to pH 10, (4) LDPE hollow fiber immersed in 30 wt% MEA solution after CO_2 loading to pH 8, and (5) LDPE hollow fiber immersed in 30 wt% MEA solution after CO_2 loading to pH 7. A sample of each type was also analyzed without rinsing and immersing in water for comparison with those thoroughly rinsed.

3.2.5. Fourier transformed infrared spectroscopy (FT-IR) analysis

External reflection spectra were recorded on a Nicolet Magna 850 FTIR spectrometer, equipped with a Golden Gate single reflection diamond ATR sample holder and a DTGS detector, with a resolution of 4 cm^{-1} and by the coaddition of 100 interferograms. Peak intensity determination was performed utilizing the Nicolet OMNIC software and intensity data was normalized using the peak at 1450 cm^{-1}. For each experimental condition, measurements were performed on at least three different samples and on three different portions of each sample in order to ensure the reproducibility of the results.

3.2.6. X-Ray Photoelectron Spectroscopy (XPS) analysis

In order to measure the amount of carbon, oxygen and nitrogen components on the surface of LDPE hollow fibers before and after contact with amine solutions, XPS measurements were carried out in a Kratos Axis-Ultra system where a UHV chamber is equipped with an electrostatic-magnetic hybrid lens and a 300 W monochromatic Al Kα X-ray source (20 mA, 15 kV). The analyzed surface was approximately 400 μm by 800 μm. The angle of the X-ray beam was 60° with respect to the sample normal. The data analysis was performed using the CasaXPS software. For each experimental condition, measurements were performed on at least three samples and on three different portions of each sample in order to ensure the reproducibility of the results.

3.2.7. Contact angle and surface tension measurements

The optical contact angle analyzer (OCA 15 EC Plus, Dataphysics) was used to measure water and MEA solution contact angles of LDPE hollow fibers using the sessile drop method and the surface tension of MEA solutions was determined using the pendant drop method. The system employed a high resolution camera and specific software developed for OCA 15 EC Plus to capture and analyze the contact angle on very small and curved surfaces. For each experimental condition, measurements were performed on at least three samples and on three different portions of each sample in order to ensure the reproducibility of the results. The reported data for contact angles is the average of three obtained values. For very precise measurements, 0.15 μl testing liquid droplets were

dispensed via an ultra-thin needle with the internal diameter of 0.18 mm. In order to perform measurements at different temperatures, the apparatus was equipped with a thermostated chamber controlled with a precision of 0.01 K using a refrigerated/heating circulator with high precision external temperature control (Julabo F25-ME). Densities for pure water and all studied solutions were either measured or taken from the literature (Amundsen et al., 2009).

3.3. Results and discussion

3.3.1. FT-IR investigation

FT-IR analysis was used to study the effect of temperature, contact time, washing duration and pH on LDPE chemical stability.

The effect of MEA on LDPE was first studied using reflectance FT-IR spectroscopy. The samples were completely immersed in solutions, so the analysis could be performed on any portion of the samples. However, since the morphology on both sides of a hollow fiber can be different due to processing conditions, which in turn could cause changes in degradation susceptibility, the analysis was only done on the interior side of hollow fibers since it is the side intended to be in contact with the liquid absorbent in membrane contactors. As the contact between the polymer and the aqueous amine solution is liable to cause leaching of additives from the polymer, a blank sample (cleaned and dried LDPE hollow fiber) was used for comparison.

Fig. 3.2 depicts the FT-IR spectra of LDPE hollow fiber samples immersed in 30 wt% MEA solution and rinsed with water. The spectral region was selected as 1800-950 cm^{-1}, since no significant changes were observed in the 4000-1800 cm^{-1} spectral region (not shown). The main observations in the 1800-950 cm^{-1} spectral region are described as follows. After 8 days, four low intensity peaks were appeared, centered at 1643, 1577, 1543, 1261 and 1017 cm^{-1}. Their intensity increased notably after 30 days immersion in the same solution. The first peak is very large and often attributed to chemical functions involved in hydrogen bonding. These peaks could be related to MEA, adsorbed at the surface, or to new functional groups generated by LDPE degradation. In order to verify if these peaks can be assigned to MEA adsorbed on the polymer surface, the spectrum of pure

MEA is also reported in Fig. 3.2. As can be seen, newly observed peaks do not correspond to ones existing in pure MEA and therefore, they cannot correspond to free amine residuals. This confirms that the rinsing procedure was effective. It is worth noting that the position of the above mentioned peaks (1643, 1577, 1543, 1261 and 1017 cm^{-1}), do not correspond to those reported in previous works concerning PE auto-oxidation products, which were located at 1760, 1692, 1675 and 1410 cm^{-1} for HDPE oxidation in air at room temperature (Pages et al., 1996), at 1699, 1714 and 1740 for HDPE oxidation in air at 120°C (Pages et al., 1996; Yand et al., 2006) and at 1710-1720 cm^{-1} for LDPE oxidation in water (Messey et al., 2007). Therefore, the newly observed peaks in Fig. 3.2 might not correspond to the LDPE auto-oxidation products. The appropriate assignment of these peaks requires more attention.

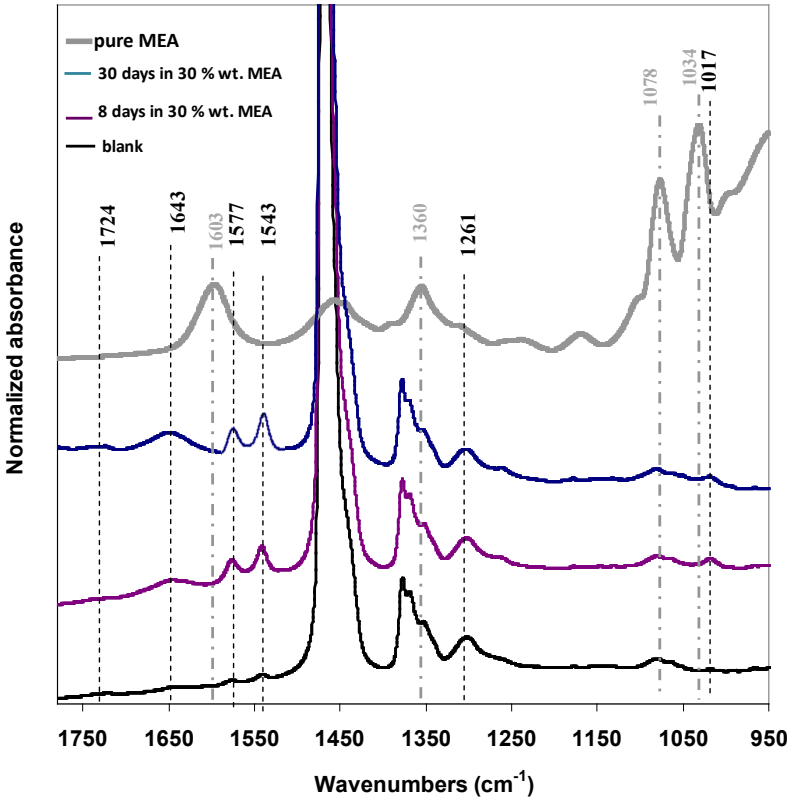

Figure 3.2. FT-IR spectra of degraded LDPE hollow fibers in contact with MEA solution at 25°C.

In order to verify the irreversibility of the above mentioned changes after 8 days contact in 30 wt% MEA solution, samples were immersed in deionised water for various

lengths of time. FT-IR spectra are reported in Fig. 3.3. It can be seen that the intensity of the vibration at 1577 and 1543 cm^{-1} rapidly decreases during the first 8 days of washing. This indicates that these two peaks are partially attributed to chemical species which can be removed from the surface by washing, either because they are not chemically bonded or because they could react with water and redissolve. However, for washing durations longer than 8 days, no change in the intensity of these peaks is observed, which clearly shows the existence of chemical bonds on the surface. On the other hand, the intensity of the peaks located at 1643 and 1017 cm^{-1} does not reduce even after 40 days of washing, which obviously indicates that these peaks do not correspond to physically adsorbed species, but to those chemically bonded to the LDPE hollow fibers.

It is well known that oxidation can induce -COOH groups in PE, but this vibration, if present in the form of the COO^- salts, would appear at a frequency between 1730-1700 cm^{-1} or around 1580 cm^{-1} (Massey et al., 2007). Therefore, these newly observed bands cannot be attributed to acid groups. According to the peak positions, a possible assignment would be the amide II vibration for the 1543 cm^{-1} band and C=O valence vibration of unsaturated ketones, aldehydes or acid groups for the 1577 cm^{-1} vibration. In the case of the 1643 cm^{-1} peak, on the basis of its position and width, our proposed assignment is the secondary amide I vibration (C=O valence vibration of amide groups), which slightly shifts in position when the amide group forms hydrogen bonds with different species. These assignments clearly indicate that amide groups are present at the PE surface. These amide groups could result from successive oxidation, which would introduce –COOH groups, followed by the reaction of –COOH groups with the amine, leading to the formation of secondary amide groups on the LDPE surface, according to the following scheme:

$$PE - COO + NH_2 - CH_2 - CH_2 - OH \rightarrow PE - CO - NH - CH_2CH_2 - OH \quad (3.1)$$

The second peak at 1017 cm^{-1} that does not change in intensity with further washing, is in a typical position of amine ν(C-N) or alcohol ν(C-O) valence stretching vibrations and could be related to the C-N or C-O bonds of the MEA attached to the amide group.

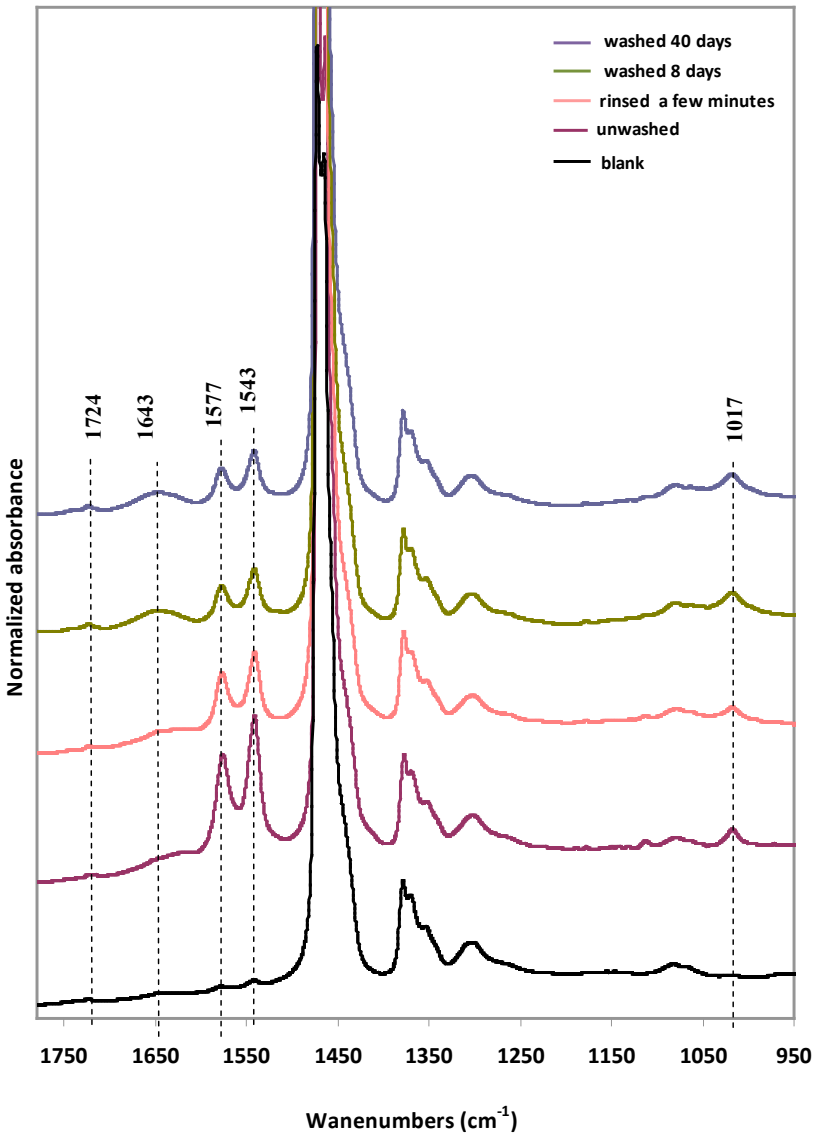

Figure 3.3. FT-IR spectra of LDPE hollow fibers kept in contact with MEA solution at 25°C: Effect of washing duration.

According to the aforementioned peak assignments, it is proposed that the mechanism of chemical alteration of LDPE hollow fibers in presence of amine solutions can be represented by the following series of reactions:

1. First, PE undergoes an auto-oxidative degradation which is attributed to the decomposition of hydroperoxides and is a self-initiating phenomenon (Chien and Wang,

1975). The auto-oxidation mechanism of polyethylene has been represented using the following equations (Rychly et al., 1997):

$$2PEOOH \longrightarrow PE^{\bullet} + PEOO^{\bullet} + \alpha V \quad (3.2)$$

$$PEOO^{\bullet} + PE \rightarrow PEOOH + PE^{\bullet} \quad (3.3)$$

$$PE^{\bullet} + O_2 \rightarrow PEOO^{\bullet} \quad (3.4)$$

$$2PEOO^{\bullet} \rightarrow ketones, acids, aldehydes \quad (3.5)$$

where $PEOOH$, $PEOO^{\bullet}$ and $PE^{\bullet}$ represent, polyethylene hydroperoxide, polyethylene peroxy radicals, and polyethylene alkyl radical, respectively. α and V represent, respectively, the number and type of volatile species generated by $PEOOH$ decomposition. Carbonyl group (C=O) containing products (aldehydes, ketones and carboxylic acids) are formed during termination reactions in this process.

2. The second step is the reaction between MEA and –COOH groups of LDPE samples due to the auto-oxidative degradation to form CO-NH-CH_2-CH_2-OH.

Fig. 3.4 shows the effect of pH on chemical alteration of LDPE hollow fibers as observed by FT-IR spectroscopy. The increase in CO_2 loading, which is accompanied by the decrease in the solution pH from 12 to 7, leads to a decrease in the intensity of all degradation peaks. The chemical degradation of LDPE is therefore remarkably suppressed in presence of CO_2. This can arise for two reasons. First, it has been shown (Gugumus, 2001) that an alkaline environment accelerates the auto-oxidation of polyolefins, while acidic media retards this phenomenon, leading to a decrease in generation of C=O groups in polyolefins. Second, even if an auto- oxidation occurs in MEA loaded solution to form C=O groups on the LDPE surface, the reaction of MEA with these groups to form amide groups seems to be less probable compared with the reaction of MEA with CO_2 (Masohan et al., 2009).

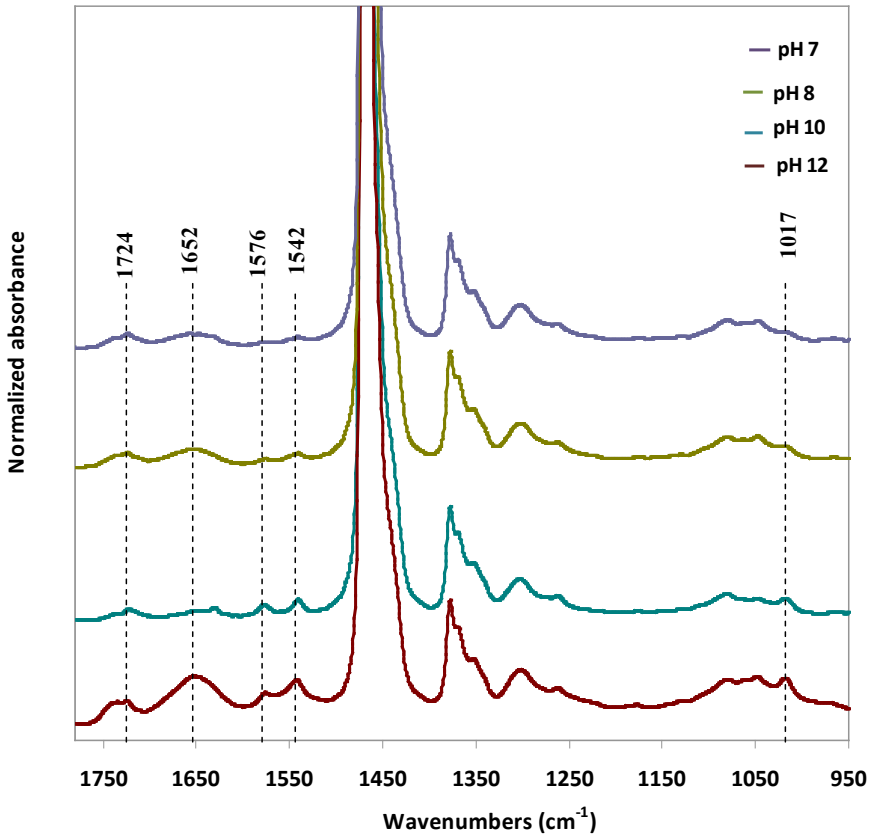

Figure 3.4. FT-IR spectra of LDPE hollow fibers kept in contact with MEA solution at 25°C: Effect of pH.

Fig. 3.5 illustrates the effect of temperature on the chemical degradation of LDPE hollow fibers in contact with 30 wt% MEA solution. The samples were left in contact with the amine solutions for 30 days to ensure that reactions were complete. As can be seen, in addition to peaks appearing in Fig. 3.2, the 1724 cm^{-1} peak that was too close to background noise to ascertain at room temperature, becomes clearly visible at 65°C. The peaks at 1261, 1577 and 1543 cm^{-1} are more intense at 65°C when compared to those at 25°C, indicating the accelerating effect of temperature on the chemical alteration of LDPE hollow fibers. The 1261 cm^{-1} band position is compatible with an amide III band (Bellamy, 1962) whereas, the 1724 cm^{-1} band is clearly located in the carbonyl spectral region. The existence of a peak at this position has already been reported for oxidation of PE in water.

It was assigned to COO^- groups formed by treatment in water/buffer solution at pH 10 (Kumar et al., 2002). This could be due to acid groups (generated by oxidation) that did not react with MEA to produce amide groups, probably due to the steric hindrance or because they were not present on the surface but near the surface where MEA could not easily diffuse and be available for reaction.

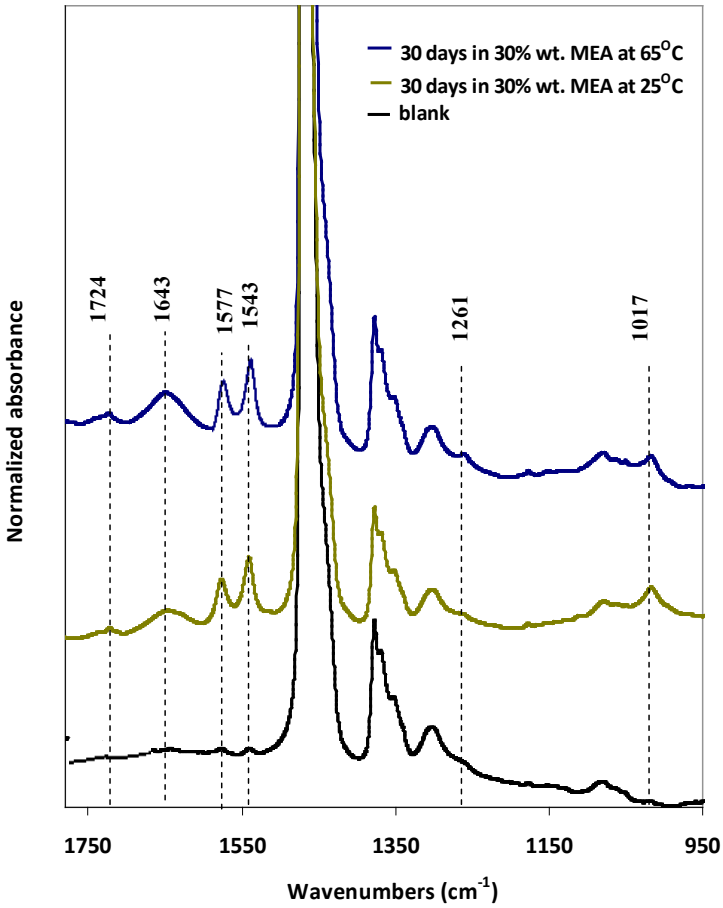

Figure 3.5. FT-IR spectra of LDPE hollow fibers kept in contact with MEA solution at 25 and 65°C: Effect of contact temperature.

3.3.2. XPS study on the change in surface elemental composition of LDPE hollow fibers in contact with amine solutions

XPS is a surface-sensitive method providing a quantitative analysis of the surface composition. It gives information on approximately the first 5 μm of sample thickness.

Therefore, it is one of the most useful methods for surface analysis and can give information on elemental compositions, as well as on chemical groups present at the surface. XPS measurements were performed using LDPE samples kept in contact with fresh MEA solutions at 25 and 65^{o}C.

XPS elemental analysis was performed to determine the surface composition of elemental oxygen and nitrogen in LDPE hollow fibers after 1 month contact with 30 wt% MEA solutions at both temperatures. The results show an increase in oxygen and nitrogen surface elemental composition of LDPE hollow fibers after 1 month contact with 30 wt% MEA solutions at 25 and 65^{o}C (Table 3.2 and Fig. 3.6).

Table 3.2. XPS elemental analysis of LDPE hollow fiber samples in contact with MEA solutions at 25 and 65°C.

Atom	Blank LDPE hollow fiber	LDPE immersed 30 days in 30 wt% MEA at 25^{O}C and 8 days in water	LDPE immersed 30 days in 30 wt% MEA at 65^{O}C and 8 days in water
O	2.52 %	4.55 %	5.71 %
N	0.15 %	0.9 %	1.84 %
C	96.25 %	93.44 %	91.55 %

As can be seen, an increase in surface oxygen from 2.52% (blank LDPE hollow fiber) to 4.55% and 5.71% at 25 and 65^{o}C, respectively, is observed for LDPE hollow fibers after 1 month exposure to MEA. This increase indicates the higher rate of auto-oxidation of LDPE at higher temperature and confirms the generation of the peak at 1724 cm^{-1} at 65^{o}C (Fig. 3.5) related to the formation of carbonyl groups. In addition, there is an increase in surface elemental nitrogen from 0.15% (blank sample) to 0.9% and 1.4% at 25 and 65^{o}C, respectively, after 1 month contact with 30 wt% MEA solutions. The increase in surface elemental nitrogen from 25 and 65^{o}C is in good agreement with the generation of a new band at 65^{o}C positioned at 1261 cm^{-1}, which was assigned as amide III (Fig. 3.5). This can be explained by the fact that, at higher temperature, more carbonyl groups are available to react with MEA to form amide groups (Fig. 3.5). It is worth noting that the extraction of

the individual bond contribution was extremely difficult, and is therefore not reported, since the total amount of carbon-oxygen bond intensities were very low.

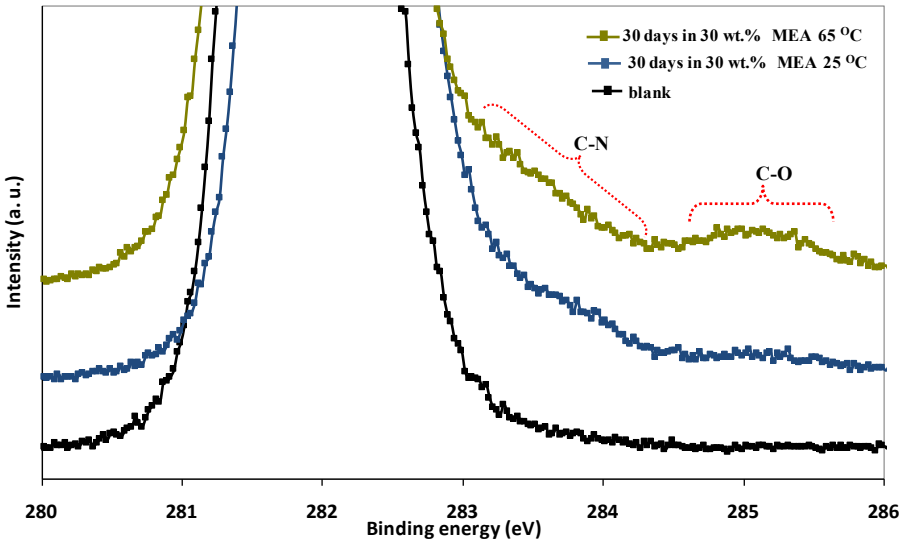

Figure 3.6. C1s XPS spectra of LDPE hollow fibers kept in contact with MEA solution at 25°C.

Table 3.3. Surface tension and CO_2 loading for the aqueous MEA solutions.

Solution	CO_2 loading (mol of CO_2/mol of MEA)[1]	Surface tension (mN/m) at 25°C
Without CO_2 loading		
30 wt.% MEA	–	61.1±0.2
With CO_2 loading		
pH 10 (CO_2 loaded 30 wt.% MEA)	0.397	64.1±0.2
pH 8 (CO_2 loaded 30 wt.% MEA)	0.722	68.1±0.2
pH 7 (CO_2 loaded 30 wt.% MEA)	0.988	70.4±0.2

[1]CO_2 loading values are estimated based on the work by Park et al. (2003).

3.3.2. Surface tension and contact angle analyses

MEA decreases the surface tension of water (72 mN/m at 25°C (Jasper, 1972)) (Table 3.3) and seems therefore to behave as a typical capillary active substance.

However, the addition of CO_2 in an aqueous MEA solution leads to an increase in surface tension (Table 3.3). Similar results were reported in the literature for diethanolamine (DEA) aqueous solutions (Henry, 1992). It is difficult to give a complete explanation of this behavior because of the complexity of the loaded alkanolamine solution. The reaction between MEA, a primary amine, and CO_2 in an aqueous solution leads to a complex electrolyte system containing mainly free MEA, carbamate, and protonated MEA, as well as small amounts of bicarbonate and carbonate ions. The concentration of these species is a function of CO_2 loading (mole CO_2/mole amine). Fan et al. (2009) recently studied the speciation in aqueous MEA solution at different CO_2 loadings via nuclear magnetic resonance (NMR) spectroscopy. As the CO_2 loading increased, the solution pH decreased (Table 3.3) and, therefore, the concentration of free MEA decreased. The concentration of protonated MEA gradually increased with increasing CO_2 loading and became predominant after half-molar loading. The ratio of the carbamate increased steadily and reached its maximum (ca. 41%) at half-molar loading. MEA is the only component of this mixture whose influence on water surface tension is known (Table 3.3). Indeed, the decrease of free MEA concentration in the loaded MEA solution leads to an increase in solution surface tension. As the global effect of the addition of CO_2 in an aqueous MEA solution is an increase in surface tension (Table 3.3), it is possible that the ionic species present in the solution have (i) a capillary active tendency or (ii) a capillary inactive tendency that must be less important than the capillary active behavior of free MEA in water.

The wetting tendency of liquids on material surfaces is affected by liquid surface tension and material surface energy. For a certain material (LDPE in this case), the lower the liquid surface tension, the higher its tendency to wet the solid surface. Contact angle measurements were carried out to compare the wettability of LDPE hollow fibers before (blank sample) and after the contact with MEA solutions of various pH (treated sample). Contact angle at the interface water/treated LDPE hollow fibers was also measured for

comparison. The results are presented in Table 3.3. LDPE samples kept in contact with aqueous MEA (pH 12) show a decrease in contact angle for both water (by 10%) and MEA solution (by 30%), with respect to the blank sample. Moreover, for all samples, contact angle for aqueous MEA solutions is significantly lower than the contact angle for water. Finally, both water and MEA solutions contact angles increase slightly with decreasing solution pH by CO_2 loading. These results correspond to the lower surface tension of MEA with respect to water. The hydrophobic character of blank LDPE hollow fibers with respect to water was shown to decrease significantly when the fibers were kept in contact with MEA solutions, especially for prolonged time. However, this behavior seems to be slightly attenuated by CO_2 absorption.

Since the LDPE hollow fibers used in this work were non-porous (precursors before pore formation), they were not the subject of morphological degradation. The observed behavior cannot therefore be related to pore enlargement as previously observed by Barbe et al. (2000), but rather associated to chemical degradation of LDPE hollow fibers in MEA solutions, in the presence or absence of CO_2, as proved by FT-IR and XPS analysis (§3.3.1 and §3.3.2). The increase in water and MEA contact angles with increasing CO_2 loading is consistent with the increase in the intensity of the peak positioned at 1724 cm^{-1} observed while the solution pH decreases (Table 3.4). LDPE chemical degradation seems therefore to be less important in the presence of CO_2 due to the reduction of the pH of loaded MEA solutions, which could lead to a much slower alteration of the membrane hydrophobic properties while in use in membrane contactors.

3.4. Conclusions

In this paper, a detailed study on the chemical stability of LDPE hollow fibers upon exposure to MEA solutions with and without CO_2 loading was performed on the basis of XPS, FT-IR and contact angle measurements. The results led to the conclusion that LDPE hollow fiber samples undergo a two step chemical degradation in the presence of MEA aqueous solutions. First, carbonyl groups were observed, which was attributed to an auto-oxidative degradation process of LDPE accelerated by the alkaline nature of MEA solutions. Second, the formation of amide groups was proposed to be due to a chemical

reaction between the acid groups of degraded LDPE and MEA. These chemical alterations were found to be hindered by CO_2 absorption. Further attempts on polyolefin-based stability enhancement are currently in progress in our laboratory.

Table 3.4. Water and amine interior contact angles of LDPE hollow fiber samples.

LDPE hollow fiber samples	Water contact angle (^{O}) at 25°C	30 wt% MEA contact angle (^{O}) at 25°C
Without CO_2 loading[1]		
Blank	99±1	69±1
pH 12	90±1	61±1
With CO_2 loading[2]		
pH 10	94±1	63±1
pH 8	95±1	65±1
pH 7	96±1	67±1

[1]Contact angle measurements were carried out on LDPE hollow fibers after 10 days contact with 30 wt% MEA solution followed by 8 days immersion in water.
[2]Contact angle measurements were carried out on LDPE hollow fibers after 10 days contact with CO_2 loaded MEA 30 % followed by 8 days immersion in water.

After studying the chemical degradation behavior of the membrane material (LDPE), it is important to investigate the stability of microporous LDPE hollow fiber membranes in contact with absorption solutions. A detailed study of morphological, chemical and thermal stability of the fabricated membranes in contact with MEA and AHPD (a sterically hindered alkanolamine) aqueous solutions with and without PZ addition was performed and is the subject of the following paper (Chapter 4).

Chapter 4

Morphological, Chemical and Thermal Stability of Microporous LDPE Hollow Fiber Membranes in Contact with Single and Mixed Amine Based CO_2 Absorbents

Résumé

La détérioration progressive de la stabilité morphologique et chimique des membranes dans un contacteur à membrane peut largement influencer leur mouillabilité, ce qui conduit à la réduction de l'efficacité de l'absorption du CO_2. Dans ce travail, la stabilité morphologique, chimique et thermique des membranes microporeuses à fibres creuses en polyéthylène de basse densité (LDPE), destinées à l'utilisation dans des contacteurs à membrane, a été étudiée pour des membranes en contact avec des solutions d'une amine primaire (monoéthanolamine, MEA) et d'une amine à encombrement stérique (2-amino-2-hydroxyméthyle-1,3-propanediol, AHPD). De plus, il a été étudié aussi l'effet d'une diamine (pipérazine, PZ), présentant autant une capacité d'absoption importante qu'une cinétique rapide d'absorption du CO_2, sur la stabilisation de la membrane.

Les propriétés de la surface des membranes fraiches (avant le contact avec les solutions aminées) et utilisées (après le contact avec ces solutions) ont été analysées par microscopie électronique à balayage (MEB), spectroscopie infrarouge à transformée de Fourier (FTIR), analyse thermogravimétrique (TGA) et des mesures d'angle de contact. Pour les membranes immergées dans des solutions d'amine de concentration généralement utilisée en pratique (30% en masse MEA et 11% en masse AHPD), les résultats montrent une dégradation morphologique des membranes due à l'intrusion de la solution dans les pores, ainsi qu'une dégradation chimique par l'auto-oxydation du LDPE. Cependant, l'effet est moins important en présence de la PZ. Un mécanisme en deux étapes a été proposé pour expliquer l'effet stabilisateur de la PZ. Les solutions d'amines à base de PZ sont donc considérées très appropriées pour l'absorption du CO_2 dans les contacteurs à membrane, due à leur efficacité autant dans l'absorption du CO_2 que dans la stabilisation des membranes polyoléfiniques.

Abstract

The gradual deterioration in the morphological and chemical stability of membranes in membrane contactors can extensively influence the membrane wettability, leading to reduction of CO_2 absorption efficiency. In the present work, morphological, chemical and thermal stability of microporous low density polyethylene (LDPE) hollow fiber membranes, intended to be used in membrane contactors, was studied in contact with primary amine (monoethanolamine, MEA) and sterically hindered amine (2-amino-2-hydroxymethyl-1,3-propanediol, AHPD) solutions. In addition, it was investigated the effect of a diamine (piperazine, PZ) having the operational advantages of fast CO_2 absorption rate and capacity, on membrane stabilization.

The surface properties of neat (before contact) and used (after contact with amine solutions) membranes were analyzed using scanning electron microscopy (SEM), Fourier transform infrared spectroscopy (FTIR), thermogravimetric analysis (TGA) and contact angle measurements. For membranes immersed in amine solutions of commonly used concentrations (30 wt% MEA and 11 wt% AHPD), the results show morphological degradation of membranes, caused by the intrusion of the solution into the pores, as well as chemical degradation caused by the LDPE auto-oxidation. However, a less significant effect was found by the addition of PZ. A two-step mechanism was proposed to explain the stabilizing effect of PZ. PZ containing amine solutions are suggested as strong candidates for CO_2 absorption in membrane contactors due to their efficient dual-function properties (high CO_2 absorption efficiency and polyolefin membrane stabilization).

4.1. Introduction

Carbon dioxide (CO_2) is one of the major greenhouse gases and thus is believed to be the main responsible factor for climatic changes. Various separation processes for CO_2 capture have been developed. Among them, absorption using amine-based absorbents is the most common industrial process mainly due to the high CO_2 removal efficiency (Yang et al., 2008). However, due to the direct contact of the two fluid phases (G and L), the use of conventional gas-liquid contactors (bubble columns, sieve trays or packed towers) often leads to several technical problems such as foaming, emulsions, unloading and flooding. In order to overcome such operational problems, gas/liquid membrane contactors (GLMC) have been proposed as promising alternatives, offering several important advantages over conventional gas/liquid absorption equipments (Scholes et al., 2010; Favre, 2011; Luis et al., 2012).

Membrane stability during CO_2 absorption in GLMC is of great importance in industrial applications. Membrane instability, which can be either chemical or morphological, leads to an increase in mass transfer resistance, which can result in the reduction of absorption efficiency (Zhang et al., 2008). Very few studies have been reported in the open literature on the instability of porous membrane in contact with different solutions. In the case of morphological stability, Barbe et al. (2000) reported surface morphological changes of microporous polypropylene (PP) flat membranes after 72 h contact with water, due to pore intrusion by the liquid meniscus. Similar behavior was observed in the case of polypropylene (PP), polyvinilydene fluoride (PVDF), polyethersulfone (PES) and polystyrene (PS) membranes exposed to various liquid absorbents such as alkanolamine solutions, Selexol^{TM} (a mixture of dimethyl ethers of polyethylene glycol) and dimethyl formamide (Dindore et al., 2004; Porcheron and Dozds, 2009; Rongwong et al., 2009). Concerning the chemical stability of membranes, some authors reported the possibility of chemical reactions between membranes and amine absorbents. Wang et al. (2004a) reported the possibility of chemical reaction between PP and diethanolamine (DEA) after 30 days contact, resulting in the deterioration of membrane hydrophobicity. Franco et al. (2008) attributed the increase in the elemental oxygen of PP membrane surface from 0.78 to 1.49% to the oxidation of the membrane after 68 h use in

the membrane contactor in contact with MEA. Lv et al. (2010) investigated the changes in surface hydrophobicity of PP hollow fiber membranes in contact with amine solutions. The authors mentioned that improving the surface hydrophobicity of membranes may be an effective way of overcoming wetting problems.

In our previous work, a detailed study was performed on the chemical alteration of non-porous low density polyethylene (LDPE) hollow fibers in contact with aqueous solutions of monoethanolamine (MEA) (Mosadegh Sedghi et al., 2011). It was reported that the instability of LDPE was mainly due to its auto-oxidation, which is enhanced in the presence of aqueous MEA solutions. This auto-oxidative degradation results in the generation of a functional layer on the fiber surface leading to the increase in the material wettability which in turn affects the CO_2 absorption efficiency. Therefore, an efficient way to inhibit the degradation of polyolefin based membranes in contact with amine solutions, extensively used for CO_2 capture, is highly desirable.

Hindered amine light stabilizers (HALS, the amine derivatives of 2,2,6,6-tetramethylpiperidine) are well-known industrial stabilizers for polymers (Klemchuk and Gande, 1989; Klemchuck and Gande, 1990). Since the auto-oxidation of polyolefins follows a series of radical reactions (Chien and Wang, 1975), these additives are added to polymers during the fabrication process, mainly to terminate the auto-oxidation reactions by the formation of nitroxide radicals (Step and Turro, 1994). The prohibiting effect of HALS on the auto-oxidation of PP was discussed by Massey et al. (2007). However, in the case of stabilizer-free polyolefin membranes for CO_2 absorption, it would be interesting to verify whether the same stabilizing effect could be obtained by the addition of HALS directly in the absorption liquid. The proper selection of the liquid absorbent could then provide both efficient CO_2 absorption and membrane stability. Further, HALS content would be stable, and therefore not deplete with time, leading to longer membrane stability. This work aims to introduce such a dual-function absorbent for CO_2 capture in GLMC using porous LDPE membranes. Since most of the commonly used stabilizers are derivatives of piperidine (Pip), a possible choice for liquid absorbent is piperazine (PZ), which has a molecular structure similar to that of piperidine (Fig. 4.1).

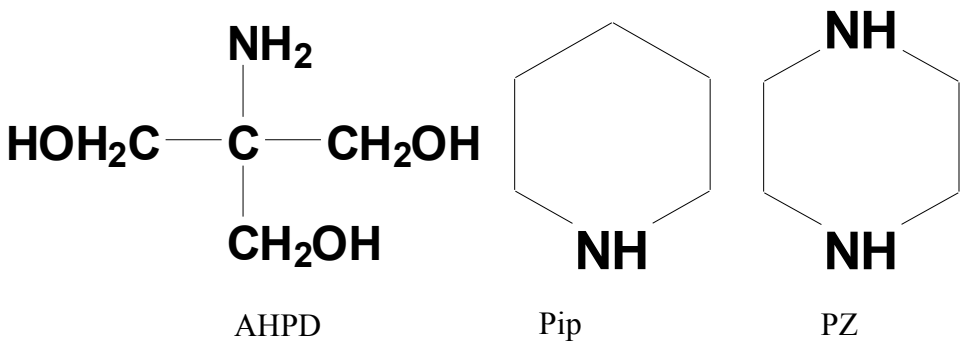

Figure 4.1. Structure of piperazine (Pz), piperidine (Pip) and 2-amino-2-hydroxymethyl-1,3-propanediol (AHPD).

The effect of PZ in the improvement of CO_2 absorption efficiency has already been reported in the literature (Bishnoi and Rochelle, 2002; Cullinane et al., 2004; Cullinane et al., 2006; Khalili et al., 2009). PZ, a diamine, has higher absorption capacity and reaction rate compared to MEA, the most commonly used solvent in CO_2 capture technology (Bishnoi and Rochelle, 2000). In addition, recent studies performed in our laboratory on absorption kinetics, thermodynamics and regenerative capacity of CO_2 absorbents showed that the AHPD-PZ aqueous mixture could be an interesting alternative to conventional amine solutions (Bougie et al., 2009; Bougie and Iliuta, 2010a; Bougie and Iliuta 2010b). In this context, the present paper investigates the stabilizing effect of PZ on LDPE hollow fiber membranes intended to be used for CO_2 capture in GLMC, in contact with MEA (primary amine) and AHPD (sterically hindered amine) (Fig. 4.1) aqueous solutions. Morphological, chemical and thermal stability of the membranes in contact with the above mentioned absorbents have been investigated.

4.2. Experimental

4.2.1. Chemicals and materials

MEA, AHPD and PZ with minimum purity of 99% were used to prepare aqueous solutions of single and mixed amines. All chemicals (Laboratoire MAT, Canada) were used without further purification. All single and mixed aqueous amine solutions used in this work were prepared with deionized water. Microporous LDPE hollow fiber membranes

were fabricated using a novel method (Mosadegh Sedghi et al., 2012b). General characteristics of fabricated LDPE hollow fiber membranes are presented in Table 4.1.

Table 4.1. Characteristics of LDPE hollow fiber membrane.

Fiber inner diameter (mm)	1.8
Fiber outer diameter (mm)	2.5
Fiber density (g/cm^3)	0.770
Fiber porosity (%)	48

4.2.2. Hollow fiber membrane immersion in amine solutions

The composition of the amine solutions is shown in Table 4.2. The total amine concentration was kept constant (30 wt% for MEA and 11 wt% for AHPD solutions). 30 mm long LDPE hollow fiber membranes were completely immersed in the solutions, loaded in small vials. The vials were sealed in order to prevent air penetration and placed in an oven at 65°C (to enhance the interaction between the fiber surface and the liquid absorbent) for 30 days. At the end of the contact period, hollow fibers were taken out of solutions and rinsed thoroughly with deionized water. In order to remove all molecules which were physically adsorbed on the surface, the membranes were immersed into deionized water for an additional 2 days. Water was changed daily. Fibers were finally dried overnight at 50°C.

Table 4.2. Density and surface tension of solutions at 25°C.

Liquid	**Density (g/cm^3)**	**Surface tension (mN/m)**
Water	0.997	72.0 ± 0.1
MEA 30 wt%	1.008	64.0 ± 0.1
MEA 25 wt% + PZ 5 wt%	1.010	64.8 ± 0.1
AHPD 11 wt%	1.024	71.3 ± 0.1
AHPD 10.11 wt% + PZ 0.89 wt%	1.026	71.9 ± 0.1

4.2.3. Hollow fiber membrane characterization

Neat (before immersion in amine solutions) and used (after immersion in amine solutions) LDPE hollow fiber membranes were characterized from different aspects to analyze their morphological, chemical and thermal stability before and after contact with amine solutions.

4.2.3.1. Scanning electron microscopy (SEM)

The structure of hollow fiber membranes was investigated using a scanning electron microscope (SEM) (JEOL, JSM-840a). To calculate the pore diameter distribution, the images were digitized and analyzed using Image-Pro-Plus Version 5.0 software.

4.2.3.2. Fourier transformed infrared spectroscopy (FTIR)

FTIR experiments were carried out to analyze the chemical composition of membranes before and after contact with amine solutions. External reflection spectra were recorded on a Nicolet Magna 850 FTIR spectrometer, equipped with a Golden Gate single reflection diamond ATR sample holder and a DTGS detector, with a resolution of 4 cm^{-1} and by coaddition of 100 interferograms. Band intensity determination was performed using the Nicolet OMNIC software and intensity data was normalized using the band at 1450 cm^{-1}. For each experimental condition, measurements were performed on at least three different portions of each sample in order to ensure the reproducibility of the results.

4.2.3.3. Thermogravimetry (TGA)

The thermal stability of hollow fiber membranes before and after contact with amine solutions was analyzed by thermogravimetric analysis (TGA), using a TA Instruments TGA, model Q5000 IR from ambient temperature to 950°C at a heating rate of 10 °C/min under air.

4.2.3.4. Contact angle and surface tension measurements

An optical contact angle analyzer (OCA 15 EC Plus, Dataphysics) was used to measure contact angles of membrane with water and amine solutions using the sessile drop method, as well as the surface tension of amine solutions using the pendant drop method. The system employed a high resolution camera and specific software developed for OCA

15 EC Plus to capture and analyze the contact angle on very small and curved surfaces. For each experimental condition, measurements were performed on at least three samples in order to ensure the reproducibility of the results. The reported data for contact angles is the average of three obtained values. For very precise measurements, 0.15 µl testing liquid droplets were dispensed via an ultra-thin needle with an internal diameter of 0.18 mm. The apparatus was equipped with a thermostated chamber controlled with a precision of 0.01 K using a refrigerated/heating circulator with high precision external temperature control (Julabo F25-ME). Densities for pure water and all studied solutions were measured using a calibrated pycnometer having a bulb volume of 1×10^{-5} m^3 and a Mettler AE240 balance with a precision of $\pm1\times10^{-3}$ g.

4.3. Results and discussion

4.3.1. Morphological stability

Since any alteration in the porous structure of membranes can directly affect the CO_2 absorption efficiency in membrane contactors, morphological stability of the membranes in contact with amine solutions was primarily investigated using SEM microscopy to determine possible changes in the shape and size of the pores, as well as any damages in cell walls. Fig. 4.2 shows SEM images of the porous structure of LDPE hollow fiber membranes, before and after 30 days contact with amine solutions (MEA, AHPD, MEA/PZ and AHPD/PZ). In the neat fiber (Fig. 4.2a), cell walls are relatively homogeneous and small. In comparison, the membrane surface significantly underwent morphological degradation after 30 days contact with MEA 30 wt% aqueous solution (Fig. 4.2b), after which membrane pores were remarkably enlarged. However, pore enlargement was significantly reduced by the addition of small amount of PZ in MEA solutions (Fig. 4.2c). The pore enlargement phenomenon was previously reported for porous membranes in contact with liquids with low surface tension (Kamo et al., 1992; Porcheron and Dozds, 2009; Franco et al., 2011). Surface tensions of single and mixed aqueous amine solutions are presented in Table 4.2. The values are in agreement with the degradation level observed by SEM images, indicating that the structural stability of membrane pores (morphological stability) is strongly associated with the surface tension of the contact solution (absorbent).

Solutions with lower surface tension can penetrate more easily into the pores. Upon diffusion, the liquid meniscus exerts an additional force onto the pore walls and pushes them away. Depending on the surface tension of the solution, this process can continue until the complete rupture of the wall.

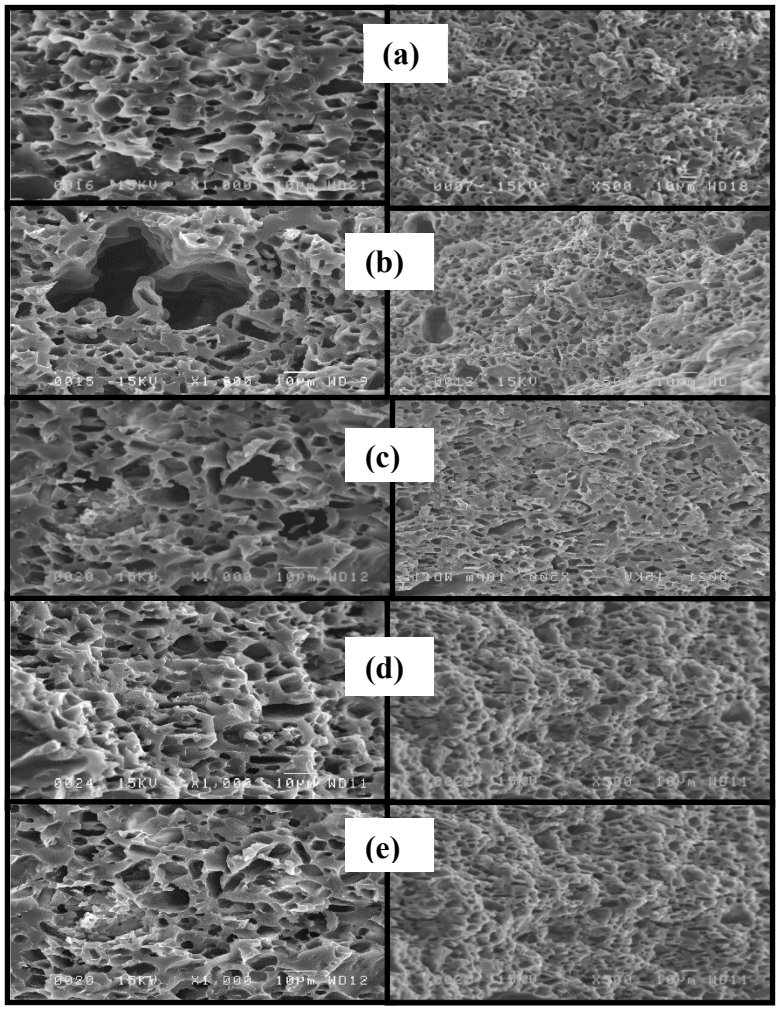

Figure 4.2. SEM micrographs of LDPE hollow fiber membranes: a) neat; b) after 30 days contact with 30 wt% MEA; c) after 30 days contact with MEA/PZ:25/5 wt%; d) after 30 days contact with 11 wt% AHPD; e) after 30 days contact with AHPD/PZ:10.11/0.89 wt%.

SEM images reveal that single MEA amine solutions can easily penetrate into the LDPE membrane pores, swelling the pores and breaking the walls between the membrane pores. However, the addition of PZ to MEA increases the surface tension of the solution, reducing the solution diffusion into the pores and stabilizing the pore structures. In case of

AHPD, however, the structural deformation is much less significant (Fig. 4.2d). Due to its large molecular size, hindered structure (Fig. 4.1) and high surface tension (Table 4.2), AHPD seems to have a lesser tendency to penetrate into the membrane pores, acting therefore as a stabilizer.

Fig. 4.3 illustrates the pore size distribution of neat and used hollow fiber membranes. For the neat membrane, more than 60% of pores were in the diameter range of 2-5 μm. However, this number decreased to about 12% and 35%, respectively, for membranes kept in contact with MEA and AHPD solutions. Moreover, larger diameters of 16-25 μm, which were completely absent in the neat membrane occupy, respectively, around 10% and 3% of pores for the membranes in contact with the above mentioned solutions. The order of pore size distribution for the membranes in contact with amine solutions, from the largest to the narrowest, is the following: MEA > AHPD > MEA/AHPD > AHPD/PZ. This confirms the stabilizing effect of PZ in the structural deformation of pores.

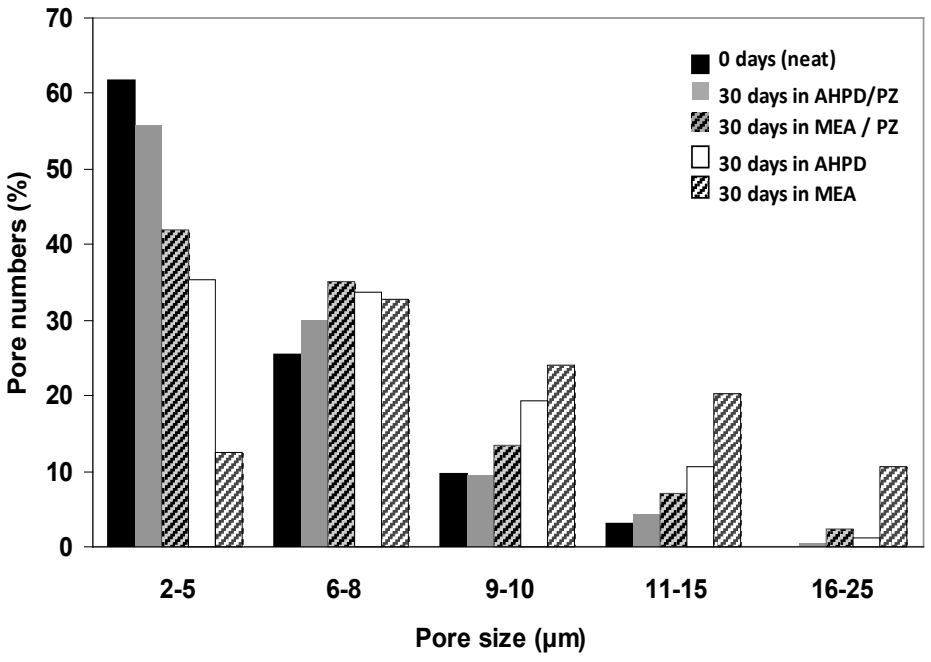

Figure 4.3. Pore size distribution of LDPE hollow fiber membranes.

4.3.2. Chemical stability

In our previous work, a detailed study was performed on the chemical effect of MEA solutions on non-porous LDPE hollow fibers (Mosadegh Sedghi et al., 2013). The formation of carbonyl (C=O), as well as the amide groups (N-C=O) on the hollow fiber surfaces after contact with MEA solutions was confirmed using FTIR and XPS analysis. In addition, a two-step mechanism for such chemical degradation was proposed. It was concluded that the auto-oxidation of polyolefins is enhanced in the presence of amines. The effect of PZ on retarding the auto-oxidation of LDPE in contact with MEA and AHPD is now investigated by comparing the FTIR spectra of the neat and used microporous LDPE membranes, with and without the addition of PZ in the aqueous solvent.

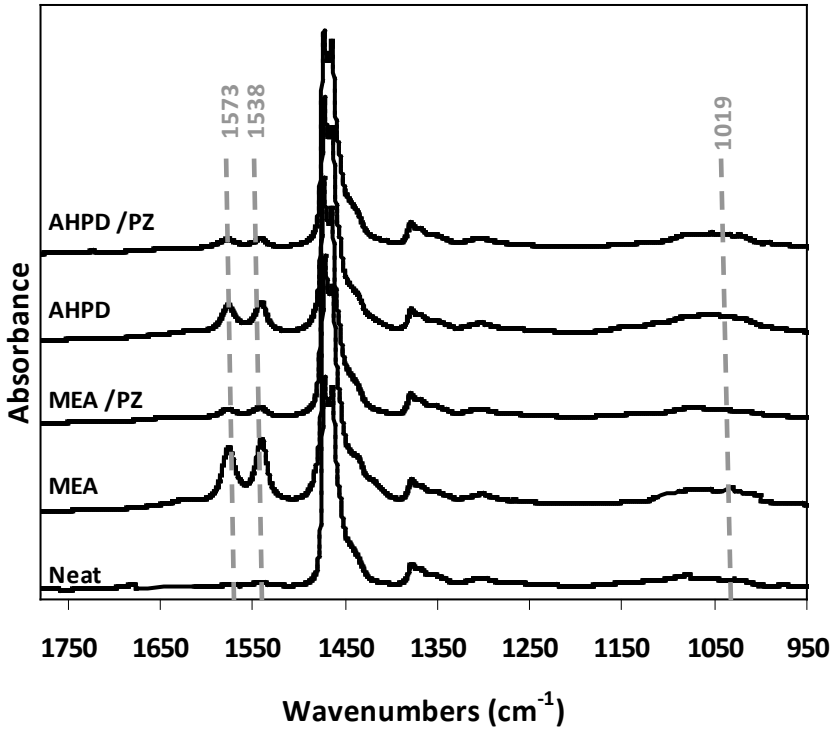

Figure 4.4. FTIR spectra of LDPE hollow fiber membranes.

As seen in Fig. 4.4, for membranes immersed in MEA three absorption bands around 1019, 1538 and 1573 cm^{-1} are observed, which are absent in the IR spectra of the neat membrane. Since the membranes were thoroughly washed with water, the above

mentioned bands cannot correspond to free amine residuals on the surface and are attributed to the chemical bonds generated by chemical interaction between the membrane and MEA solution. It was observed that these bands become less intense for the membrane in contact with AHPD, indicating that LDPE membranes are more chemically compatible with AHPD than with MEA solutions. Due to the higher surface tension of the aqueous AHPD solution in respect to that of MEA (Table 4.2), the tendency of AHPD to diffuse into the membrane pores is less significant than in the case of MEA, leading to less interaction between the membranes and the AHPD solution.

A possible assignment for the above mentioned bands would be the amide vibration for the 1538 cm^{-1} band and C=O valence vibration of unsaturated ketones, aldehydes or acid groups for the 1573 cm^{-1} vibration (Rongwong et al., 2009). The 1019 cm^{-1} band is in a typical position for amine ν(C-N) or alcohol ν(C-O) valence stretching vibrations and could be related to the C-N or C-O bonds of the MEA attached to the amide group. After membrane immersion in PZ containing amine solutions, the intensity of all these bands remarkably decrease with respect to those of LDPE, suggesting that PZ acts as a chemical stabilizer for the membrane surface. This chemical stabilization effect could arise from two aspects: PZ acts as a surface inactive substance, by increasing the solution surface tension and inhibiting pore intrusion by the liquid meniscus. On the other hand, PZ is a symmetric diamine with similar structure to that of commonly known HALS (derivatives of piperidine) and could therefore be able to retard the membrane auto-oxidation. It is widely accepted that the outstanding efficiency in polymer stabilizing technology is due to the regenerative scavenging capability of HALS (Chmela et al., 1989; Scoponi et al., 2000; Hodgson and Coote, 2010). These materials are especially characterized by the nitrogen atom bonded to a six membered-ring (Fig. 4.1) and can protect polymer surfaces against photo-oxidative damage via the formation of nitroxide radicals (Chmela et al., 1989; Scoponi et al., 2000; Hodgson and Coote, 2010). Extensive investigations on HALS stabilization mechanism reveal different radical reaction pathways, mostly including the decomposition of hydroperoxides, peracids and ozone (Pospìsil and Nešpůrek, 1995). The most essential part of HALS stabilization mechanism, the regenerative radical scavenging, is best described in the so-called “Denisov cycle”, as shown in Fig. 4.5.

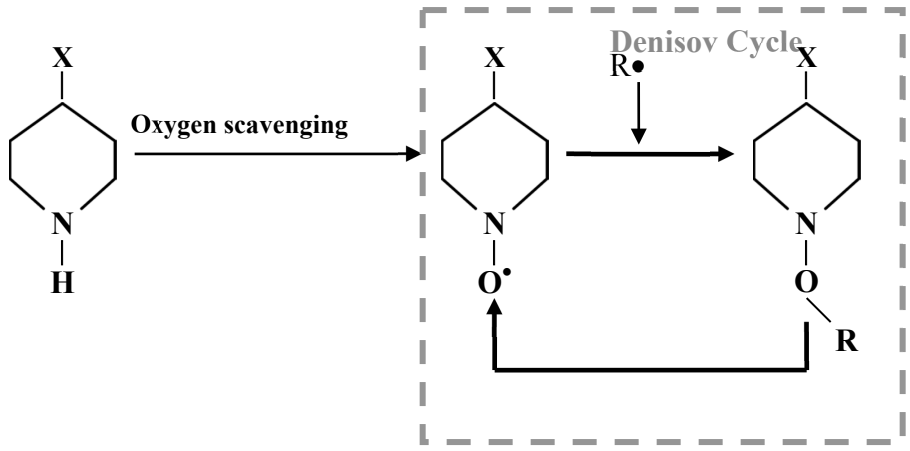

Figure 4.5. Radical scavenging of HALS in Denisov cycle.

Besides the photo-oxidative degradation, HALS can also act as stabilizers for auto-oxidative degradation of polyolefins. Massey et al. (2007) reported a remarkable contribution of HALS in retarding the oxidative degradation of LDPE in water, through scavenging of oxygen present at the polymer surface. Having a similar structure (nitrogen atoms in a six-membered ring), PZ seems to behave in a similar manner through the formation of nitroxide radicals. Based on the above mentioned explanation, a two-step mechanism is proposed to explain the effect of PZ on auto-oxidation of porous LDPE membranes in contact with amine based absorbents: PZ scavenges the oxygen present in the bulk solution and around the membrane surface, to form nitroxide radicals. Once formed, the nitroxide radicals can be involved in termination reactions by coupling with amine molecules to form larger sized molecules. The formation of such large molecules can create a steric hindrance (resistance) which decreases the interaction between membrane and amine solution and hinders the auto-oxidative degradation of the membrane.

4.3.3. Wettability of hollow fiber membranes

Along with structural alterations, the intrusion of absorbent molecules in membrane pores and their interaction with the polymer can significantly affect membrane hydrophobicity. Hydrophobicity of membrane surface and pore resistance to wetting were quantified by contact angle measurements. The wetting tendency of liquids on the membrane surface is affected by liquid surface tension and membrane surface energy.

The static contact angles of neat membrane with water, single amines and mixed amine solutions are presented in Table 4.3. It can be observed that membrane wettability increases as the liquid surface tension decreases. The highest water contact angle of 128.4° shows the ultra-hydrophobic characteristics of the microporous LDPE hollow fiber membranes used in the present study. Membrane contact with MEA and AHPD aqueous solutions leads to a decrease in the contact angle to 111.7° and 118.1°, respectively. These results are in good agreement with the surface tension of solutions, MEA and AHPD acting as capillary active substances and decreasing the surface tension of water (Hodgson and Coote, 2010). However, both MEA and AHPD contact angles rise upon addition of PZ, due to the higher surface tension and the hindrance effect caused by the presence of PZ in MEA and AHPD solutions (see §4.3.2.).

On the other hand, it can also be seen that water contact angles of membrane immersed in MEA and AHPD solutions are significantly lower than water contact angle of neat membrane, showing an increase in wettability of membrane surface after contact with amine solutions (Table 4.3). This is mainly attributed to chemical alterations of membrane surface, caused by auto-oxidation of LDPE enhanced in the presence of amines. These can form hydrophilic functional groups like acids, alcohols, amides, ketones and aldehydes on the membrane surface, thus decreasing the surface hydrophobicity, and consequently, increasing membrane wettability (Rongwong et al., 2009). In addition to chemical properties, the wettability of the surface is also influenced by its morphological structure (Dindore et al., 2004). Therefore, the deformation of membrane pore structure (see §4.3.1) is also responsible for the increase in membrane wettability. However, the increase in the contact angles of both MEA and AHPD solutions after the addition of PZ confirms the stabilizing effect of PZ in chemical and morphological alteration of membrane surface, resulting in enhanced membrane surface hydrophobicity and reduced membrane wettability.

Table 4.3. Static contact angle of neat and used hollow fiber membranes.

Neat		
Liquid		Average contact angle (^{O})
Water		128± 1
MEA 30 wt%		111± 1
MEA 25 wt% + PZ 5 wt%		116± 1
AHPD 11 wt%		118± 1
AHPD 10.11 wt% + PZ 0.89 wt%		121 ± 1
Used		
Liquid	Liquid in contact with membranes (immersion liquid)	Average contact angle (^{O})
Water	MEA 30 wt%	112± 1
	MEA 25 wt% + PZ 5 wt%	116± 1
	AHPD 11 wt%	118± 1
	AHPD 10.11 wt% + PZ 0.89 wt%	121± 1

4.3.4. Thermal stability

TGA was used to study the influence of amines on membrane degradation and the effect of Pz on thermal stabilization. Fig. 4.6 shows the TGA curves of neat and used membranes in the temperature range of 200-600°C. Weight loss was observed at lower temperatures for all used membranes in comparison to the neat one, showing that the thermal resistance of the membrane is weakened by its immersion in the amine solutions. However, it is restored to a great extent after the addition of PZ in MEA and AHPD solutions. It is believed that Pz acts in a similar way as HALS molecules, which are well known to enable thermal stabilization of polyolefins, in addition to its oxidative stabilization effects (Gugumus, 1990; Zweifel, 2001).

Membrane stability can quantitatively be studied either by comparison of temperatures at which membrane reach 50% of its initial weight, or by comparison of membrane weight at a certain temperature. Thermal stability data and decomposition level

of membranes are summarized in Table 4.4. Membrane decomposition level shows the level of instability of used membranes at a certain temperature ($T_{50\%}$ of the neat membrane) in comparison to that of the neat one. This data indicate that membrane stability varies in the following order: Neat > MEA > AHPD > MEA/AHPD > AHPD/PZ.

Table 4.4. Membrane stability data and decomposition level.

Sample	[a]T_{in} (°C)	[b]T_{fi} (°C)	[c]$T_{50\%}$ (°C)	[d]Decomposition level (%)
Neat	275	550	484	50
AHPD/PZ	247	535	446	75
AHPD	243	515	433	94
MEA/PZ	235	498	429	97
MEA	237	504	411	96

a) Initial decomposition temperature, b) Final decomposition temperature, c) Decomposition temperature at 50% weight, d) Membrane weight at $T_{50\%}$ of the neat membrane (484°C).

4.4. Conclusions

The stability of microporous LDPE hollow fiber membranes intended to be used for CO_2 capture in membrane contactors was studied in contact with 30 wt% MEA and 11 wt% AHPD aqueous solutions with and without the addition of PZ. The surface of membranes immersed in MEA and AHPD solutions underwent morphological, chemical and thermal degradation. However, such instability was found to be restored to a great extent by the addition of PZ. It was proposed that the stabilizing effect of PZ in amine solutions arises from a two-step mechanism including the formation of nitroxide radicals, through the oxidation of PZ, followed by the reaction between the oxidized PZ and amine molecules. Resulting large size molecules are proposed to have a steric hindrance effect. For their efficient dual-function properties (high CO_2 absorption efficiency and polyolefin membrane stabilization) PZ containing amine solutions are therefore suggested as good candidates for CO_2 absorption in membrane contactors.

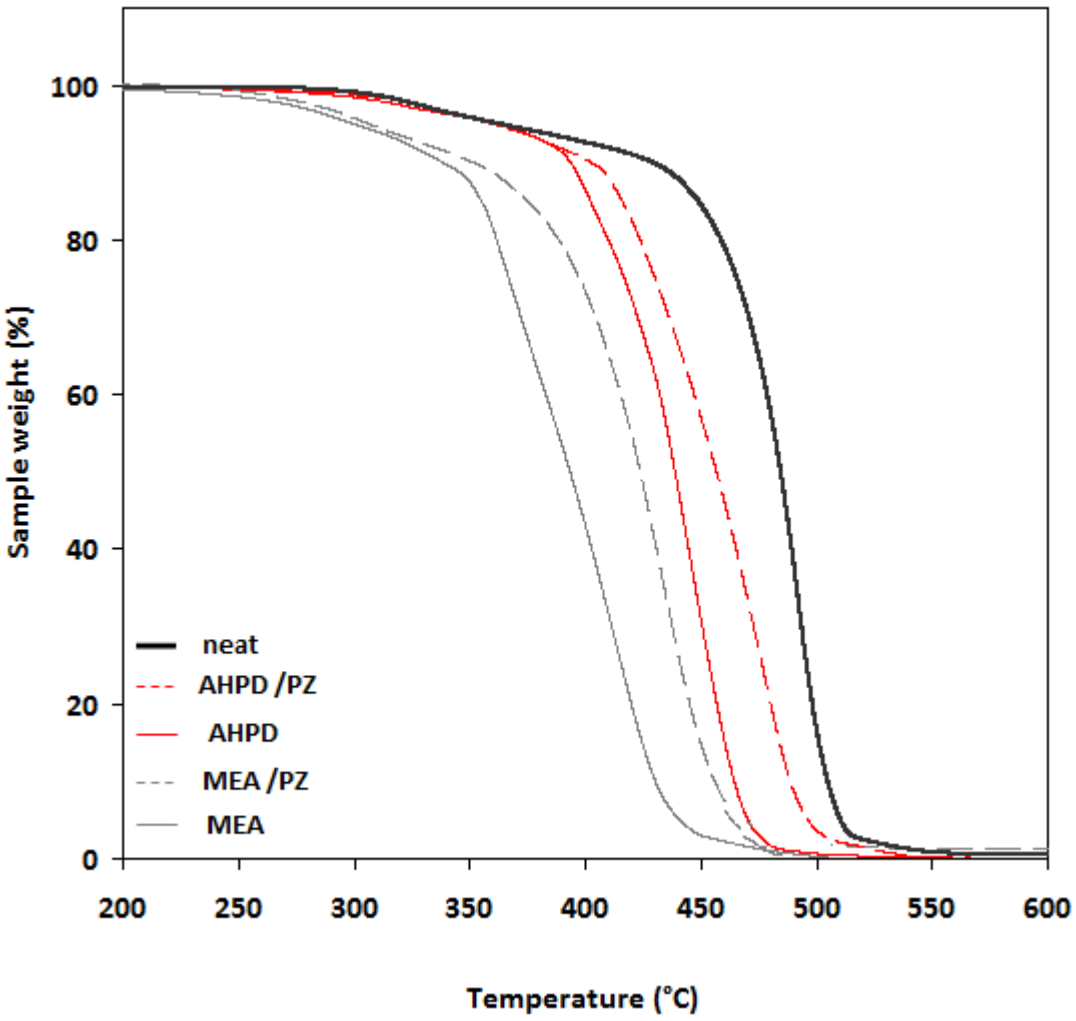

Figure 4.6. TGA curves of LDPE hollow fiber membranes.

5. General conclusions and recommendations for future works

Highly hydrophobic microporous LDPE *hollow fiber membranes* intended to be used for CO_2 capture in GLMC were prepared using melt-extrusion of LDPE/NaCl blends followed by salt leaching in water. Membrane porosity, which is strongly dependent on the amount of salt removed from the hollow fiber structure, was shown to increase with increasing initial salt content. It was observed that for samples with initial salt content below 60 wt%, the leaching could not be completed and an important amount of salt remained in the samples after 160 min leaching. However, for samples with salt content of 60 wt% and higher, the percentage of salt removal reached 100% after 160 min. SEM micrographs revealed the roughness created on the surface of hollow fiber membranes due to the formation of micropapillas formed by the addition of NaCl to the LDPE matrix. Moreover, the surface roughness was shown to increase by the increase of the initial salt content. The roughness created on the membrane surface led to a remarkable increase in water contact angle (hydrophobicity) from 98^o for neat LDPE to 130^o for hollow fibers prepared with 68 wt% NaCl.

The investigated mechanical properties (Young's modulus, tensile strength, and strain at break) were shown to be highly dependent on the initial salt content, but can be directly related to the final structure of the hollow fibers through the porous structure produced. Several important conclusions derived from mechanical properties analysis: i) Young's modulus increased from the neat sample to the sample with initial salt content of 50 wt%, due to salt remained in the sample (unleached), which increased the material rigidity; ii) with the increase of the initial salt content from 60 to 68 wt%, the Young's modulus decreased as a result of complete salt leaching and pore formation; iii) the stress at break decreased with the increase of the initial salt content, due to the combined effects of residual salts in LDPE structure and those removed by leaching; iv) the tensile stress slightly increased for the sample prepared with 68 wt% initial salt content compared to the one with 60 wt%, probably due to a change in the volume fraction of open/close pores with the increase in material porosity; v) a sharp drop in elongation at break was observed for

samples with initial salt contents of 0-50 wt%, followed by a slight increase from 50 wt% to 60 wt%, since the material was already brittle; vi) a slight increase in elongation at break was observed when the initial salt content increased from 60 to 68 wt%, due to the increase in the volume of open cells which make the sample more deformable.

The investigation of chemical stability of non-porous LDPE fibers in contact with aqueous MEA solutions revealed the auto-oxidation of LDPE material. This process was found to be accelerated by the alkaline nature of the alkanolamine which leads to the formation of C-O and C=O containing groups (ketones, aldehydes and alcohols), followed by chemical interaction of the oxidized LDPE with MEA. However, these chemical alterations were found to be hindered by the addition of CO_2 to MEA solution. The degradation process became less significant as CO_2 loading increased (pH of solution decreased), due to the acidic nature of CO_2.

In addition, the stability of microporous LDPE hollow fiber membranes in contact with 30 wt% MEA aqueous solutions and 11 wt% AHPD aqueous solutions with and without PZ addition was investigated. The surface of membranes immersed in MEA and AHPD solutions was shown to undergo morphological, chemical and thermal degradations, but they were more important in case of MEA. However, the degradation process was found to be restored to a great extent by addition of PZ. It was proposed that the stabilizing effect of PZ in MEA and AHPD solutions arises from a two-step mechanism including the formation of nitroxide radicals, through the oxidation of PZ, followed by the reaction between the oxidized PZ and alkanolamine molecules. Resulting large size molecules are proposed to have a steric hindrance effect. For their efficient dual-function properties (high CO_2 absorption efficiency and polyolefin membrane stabilization), PZ containing alkanolamine solutions (especially AHPD/PZ) are therefore suggested as good candidates for CO_2 absorption in membrane contactors.

The results of this project demonstrated that template-leaching is a solvent-free method that can be used as a continuous membrane fabrication process and might be applicable to a variety of polymers. Having much less environmental impacts, solvent-free approaches for highly hydrophobic membrane fabrication are most desirable for preventing wetting in GLMC. New research in this area would be very much welcome for making the

gas separation process in GLMC attractive and competitive for industrial applications. Further investigations on membrane fabrication through melt extrusion coupled with the salt leaching technique can be directed towards reducing of the membrane pore size and acceleration of the leaching time. In addition, since the fabricated membranes are aimed for CO_2 absorption in GLMC, future investigations will have to evaluate the absorption efficiency in different conditions (different absorbent solutions, gas concentrations and temperatures) and membrane wettability in long term operation.

References

D. Aaron, C. Tsouris, Separation of CO_2 from Flue Gas: A Review, Sep. Sci. Technol. 40 (2005) 321-348.

T.G. Amundsen, L.E. Øi, D.A. Eimer, Density and Viscosity of Monoethanolamine + Water + Carbon Dioxide from (25 to 80) °C, J. Chem. Eng. Data. 54 (2009) 3096-3100.

S. Atchariyawut, R. Jiraratananon, R. Wang, Separation of CO_2 from CH_4 by gas–liquid membrane contacting process. J. Membr. Sci. 304 (2007) 163-172.

A.-M. Barbe, P.-A. Hogan and R.-A. Johnson, Surface morphology changes during initial usage of hydrophobic, microporous polypropylene membranes, J. Membr. Sci. 17 (2000) 149-156.

D. Bargeman, D.F. van Voorst Vader, Effect of Surfactants on Contact Angles at Nonpolar, J. Colloid Interface Sci. 42 (1973) 467-472.

L.J. Bellamy, The Infrared Spectra of Complex Molecules, 2nd edition, Methuen, London, 1962, pp. 425.

E.A. Bevilacqua, E.S. English, J.S. Gall, Mechanism of Polyethylene Oxidation, J. Appl. Polym. Sci. 8 (1964) 1691-1698.

S. Bishnoi, G.T. Rochelle, Absorption of carbon dioxide into aqueous piperazine: reaction kinetics, solubility and mass transfer, Chem. Eng. Sci., 55 (2000) 5531-5543.

S. Bishnoi, G.T. Rochelle, Thermodynamics of piperazine/ methyldiethanolamine/ water/carbon dioxide. Ind. Eng. Chem. Res. 41 (2002) 604-612.

R. Bloosey, Self-cleaning surfaces-virtual realities, Nat. Mater. 2 (2003) 301-306.

S. Boributh, S. Assabumrungrat, N. Laosiripojana, R. Jiraratananon, A Modeling Study on the Effects of Membrane Characteristics and Operating Parameters on Physical Absorption of CO_2 by Hollow Fiber Membrane Contactor, J. Membr. Sci. 380 (2011) 21-33.

Y. Boguslavsky, T. Fadida, Y. Talyosef, J.-P. Lellouche, Controlling the Wettability Properties of Polyester Fibers Using Grafted Functional Nanomaterials, J. Mater. Chem. 21 (2011) 10304-10310.

S. Boributh, W. Rongwong, S. Assabumrungrat, N. Laosiripojana, R. Jiraratananon, Mathematical Modeling and Cascade Design of Hollow Fiber Membrane Contactor for CO_2 Absorption by Monoethanolamine, J. Membr. Sci. 401 (2012) 175-189.

F. Bougie, J. Lauzon-Gauthier, M.C. Iliuta, Acceleration of the reaction of carbon dioxide into aqueous 2-amino-2- hydroxymethyl-1,3-propanediol solutions by piperazine addition, Chem. Eng. Sci. 64 (2009) 2011-2019.

F. Bougie, M.C. Iliuta, Analysis of regeneration of sterically hindered alkanolamines aqueous solutions with and without activator, Chem. Eng. Sci. 65 (2010a) 4746–4750.

F. Bougie, M.C. Iliuta, CO_2 Absorption into Mixed Aqueous Solutions of 2-Amino-2-hydroxymethyl-1,3-propanediol and Piperazine, Ind. Eng. Chem. Res. 49 (2010b) 1150-1159.

F. Bougie, M.C. Iliuta, CO_2 Absorption in Aqueous Piperazine Solutions: Experimental Study and Modeling, J. Chem. Eng. Data, 56 (2011) 1547-1554.

F. Bougie, M.C. Iliuta, Analysis of Young-Laplace equation parameters and their influence on efficient CO_2 capture in membrane contactors, Sep. Purif. Technol. 118 (2013) 806-815.

R. Bounaceur, N. Lape, D. Roizard, C. Vallieres, E. Favre, Membrane processes for post-combustion, Energy 31 (2006) 2556-2570.

A.B.D. Cassie, S. Baxter, Wettability of Porous Surfaces, Trans. Faraday. Soc. 40 (1944) 546-551.

E. Chabanon, carbon dioxide capture: A parametric study, Energy 31 (2006) 2556-2570.

Canadian Protection Environmental Act (CEPA), 1999, http://www.ec.gc.ca/lcpe-cepa/default.asp?lang=En&n=26A03BFA-1.

A. Chabanon, C. Bouallou, J.C. Remigy, E. Lasseuguette, Y. Medin, E. Favre, P.T. Nguyen, D. Roizard, Study of an Innovative Gas-Liquid Contactor for CO_2 Absorption, Energy Procedia 4 (2011a) 1769-1776.

E. Chabanon, D. Roizard, E. Favre, Membrane Contactors for Post Combustion Carbon Dioxide Capture: A Comparative Study of Wetting Resistance on Long Time Scales, Ind. Eng. Chem. Res. 50 (2011b) 8237-8244.

S. Chakravati, A.Gupta, B. Hunek, Advanced technology for the capture of carbon dioxide from flue gases. In: 1st National Conference on Carbon Sequestration, Washington, DC, 2001.

J. Chen, J.D. Li, C.X. Chen, Surface modification of polyvinylidene fluoride (PVDF) membranes by low-temperature plasma with grafting styrene, Plasma Sci. Technol. 11 (2009) 42-47.

Sh.-Ch. Chen, S.-H. Lin, R.-D. Chien, Y.-H. Wang, H.-C. Hsiao, Chemical Absorption of Carbon Dioxide with Asymmetrically Heated Polytetrafluoroethylene Membranes, J. Environ. Manag. 92 (2011) 1083-1090.

J.C.W. Chien, D.S.T. Wang, Autoxidation of Polyolefins. Absolute Rate Constants and Effect of Morphology, Macromolecules 8 (1975) 920-928.

A.E. Childress, P. Le-Clech, J.L. Daugherty, C. Chen, G.L. Leslie, Mechanical analysis of hollow fiber membrane integrity in water reuse applications, Desalination 80 (2005) 5-14.

S. Chmela, D.J. Carlsson, D.M. Wiles, Photo-stabilizing efficiency of N-substituted hindered amines in polypropylene: Effects of processing conditions and exposure to a protonic acid, Polym. Degrad. Stab. 26 (1989) 185-195.

S.-H. Choi, F. Tasselli, J.C. Jansen, G. Barbieri, E. Drioli, Effect of the preparation conditions on the formation of asymmetric poly(vinylidene fluoride) hollow fibre membranes with a dense skin, Eur. Polym. J. 46 (2010) 1713-1725.

W.-J. Choi, J.-B. Seo, S.-Y. Jang, J.-H. Jung, K.-J. Oh, Removal characteristics of CO_2 using aqueous MEA/AMP solutions in the absorption and regeneration process, J. Environ. Sci. 21 (2009) 907-913.

R.K.M. Chu, H.E. Naguib, N. Atalla, Synthesis and Characterization of Open-Cell Foams for Sound Absorption With Rotational Molding Method, Polym. Eng. Sci. 49 (2009) 1744-1754.

A.L. Cordeiro, M. Nitschke, A. Janke, R. Helbig, F. D'Souza, G.T. Donnelly, P.R. Willemsen, C. Werner, Fluorination of poly(dimethylsiloxane) Surfaces by Low Pressure CF_4 Plasma- Physicochemical and Antifouling Properties, eXPRESS Polym. Lett. 3 (2009) 70-83.

J.T. Cullinane, G.T Rochelle, Carbon dioxide absorption with aqueous potassium carbonate promoted by piperazine. Chem. Eng. Sci., 59 (2004) 3619-3630.

J.T. Cullinane, G.T. Rochelle, Kinetics of carbon dioxide absorption into aqueous potassium carbonate and piperazine, Ind. Eng. Chem. Res. 45 (2006) 2531-2545.

R. Dangtungee, P. Supaphol, Melt rheology and extrudate swell of sodium chloride-filled low-density polyethylene: Effects of content and size of salt particles, Polym. Test. 29 (2010) 188-195.

J. Davison, Performance and costs of power plants with capture and storage of CO_2, Energy 32 (2007) 1163–1176.

D. deMontigny, P. Tontiwachwuthikul, A. Chakma, Using Polypropylene and Polytetrafluoroethylene Membranes in a Membrane Contactor for CO_2 Absorption, J. Membr. Sci. 277 (2006) 99-107.

V.Y. Dindore, D.W.F. Brilman, F.H. Geuzebroek, G.F. Versteeg, Membrane-Solvent Selection for CO_2 Removal Using Membrane Gas-Liquid Contactors, Sep. Purif. Technol. 40 (2004) 133-145.

V.Y. Dindore, D.W.F. Brilman, F.H. Geuzebroek, G.F. Versteeg, Hollow Fiber Membrane Contactor as a Gas-Liquid Model Contactor, Chem. Eng. Sci. 60 (2005) 467-479.

T.C. Drage, K.M. Smith, C. Pevida, A. Arenillas, C.E. Snape, Development of adsorbent technologies for post-combustion CO_2 capture, Energy Procedia 1 (2009) 881-884.

Ch. Du, Y.-Y. Xu and B.-K. Zhu, Structure formation and characterization of PVDF hollow fiber membranes by melt-spinning and stretching method, J. Appl. Polym. Sci. 106 (2007) 1793-1799.

S.J. Ebbens, J.P.S. Badyal, Surface Enrichment of Fluorochemical-Doped Polypropylene Films, Langmuir 17 (2001) 4050-4055.

H.Y. Erbil, A.L. Demirel, Y. Avci, O. Mert, Transformation of a Simple Plastic into a Superhydrophobic Surface, Sci. 299 (2003) 1377-1380.

O. Falk-Pedersen, H. Dannström, Separation of Carbon Dioxide From Offshore Gas Turbine Exhaust, Polym. Adv. Technol. 19 (1997) 1616-1622.

G.-J. Fan, A.G.H. Wee, R. Idem, P. Tontiwachwuthikul, NMR Studies of Amine Species in MEA-CO_2-H_2O System: Modification of the Model of Vapor-Liquid Equilibrium (VLE), Ind. Eng. Chem. Res. 48 (2009) 2717–2720.

Z.P. Fan, W.L. Liu, Z.J. Wei, J.S. Yao, X.L. Sun, M. Li, X.Q. Wang, Fabrication of Two Biomimetic Superhydrophobic Polymeric Surfaces, Appl. Surf. Sci. 257 (2011) 4296-4301.

L. Feng, Sh. Li, Y. Li, H. Li, L. Zhang, L. Jiang, D. Zhu, Super-Hydrophobic Surfaces: From Natural to Artificial, Adv. Mater. 14 (2002) 1857-1860.

L. Feng, Y. Song, J. Zhai, B. Liu, J. Xu, L. Jiang, D. Zhu, Creation of a Superhydrophobic Surface from an Amphiphilic Polymer, Angew. Chem. Int. Ed. 42 (2003) 800-802.

E. Favre, Membrane processes and postcombustion carbon dioxide capture: challenges and prospects. Chem. Eng. J. 171 (2011) 782-93.

J. D. Figueroa, T. Fout, S. Plasynski, H. McIlvried, R.D. Srivastava, Advances in CO_2 capture technology-The U.S. Department of Energy's Carbon Sequestration Program, internati onal journa l of greenhouse gas control 2 (2008) 9-20.

H.W. Fox, W.A. Zisman, The Spreading of Liquids on Low Energy Surfaces II. Modified Tetrafluoroethylene Polymers, J. Colloid Sci. 7 (1952) 109-121.

J.A. Franco, S.E. Kentish, J.M. Perera, G.W. Stevens, Fabrication of a superhydrophobic polypropylene membrane by deposition of a porous crystalline polypropylene coating, J. Membr. Sci. 318 (2008) 107-113.

J. Franco, D. deMontigny, S. Kentish, J. Perera, G. Stevens, A Study of the Mass Transfer of CO_2 through Different Membrane Materials in the Membrane Gas Absorption Process, Sep. Sci. Tech. 43 (2008) 225-244.

J.A. Franco, S.E. Kentish, J.M. Perera, G.W. Stevens, Poly(tetrafluoroethylene) Sputtered Polypropylene Membranes for Carbon Dioxide Separation in Membrane Gas Absorption, Ind. Eng. Chem. Res. 50 (2011) 4011-4020.

A.C.M. Franken, J.A.M. Nolten, M.H.V. Mulder, D. Bargeman, C.A. Smolders, Wetting Criteria for the Applicability of Membrane Distillation, J. Membr. Sci. 33 (1987) 315-328.

P. Freund, Making deep reductions in CO_2 emissions from coal-fired power plant using capture and storage of CO_2, Proc. Instn. Mech. Engrs Part A: J. Power and Energ 217 (2013) 1-7.

R.K.Y. Fu, Y.F. Mei, G.J. Wan, G.G. Siu, P.K. Chu, Y.X. Huang, X.B. Tian, S.Q. Yang, J.Y. Chen, Surface Composition and Surface Energy of Teflon Treated by Metal Plasma Immersion Ion Implantation, Surf. Sci. 573 (2004) 426-432.

A. Gabelman, S.-T. Hwang, Hollow Fiber Membrane Contactors, J. Membr. Sci. 159 (1999) 61-106.

M.C. Garcia-Payo, M.A. Izquierdo-Gil, C. Fernández-Pineda, Air Gap Membrane Distillation of Aqueous Alcohol Solutions, J. Membr. Sci. 169 (2000) 61-80.

G.A. George, M. Ghaemy, Hydroperoxide formation in the early stages of polypropylene photo-oxidation, Polym. Degrad. Stabil. 33 (1991) 411-428.

R.W. Gore, Process for Producing Porous Products, *US Patent* 1976, US3953566 A.

F. Gugumus, Plastic Additives, Chapter 1, 3rd ed., Hanser publishers, New York, 1990.

F. Gugumus, Re-examination of the thermal oxidation reactions of polymers: 1. New views of an old reaction, Polym. Degrad. Stabil. 74 (2001) 327-339.

N. Hedin, L. Andersson, L. Bergstrom, J. Yan, Adsorbents for the post-combustion capture of CO_2 using rapid temperature swing or vacuum swing adsorption, Appl. Energy 104 (2013) 418-433.

J.L. Henry, L.A. Ruaya, A. Carton, The kinetics of polyolefin oxidation in aqueous media, J. Polym. Sci. 30 (1992) 1693-1703.

J.L. Hodgson, M.L. Coote, Clarifying the mechanism of the Denisov cycle: How do hindered amine light stabilizers protect polymer coatings from photo-oxidative degradation, Macromolecules 43 (2010) 4573-4583.

X. Hu, Y. Chen, H. Liang, Ch. Xiao, Preparation of Pressure Responsive Hollow Fiber Membrane by Melt-Spinning of Polyurethane-Poly(vinylidene fluoride)-Poly(ethylene glycol) Blends, Mater. Manuf. Proc. 25 (2010) 1018-1020.

X.Y. Hu, Y.B. Chen, H. X. Liang, C.F. Xiao, Preparation of polyurethane/poly(vinylidene fluoride) blend hollow fibre membrane using melt spinning and stretching, Mater. Sci. Technol., 27 (2011) 661-665.

R. Riemer, IEA GHG, 1993. The Capture of Carbon dioxide from Fossil Fuel Fired Power Stations. Green House Gas Report IEA GHG/SR_2, Cheltenham, UK.

IEA, 2004. Prospects for CO_2 Capture and Storage. OECD/IEA, Paris, France.

B. Metz, O. Davison, H. de Coninck, M. Loos, L. Meyer, IPCC, 2005. Intergovernmental Panel on Climate Change (IPCC) Special Report on Carbon Dioxide Capture and Storage. Cambridge University Press, Cambridge, UK.

A.F. Ismail, P.Y. Lai, Development of defect-free asymmetric polysulfone membranes for gas separation using response surface methodology, Sep. Purif. Technol. 40 (2004) 191-207.

A. Ismail, N. Yaacob, Performance of Treated and Untreated Asymmetric Polysulfone Hollow Fiber Membrane in Series and Cascade Module Configurations for CO_2/CH_4 Gas Separation System, J. Membr. Sci. 275 (2006) 151-165.

D.R. Iyengar, S.M. Perutz, C.A. Dai, C.K. Ober, E.J. Kramer, Surface Segregation Studies of Fluorine-Containing Diblock Copolymers, Macromolecules 29 (1996) 1229-1234.

J.J. Jasper, The Surface Tension of Pure Liquid Compounds, J. Phys. Chem. Ref. Data 1 (1972) 841-850.

C. Jian, L. Jiding, C. Cuixian, Surface Modification of Polyvinylidene Fluoride (PVDF) Membranes by Low Temperature Plasma with Grafting Styrene, Plasma Sci. Technol. 11 (2009) 42-47.

M. Jin, X. Feng, J. Xi, K. Cho, L. Feng, L. Jiang, Superhydrophobic PDMS Surface with Ultra Low Adhesive Force, Macromol. Rapid. Commun. 26 (2005) 1805-1809.

J. Kamo, T. Hirai, K. Kamada, Solvent induced morphological change of microporous hollow fiber membranes, J. Membr. Sci. 70 (1992) 217-224.

S. Karoor, K.K. Sirkar, Gas Absorption Studies in Microporous Hollow Fiber Membrane Modules, Ind. Eng. Chem. Res. 32 (1993) 674-681.

H. Kawakami, M. Mikawa, S. Nagaoka, Formation of surface skin layer of asymmetric polyimide membranes and their gas transport properties, J. Membr. Sci. 137 (1997) 241-251.

Sh. Kazama, M. Sakashita, Gas separation properties and morphology of asymmetric hollow fiber membranes made from cardo polyamide, J. Membr. Sci. 243 (2004) 59-68.

A. Keller, M.J. Marchin, Oriented crystallization in polymers, J. Macromol. Sci., Bl (1967) 41-47.

P. Keshavarz, J. Fathikalajahi, S. Ayatollahi, Analysis of CO_2 Separation and Simulation of a Partially Wetted Hollow Fiber Membrane Contactor, J. Hazard. Mater. 152 (2008) 1237-1247.

B.S. Khaisiri, D. deMontigny, P. Tontiwachwuthikul, R. Jiraratananon, Comparing Membrane Resistance and Absorption Performance of Three Different Membranes in a Gas Absorption Membrane Contactor, Sep. Purif. Technol. 65 (2009) 290-297.

F. Khalili, A. Henni, A.L.L. East, p*K*a Values of Some Piperazines at (298, 303, 313, and 323) K, J. Chem. Eng. Data, 54 (2009) 2914-2917.

M.T. Khorasani, H. Mirzadeh, Z. Kermani, Wettability of Porous Polydimethylsiloxane Surface: Morphology Study, Appl. Surf. Sci. 242 (2005) 339-345.

B.-S. Kim, P. Harriot, Critical Entry Pressure for Liquids in Hydrophobic Membranes, J. Colloid Interface Sci. 115 (1987) 1-8.

S.S. Kim, D.R. Lloyd, Microporous membrane formation via thermallyinduced phase separation. III. Effect of thermodynamic interactions on the structure of isotactic polypropylene membranes, J. Membr. Sci. 64 (1991) 13-29.

J.J. Kim, T.S. Jang, Y.D. Kwon, U.Y. Kim, S.S. Kim, Structural Study of Microporous Polypropylene Hollow Fiber Membranes Made by the Melt-Spinning and Cold Stretching Method, J. Membr. Sci. 93 (1994) 209-215.

J.-J. Kim, J.-R. Hwang, U.-Y. Kim and S.-S. Kim, Operation parameters of melt-spinning of polypropylene hollow fiber membranes, J. Membr. Sci. 108 (1995) 25-36.

Y.-S. Kim, S.-M. Yang, Absorption of Carbon Dioxide through Hollow Fiber Membranes Using Various Aqueous Absorbents, Sep. Purif. Technol. 21 (2000) 101-109.

K.S. Kim, K.H. Lee, K. Cho, C.E. Park, Surface Modification of Polysulfone Ultrafiltration Membrane by Oxygen Plasma Treatment, J. Membr. Sci. 199 (2002) 135-145.

J. Kim, Effects of Precursor Properties on the Preparation of Polyethylene Hollow Fiber Membranes by Stretching, J. Membr. Sci. 318 (2008) 201-209.

S. Kirk, M. Strobel, Ch.-Y. Lee, St. J. Pachuta, M. Prokosch, H. Lechuga, M.E. Jones, Ch. S. Lyons, S. Degner, Y. Yang, M.J. Kushner, Fluorine Plasma Treatments of Polypropylene Films, 1 – Surface Characterization, Plasma Process Polym. 7 (2010)107-122.

P.P. Klemchuk, M. E. Gande, Stabilization mechanisms of hindered amines, Makromol. Chem. Macromol. Symp. 28 (1989) 117-144.

P.P. Klemchuk, M.E. Gande, E. Cordola, Hindered amine mechanisms: Part III-Investigations using isotopic labelling, Polym. Degrad. Stabil. 27 (1990) 65-74.

P. Kosaraju, A. S. Kovvali, A. Korikov, K.K. Sirkar, Hollow Fiber Membrane Contactor Based CO2 Absorption-Stripping Using Novel Solvents and Membranes, Ind. Eng. Chem. Res. 44 (2005) 1250-1258.

B. Krause, M.E. Boerrigter, N.F.A. van der Vegt, H. Strathmann, M. Wessling, Novel open-cellular polysulfone morphologies produced with trace concentrations of solvents as pore opener, J. Membr. Sci. 187 (2001) 181–192.

H. Kreulen, C.A. Smolders, Microporous Hollow Fiber Membrane Modules as Gas-Liquid Contactors, J. Membr. Sci. 78 (1993) 217-238.

P.S. Kumar, J.A. Hogendoorn, P.H.M. Feron, G.F. Versteeg, New Absorption Liquids for the Removal of CO_2 from Dilute Gas Streams Using Membrane Contactors, Chem. Eng. Sci. 57 (2002) 1639-1651.

K.H. Lee, S.H. Yeon, B. Sea, Y.I. Park, Hollow Fiber Membrane Contactor Hybrid System for CO_2 Recovery, Stud. Surf. Sci. Catal. 153 (2004) 423-428.

S.Y. Lee, S.Y. Park, H.S. Song, Lamellar Crystalline Structure of Hard Elastic HDPE Films and its Influence on Microporous Membrane Formation, Polymer 47 (2006) 3540-3547.

Y. Lee, S.-H. Park, K.-B. Kim, and J.-K. Lee, Fabrication of Hierarchical Structures on a Polymer Surface to Mimic Natural Superhydrophobic Surfaces, Adv. Mater. 19 (2007) 2330-2335.

K. Lee, Y.S. Kim, K. Shin, Hierarchically-Structured Artificial Water-Repellent Leaf Surfaces Replicated from Reusable Anodized Aluminum Oxide, Macromol. Res. 20 (2012) 762-767.

J.-L. Li, B.-H. Chen, Review of CO_2 Absorption Using Chemical Solvents in Hollow Fiber Membrane Contactors, Sep. Purif. Technol. 41 (2005) 109-122.

S.-H. Lin, P.-C. Chiang, Ch.-F. Hsieh, M.-H. Li, K.-L. Tung, Absorption of Carbon Dioxide by the Absorbent Composed of Piperazine and 2-amino-2-methyl-1-propanol in PVDF Membrane Contactor, J. Chin. Inst. Chem. Eng. 39 (2008) 13-21.

S.-H. Lin, Ch.-F. Hsieh, M.-H. Li, K.-L. Tung, Determination of Mass Transfer Resistance during Absorption of Carbon Dioxide by Mixed Absorbents in PVDF and PP Membrane Contactor, Desalination 249 (2009) 647-653.

S.-H. Lin, K.-L.W.-J. Tung, H.-W. Chang, Absorption of Carbon Dioxide by Mixed Piperazine-Alkanolamine Absorbent in a Plasma-Modified Polypropylene Hollow Fiber Contactor, J. Membr. Sci. 333 (2009a) 30-37.

S.-H. Lin, K.-L. Tung, H.-W. Chang, K.-R. Lee, Influence of Fluorocarbon Flat Membrane Hydrophobicity on Carbon Dioxide Recovery, Chemosphere 75 (2009b) 1410-1416.

D.R. Lloyd, S.S Kim, K.E. Kinzer, Microporous membrane formation via thermallyinduced phase separation. II. Liquid-liquid phase separation, J. Membr. Sci. 64 (1991) l-11.

X. Lu, Ch. Zhang, H. Yanchun, Low-Density Polyethylene Superhydrophobic Surface by Control of its Crystallization Behavior, Macromol. Rapid Commun. 25 (2004) 1606-1610.

J.-G. Lu, Y.-F. Zheng, M.-D. Cheng, Wetting Mechanism in Mass Transfer Process of Hydrophobic Membrane Gas Absorption, J. Membr. Sci. 308 (2008) 180-190.

J.-G. Lu, Y. Ji, H. Zhang, M.-D. Chen, CO_2 Capture Using Activated Amino Acid Salt Solutions in a Membrane Contactor, Sep. Sci. Technol. 45 (2010) 1240-1251.

P. Luis, T.V. Gerven, B. Van der Bruggen, Recent Developments in Membrane-Based Technologies for CO_2 Capture, Prog. Energy Comb. Sci. 38 (2012) 419-448.

Y. Lv, X. Yu, S.-T. Tu, J. Yan, E. Dahlquist, Wetting of Polypropylene Hollow Fiber Membrane Contactors, J. Membr. Sci. 362 (2010) 444-452.

Y. Lv, X. Yu, J. Jia, S.-T. Tu, J. Yan, E. Dahlquist, Fabrication and Characterization of Superhydrophobic Polypropylene Hollow Fiber Membranes for Carbon Dioxide Absorption, Appl. Energy 90 (2012) 167-174.

M. Ma, R.M. Hill, Superhydrophobic Surfaces, Curr. Opin Colloid Interface Sci. 11 (2006) 193-202.

J. Ma, N. Sun, X. Zhang, N. Zhao, F. Xiao, W. Wei, Y. Sun, A short review of catalysis for CO_2 conversion, Catal. Today 148 (2009) 221-231.

A. Malek, K. Li, W.K. Teo, Modeling of Microporous Hollow Fiber Membrane Modules Operated under Partially Wetted Conditions, Ind. Eng. Chem. Res. 36 (1997) 784-793.

Sh. Ma'mun, H.F. Svendsen, K.A. Hoff, O. Juliussen, Selection of New Absorbents for Carbon Dioxide Capture, Energy Convers. Manage. 48 (2007) 251-258.

A. Mansourizadeh, A.F. Ismail, Hollow Fiber Gas-Liquid Membrane Contactors for Acid Gas Capture: A Review, J. Hazard. Mater. 171 (2009) 38-53.

A. Mansourizadeh, A.F. Ismail, T. Matsuura, Effect of Operating Conditions on the Physical and Chemical CO_2 Absorption through the PVDF Hollow Fiber Membrane Contactor, J. Membr. Sci. 353 (2010) 192-200.

A. Mansourizadeh, Experimental Study of CO_2 Absorption/Stripping via PVDF Hollow Fiber Membrane Contactor, Chem. Eng. Res. Des. 90 (2012) 555-562.

A. Mansourizadeh, S. Mousavian, Structurally developed microporous polyvinylidene fluoride hollow-fiber membranes for CO_2 absorption with diethanolamine solution, J. Polym. Res. 20 (2013) 99-111.

S.A.M. Marzouk, M. H. Al-Marzouqi, M. Teramoto, N. Abdullatif, Z.M. Ismail, Simultaneous removal of CO_2 and H_2S from pressurized CO_2-H_2S-CH_4 gas mixture using hollow fiber membrane contactors, Sep. Purif. Technol. 86 (2012) 88-97.

A. Masohan, M. Ahmed, S.K. Nirmal, A. Kumar, M.O. Garg, A simple pH-based method for estimation of CO_2 absorbed in alkanolamines, Indian J. Sci. Technol. 4 (2009) 59-64.

S. Massey, A. Adnot, A. Rjeb, D. Roy, Action of water in the degradation of low-density polyethylene studied by X-ray photoelectron spectroscopy, eXPRESS Polymer Lett. 1 (2007) 506–511.

H. Matsumoto, H. Kitamura and T. Kamata, Effect of Membrane Properties of Microporous Hollow fiber Gas-Liquid Contactor on CO_2 Removal from Thermal Power Plant flue gas, J. Chem. Eng. Jpn. 28 (1995) 125-128.

M. Mavroudi, S.P. Kaldis, G.P. Sakellaropoulos, Reduction of CO_2 Emissions by a Membrane Contacting Process, Fuel 82 (2003) 2153-2159.

M. Mavroudi, S.P. Kaldis, G.P. Sakellaropoulos, A study of Mass Transfer Resistance in Membrane Gas-Liquid Contacting Processes, J. Membr. Sci. 272 (2006) 103-115.

L. Mei, D. Zhang, Q. Wang, Morphology Structure Study of Polypropylene Hollow Fiber Membrane Made by the Blend-Spinning and Cold-Stretching Method, J. Appl. Polym. Sci. 84 (2002) 1390-1394.

M. Mikawa, Sh. Nagaoka, H. Kawakami, Gas permeation stability of asymmetric polyimide membrane with thin skin layer: effect of molecular weight of polyimide, J. Membr. Sci. 208 (2002) 405-414.

M.K. Mondal, H.K. Balsora, P. Varshney, Progress and trends in CO_2 capture/separation technologies: A review, Energy 46 (2012) 431-441.

S. Mosadegh Sedghi, J. Brisson, D. Rodrigue, M.C. Iliuta, Chemical alteration of LDPE hollow fibers exposed to monoethanolamine solutions used as absorbent for CO_2 capture process, Sep. Purif. Technol. 80 (2011) 338-344.

S. Mosadegh-Sedghi, J. Brisson, D. Rodrigue, M.C. Iliuta, Morphological, Chemical and Thermal Stability of Microporous LDPE Hollow Fiber Membranes in Contact with Single and Mixed Amine Based CO_2 Absorbents, Sep. Purif. Technol. 96 (2012a) 117-123.

S. Mosadegh Sedghi, D. Rodrigue, J. Brisson, M.C. Iliuta, Microporous and highly hydrophobic polymeric hollow fiber membranes and methods for preparation thereof, US Patent pending, 2012b.

S. Mosadegh-Sedghi, D. Rodrigue, J. Brisson, M.C. Iliuta, Highly hydrophobic microporous LDPE hollow fiber membranes by melt-extrusion coupled with salt-leaching technique, Adv. Polym. Technol. 24 (2013) 584-592.

M. Narkis, E. Joseph, Tensile Properties of Rigid Polymeric Foams Produced by Salt Extraction, J. Cell. Plast. 14 (1978) 45-48.

P.T. Nguyen, E. Lasseuguette, Y. Medina-Gonzalez, J.C. Remigy, D. Roizard, E. Favre, A Dense Membrane Contactor for Intensified CO_2 Gas/Liquid Absorption in Post Combustion Capture, J. Membr. Sci. 377 (2011) 261-272.

N. Nishikawa, M. Ishibashi, H. Ohta, N. Akutsu, H. Matsumoto, T. Kamata, H. Kitamura, CO_2 Removal by Hollow Fiber Gas-Liquid contactor, Energy Convers. Manag. 36 (1995) 415-418.

D.C. Nymeijer, B. Folkers, I. Breebaart, M.H.V. Mulder, M. Wessling, Selection of Top Layer Materials for Gas–Liquid Membrane Contactors, J. Appl. Polym. Sci. 92 (2004) 323-334.

E. Occhiello, M. Morra, F. Garbassi, XPS and SSIMS Studies on CF_4/O_2 Plasma Treated Polycarbonate, Angew. Makromol. Chem. 173 (1989) 183-193.

A.K. Pabby, A.M. Sastre, State-of-the-art review on hollow fibre contactor technology and membrane-based extraction processes, J.Membr. Sci. 430 (2013) 263-303.

P. Pages, F. Carrascoy, J. Saurina, X. Colom, FTIR and DSC study of HDPE structural changes and mechanical properties variation when exposed to weathering aging during Canadian winter, J. Appl. Polym. Sci. 60 (1996) 153-159.

J.-Y. Park, S.J. Yoon, H. Lee, Effect of Steric Hindrance on Carbon Dioxide Absorption into New Amine Solutions: Thermodynamics and Spectroscopic Verification through Solubility and NMR Analysis, Environ. Sci. Technol. 37 (2003) 1670-1675.

J.K. Pike, T. Ho, Water-Induced Surface Rearrangements of Poly(dimethylsiloxane-urea-urethane) Segmented Block Copolymers, Chem. Mater. 8 (1996) 856-860.

I. Pinnau, W.J. Koros, A Qualitative Skin Layer Formation Mechanism for Membranes Made by Dry/ Wet Phase Inversion, J. Polym. Sci.: Part B Polym. Phys. 31(1993) 419-427.

J.C.M. Pires, F.G. Martins, M.C.M. Alvim-Ferraz, M. Simões, Recent developments on carbon capture and storage: An overview, Chem. Eng. Res. Des. 89 (2011) 1446-1460.

F. Porcheron, S. Drozdz, Hollow fiber membrane contactor transient experiments for the characterization of gas/liquid thermodynamics and mass transfer properties, Chem. Eng. Sci. 64 (2009) 265-275.

A.F. Portugal, J.M. Sousa, F.D. Magalhães, A. Mendes, Solubility of Carbon Dioxide in Aqueous Solutions of Amino Acid Salts, Chem. Eng. Sci. 64 (2009) 1993-2002.

J. Pospìsil, S. Nešpůrek, Chain-breaking stabilizers in polymers: the current status, Polym. Degrad. Stabil. 49 (1995) 99-110.

P.S. Puri, Fabrication of hollow fibre gas separation membranes, Gas Sep. Purif. 4 (1990) 29-36.

E. Puukilainen, A. Tapani, Modification of Surface Properties of Polyethylene by Perfluoropolyether Blending, J. Polym. Sci. B: Polym. Phys. 43 (2005) 2252-2258.

M. Rahbari-Sisakht, A.F. Ismail, D. Rana, T. Matsuura, A Novel Surface Modified Polyvinylidenefluoride Hollow Fiber Membrane Contactor for CO_2 Absorption, J. Membr. Sci. 415-416 (2012) 221-228.

S. Rajabzadeh, C. Liang, Y. Ohmukai, T. Maruyama, H. Matsuyama, Effect of additives on the morphology and properties of poly(vinylidene fluoride) blend hollow fiber membrane prepared by the thermally induced phase separation method, J. Membr. Sci. 423-424 (2012) 189-194.

K. Ramaratnam, V. Tsyalkovsky, V. Kelp, I. Lozinov, Ultrahydrophobic Textile Surface via Decorating Fibers with Monolayer of Reactive Nanoparticles and Non-Fluorinated Polymer, Chem. Commun. 43 (2007) 4510-4512.

E.C. Rangel, W.C.A. Bento, M.E. Kayama, W.H. Schreiner, N.C. Cruz, Enhancement of Polymer Hydrophobicity by SF_6 Plasma Treatment and Argon Plasma Immersion Ion Implantation, Surf. Interface Anal. 35 (2003) 179-183.

H.A. Rangwala, Absorption of Carbon Dioxide into Aqueous Solutions Using Hollow Fiber Membrane Contactors, J. Membr. Sci. 112 (1996) 229-240.

A.B. Rao, E.S. Rubin, A Technical, Economic, and Environmental Assessment of Amine-Based CO_2 Capture Technology for Power Plant Greenhouse Gas Control, Environ. Sci. Technol. 36 (2002) 4467-4475.

M.C. Rastogi, Surface and Interfacial Science: Applications to Engineering and Technology, Chapter 8, 1st ed., Narosa Publishing House, New Delhi, 2003.

W. Rongwong, R. Jiraratananon, S. Atchariyawut, Experimental Study on Membrane Wetting in Gas-Liquid Membrane Contacting Process for CO_2 Absorption by Single and Mixed Absorbents, Sep. Purif. Technol. 69 (2009) 118-125.

J. Rychly, L. Matisova-Rychla, K. Csmorova, L. Achimsky, L. Audouin, A. Tcharkhtchib, J. Verdub, Kinetics of mass change in oxidation of polypropylene, Polym. Degrad. Stabil. 58 (1997) 269-274.

R. Sargent, J. Alender, Soil Resistant Fibers, US Patent No. 5,560,992 (issued 1 Oct. 1996).

C.A. Scholes, K.H. Smith, S.E. Kentish, G.W. Stevens, CO_2 capture from precombustion processes-Strategies for membrane gas separation. Int. J. Greenh. Gas Con. 4 (2010) 739-755.

M. Scoponi, S. Cimmino, M. Kaci, Photo-stabilisation mechanism under natural weathering and accelerated photo-oxidative conditions of LDPE films for agricultural applications, Polymer 41 (2000) 7969-7980.

L.-Q. Shen, Z.-K. Xu, Y.-Y. Xu, Preparation and Characterization of Microporous Polyethylene Hollow Fiber Membranes, J. Appl.Polym. Sci., 84 (2002) 203-210.

A. Shojaei, S. Gholamalipour, Effect of Chemical Treatment of Teflon Powder on the Properties of Polyamide 66/Teflon Composites Prepared by Melt Mixing, Macromol. Res. 19 (2011) 613-621.

J.-Y. Shui, C.-W. Kuo, P. Chen, Fabrication of Tunable Superhydrophobic Surfaces, in Smart Materials III, SPIE Proceedings Vol. 5648, A.R. Wilson., Ed, (2005) pp.325-332.

E.N. Step, N.J. Turro, Mechanism of polymer stabilization by Hindered-Amine Light Stabilizers (HALS). Model investigations of the interaction of peroxy radicals with HALS amines and amino ethers, Macromolecules 27 (1994) 2529-2539.

M. Sun, C. Luo, L. Xu, H. Ji, Artificial Lotus Leaf by Nanocasting, Langmuir 21 (2005) 8978-8981.

K. Teshima, H. Sugimura, Y. Inoue, O. Takai, Transparent Ultra Water-Repellent Poly(ethylene terephthalate) Substrates Fabricated by Oxygen Plasma Treatment and Subsequent Hydrophobic Coating, Appl. Surf. Sci. 244 (2005) 619-622.

A. Torres-Trueba, F.A. Ruiz-Treviño, Gabriel Luna-Bárcenas, C.H. Ortiz-Estrada, Formation of integrally skinned asymmetric polysulfone gas separation membranes by supercritical CO_2, J. Membr. Sci. 320 (2008) 431-435.

UNEP, 2005. United Nations Environment Programme, Introduction to Climate Change, http://www.grida. no/climate/vital/06.htm (accessed in October 2010).

L. Verdolotti, S. Colini, G. Porta, S. Iannace, Effects of the Addition of LiCl, $LiClO_4$, and $LiCFSO_3$ Salts on the Chemical Structure, Density, Electrical, and Mechanical Properties of Rigid Polyurethane Foam Composite, Polym. Eng. Sci. 51 (2011) 1137-1144.

D. Wang, K. Li, W.-K. Teo, Porous PVDF Asymmetric Hollow Fiber Membranes Prepared with the Use of Small Molecular Additives, J. Membr. Sci. 178 (2000) 13-23.

R. Wang, D.-F. Li, C. Zhoub, M. Liua and D.-T. Liang, Impact of DEA solutions with and without CO_2 loading on porous polypropylene membranes intended for use as contactors, J. Membr. Sci. 229 (2004a) 147-157.

R. Wang, D.F. Li, D.T. Liang, Modeling of CO_2 Capture by Three Typical Amine Solutions in Hollow Fiber Membrane Contactors, Chem. Eng. Process. 43 (2004b) 849-856.

M. Wang, A. Lawal, P. Stephenson, J. Sidders, C. Ramshaw, Post-combustion CO_2 capture with chemical absorption: A state-of-the-art review, Chem. Eng. Res. Des. 89 (2011) 1609-1624.

X. Wei, B. Zhao, X.-M. Li, Z. Wang, B.-Q. He, T. He, B. Jiang, CF_4 Plasma Surface Modification of Asymmetric Hydrophilic Polyethersulfone Membranes for Direct Contact Membrane Distillation, J. Membr. Sci. 408 (2012) 164-175.

S.H. Wheale, J.P.S. Badyal, Xenon Difluoride Plasma Fluorination of Polymer Surfaces, Polymer 52 (2011) 5250-5254.

I. Woodward, W.C.E. Schofield, V. Roucoules, J.P.S. Badyal, Superhydrophobic Surfaces Produced by Plasma Fluorination of Polybutadiene Films, Langmuir 19 (2003) 3432-3438.

Z.-Y. Xi, Y.-Y. Xu, L.-P. Zhu, Ch.-H. Du, B.-K. Zhu, Effect of Stretching on Structure and Properties of Polyethylene Hollow Fiber Membranes Made by Melt-Spinning and Stretching Process, Polym. Adv. Technol. 19 (2008) 1616-1622.

S.-P. Yan, M.-X. Fang, W.-F. Zhang, S.-Y. Wang, Z.-K. Xub, Zh.-Y. Luoa, K.-F. Cen, Experimental Study on the Separation of CO_2 from Flue Gas Using Hollow Fiber Membrane Contactors without Wetting, Fuel Process. Technol. 88 (2007) 501-511.

M.-C. Yang, E.L. Cussler, Designing Hollow Fiber Contactors, AIChE 32 (1986) 1910-1916.

R. Yang, Y. Liu, J. Yu, K. Wang, Thermal oxidation products and kinetics of polyethylene composites, Polym. Degrad. Stabil. 91 (2006) 1651-1657.

H. Yang, Zh. Xu, M. Fan, R. Gupta, R.B. Slimane, A.E. Bland, I. Wright, Progress in carbon dioxide separation andcapture: A review, J. Environ. Sci. 20 (2008) 14-27.

Y. Yang, M. Strobel, S. Kirk, M.J. Kushner, Fluorine Plasma Treatments of Poly(propylene) Films, 2-Modeling Reaction Mechanisms and Scaling, Plasma Process. Polym. 7 (2010) 123-150.

X. Yang, R. Wang, L. Shi, A.G. Fane, M. Debowski, Performance Improvement of PVDF Hollow Fiber-Based Membrane Distillation Process, J. Membr. Sci. 369 (2011) 437-447.

S.-H. Yeon, B. Sea, Y.-I. Park, K.-H. Lee, Determination of Mass Transfer Rates in PVDF and PTFE Hollow Fiber Membranes for CO_2 Absorption, Sep. Sci. Technol. 38 (2003) 271-293.

S-H Yeon, K-S Lee, B Sea, Y-I Park, K-H Lee, Application of pilot-scale membrane contactor hybrid system for removal of carbon dioxide from flue gas, J. Membr. Sci. 257 (2005) 156-160.

Zh. Yuan, H. Chen, J. Zhang, D. Zhao, Preparation and Characterization of Self-Cleaning Stable Superhydrophobic Linear Low-Density Polyethylene, Sci. Technol. Adv. Mater. 9 (2008) 1-5.

Zh. Yuan, J. Bin, X. Wang, Q. Liu, D. Zhao, H. Chen, H. Jiang, Preparation and Anti-Icing Property of a Lotus-Leaf-Like Superhydrophobic Low-Density Polyethylene Coating With Low Sliding Angle, Polym. Eng. Sci. 52 (2012) 2310-2315.

J. Zhang, J. Li, Y. Han, Superhydrophobic PTFE Surfaces by Extension, Macromol. Rapid Commun. 25 (2004) 1105-1108.

H.-Y. Zhang, R. Wang, D.T. Liang, J. Tay, Theoretical and Experimental Studies of Membrane Wetting in the Membrane Gas-Liquid Contacting Process for CO_2 Absorption, J. Membr. Sci. 308 (2008) 162-170.

Y. Zhang, R. Wang, Gas–liquid membrane contactors for acid gas removal: recent advances and future challenges, Curr. Opin. Chem. Eng. 2 (2013) 255-262.

Q.-S. Zheng, Y. Yu, Z.-H. Zhao, Effects of Hydraulic Pressure on the Stability and Transition of Wetting Modes of Superhydrophobic Surfaces, Langmuir 21 (2005) 12207-12212.

H. Zweifel, Plastic Additive Handbook, 5th ed., Hanser publishers, Munich (2001), Number of pages: 1222.

Appendix A

Extrusion process for membrane fabrication

In this thesis, LDPE hollow fiber membranes were produced using Haake Rheomix TW-100 co-rotating conical twin-screw extruder. LDPE pellets were mixed thoroughly with NaCl particles to form blends containing 35, 40, 50, 60, 65 and 68 wt% salt. For comparison, a nonporous LDPE hollow fiber sample (blank) was also prepared without the addition of salt. The mixture was then fed into the extruder in two steps using a hopper. In the first step, the mixture was melt blended above the melting temperature of LDPE (≈ 112°C) to obtain a uniform polymer/salt blend. The temperature profile was controlled at 115°C for zone 1, 135°C for zone 2 and 140°C for zone 3 and the die zone (zone 4). After cooling down through a water bath at room temperature, the extrudate was pelletized using a PELL 2 pelletizer supplied by Berlyn Company (not shown). For the nonporous (blank) LDPE hollow fiber sample, the first extrusion step was skipped. In the second step, the prepared pellets were fed into the extruder using the hopper at a temperature of 115°C for zone 1, 135°C for zone 2 and 140°C for zones 3 and 4. The extruder was operated at a constant mass flow rate of 0.4 kg/h and a screw speed of 60 rpm. To produce a stable hollow fiber structure, the inside air pressure was controlled at 0.02 psig to prevent collapse. The extrudate was taken out of the hollow fiber die with an inside and outside diameters of 5 and 7 mm, respectively, and cooled down through a water bath fed by a fresh water spray and emptied by salt-rich water drains at 60°C. Finally, a take-up unit was used to control drawing speed at 250 cm/min.

Optimized extrusion conditions

- Temperature profile

In this thesis, the barrel temperature was selected as the normal temperature profile, in which the temperature of the first zone (rear zone) was selected at 115°C, which is much lower that that of the exit (die zone), in order to avoid sticking of the granules to the entrance of the barrel. Then the temperatures were gradually increased to 135°C for the second and third zones and to 140°C for the die zone. These temperatures were adjusted

according to the following reasons: i) High viscosity of the polymer melt bellow such temperatures, which makes the drawing of the fiber impossible, and ii) change in the colour of the product from white to brown at temperatures higher that the above mentioned temperatures, maybe due to the degradation of the material used for the surface modification of the salt particles to avoid agglomeration.

- Screw speed

The screw speed was selected at 60 rpm. Speeds higher than 60 rpm made the control of the structure of the final product difficult, while at speeds lower that 60 rpm salt agglomeration increased because by reducing screw speed, the stress applied on the polymer melt and salt mixture reduces, which makes it difficult for the salt particles to pass through the barrel.

- Salt particle size

The smaller the pore size of the membrane, the higher is the breakthrough pressure and therefore, the smaller is the wetting tendency of the membranes.The membranes pore size decreases with reducing salt particle size. Besides, the leaching process accelerates with the decrease of salt particle size (Table A.1). Therefore, NaCl particle size of 5-10 μm was used (smallest size commercially available).

Table A.1. Effect of salt particle size on leaching time and salt removal percentage after leaching.

Particle size (μm)	Leaching time (min)	Salt removal (%)
125-150	240	15
45-75	240	45
5-10	160	100